Energy Exchange Studies at the Earth's Surface

I. Energy Budgets of Desert, Meadow, Forest and Marsh Sites

by

Lloyd W. Gay

Technical Report No. 73-I
January 1973

ENERGY EXCHANGE STUDIES AT THE EARTH'S SURFACE

I. Energy Budgets of Desert, Meadow, Forest and Marsh Sites

by

Lloyd W. Gay

DEPARTMENT OF FOREST ENGINEERING

Oregon State University

Corvallis, Oregon 97331

WATER RESOURCES RESEARCH INSTITUTE

DISCLAIMER

The technical note series of the Department of Atmospheric Sciences of the Oregon State University is intended as an informal documentation series, not as publications. It is not intended to be a journal to burden library shelves. Its purposes included formulation of ideas, rapid communication of results to colleagues before publication so their comments can be used, and a place to dispose of negative results and ideas not quite good enough to publish.

The editor attempts to help a little, but recognizes that, in view of the purposes, the writing will often be informal and unpolished. The responsibility for the contents rests entirely with the author.

The author invites comments.

Foreword

The authors have special interest in the application of the energy budget concept to the exchange of energy at the earth's surface as a means of evaluating microclimate and its influences on biological processes. The material reported here represents such an approach applied to certain characteristic landscape types in the high, semi-arid plateau of central Oregon, lying east of the Cascade Range. The results are concerned primarily with evaluation of microclimate; they are arranged into two complementary but self-contained volumes. The first volume, by Lloyd W. Gay, discusses comparisons among the energy budget results obtained over surfaces of bare pumice, meadow, forest and marsh. The second volume, by H. Richard Holbo, provides a detailed examination of the theory, field techniques, and energy transfer processes at a pumice desert surface. There is some overlap between the two volumes to permit each to stand alone. The results should help to encourage the development and application of the energy budget concept to a wider range of surface conditions and to a variety of different types of investigations.

L.W.G.
H.R.H.

Abstract

The energy exchange characteristics of four common landscape types in the high semi-arid plateau in central Oregon, east of the Cascade Range, were evaluated during the summers of 1969 and 1971. The surfaces studied were pumice, meadow, forest, and marsh.

A portable environmental data acquisition system was developed for sampling micrometeorological variables with a high degree of precision. The construction and operation of the system is described.

The system was deployed for various periods during mid- to late summer at the four experimental sites. Clear weather periods were selected for analysis in order to examine the energy exchange processes at a time of maximum activity. The mean energy budget components for two such clear days were ($cal/cm^2 day$):

	$\bar{Q}^*$	$\bar{G}$	$\bar{H}$	$\lambda\bar{E}$
Pumice	226	- 5	-188	- 33
Meadow	351	- 9	19	-361
Forest	384	-10	-219	-155
Marsh	325	22	60	-407

where Q^* is net radiation, G is change in stored heat, H is convection, and λE is latent heat.

The maximum latent energy transfer occurred over the marsh and meadow; these surfaces were plentifully supplied with water. Latent energy transfer was enhanced at both sites by the advection of energy from the warmer surroundings. The large heat capacity of the marsh played an important role in maintaining evaporation throughout the night hours.

The studies revealed that the forest was a very effective energy exchanger. Though only moderate latent energy transfer occurred there, convection was the largest, resulting in the maximum total transfer of all the surfaces studied.

The results provide a basis for estimating maximum rates of evapotranspiration from the surfaces that are commonly found in central Oregon.

Acknowledgements

Dr. H. Richard Holbo played an important role in the development of the environmental data acquisition system that is described in this Volume. He also directed the field studies carried out at the pumice desert and at the Malheur Lake marsh. John Hyde contributed to the success of the field studies at Malheur Lake. Dr. Patrick H. Cochran was a very helpful cooperator in the pumice desert studies; the soil heat flux calculations there are derived from his measurements of pumice thermal properties.

The work upon which this publication is based was supported for the major part by funds provided by the U.S. Department of Interior, Office of Water Resources Research, as authorized under the Water Resources Research Act of 1964, and administered by the Water Resources Research Institute, Oregon State University. Support for the pumice desert study was also provided by the Pacific Southwest Forest and Range Experiment Station, Portland, under Supplement No. 58, Project FS-PNW-1203. The marsh studies at Malheur Lake received support from the U.S. Corps of Engineers, Walla Walla, Washington, through contract DACW 68-72-C-0032. The Oregon State University Graduate Research Fund provided assistance for the development of the counter system used in measuring wind velocities at the marsh site.

Contents of Volume 1

Contents of Volume 2

The Energy Budget of a Pumice Desert

H. Richard Holbo

List of Figures

List of Tables

List of Symbols

Symbol	Definition
A	psychrometric constant $°C^{-1}$
$A\downarrow$	atmospheric radiation flux density, cal/cm^2min
Cp	specific heat of air, cal/cm°C
D	day; displacement, cm
E	exponent; water vapor flux density, gm/cm^2min
E_d	electrical output of drybulb, mV
E_w	electrical output of wetbulb, mV
G	soil heat flux density, cal/cm^2min
H	hour; sensible heat flux density, cal/cm^2min
Hz	Hertz, sec^{-1}
K	diffusivity coefficient
K_E	eddy diffusivity for water vapor, cm^2/sec
K_H	eddy diffusivity for sensible heat, cm^2/sec
K_M	eddy diffusivity for momentum, cm^2/sec
$K\downarrow$	global radiation flux density, cal/cm^2min
$K\uparrow$	reflected global radiation flux density, cal/cm^2min
K*	net global radiation flux density, cal/cm^2min
Lg	longwave radiation flux density leaving the surface, cal/cm^2min
$L\downarrow$	longwave radiation flux density, incoming, cal/cm^2min
$L\uparrow$	longwave radiation flux density, outgoing, cal/cm^2min
L*	longwave radiation flux density, net, cal/cm^2min
M	model; minute; mega- (1,000,000)
N	number
p	polarity
$Q\downarrow$	allwave radiation flux density, incoming, cal/cm^2min
$Q\uparrow$	allwave radiation flux density, outgoing, cal/cm^2min
Q*	allwave radiation flux density, net, cal/cm^2min
Ri	Richardson number
T	temperature, °C or °K
T_d	drybulb temperature
T_r	temperature of reference junction
T_w	wetbulb temperature
V	voltage
VAC	voltage, alternating current
W	end of word
X	data digit
e	vapor pressure, mb
e_s	saturation vapor pressure, mb
g	acceleration due to gravity, 980 cm/sec^2
k	Von Karman's constant
mV	millivolt
n_d	number of drybulb junctions in psychrometer
n_w	number of wetbulb junctions in psychrometer
p	atmospheric pressure, mb
r	coefficient of reflectivity, longwave radiation
$rL\downarrow$	reflected longwave radiation flux density, cal/cm^2min
u	windspeed, cm/sec
x	code for bad character in data list
z	height above a reference plane, cm
z_o	roughness length, cm

Symbol	Definition
α	albedo; coefficient in the stability correction function
β	Bowen ratio
γ	exponent in the stability correction function
Δ	an operator denoting a finite difference
ε	emissivity for longwave radiation
θ	potential temperature, °C
λ	latent heat of fusion, cal/gm
λE	latent heat flux density, cal/cm^{2}min
ρ	density of air, gm/cm^3

1. THE SURFACE ENERGY BUDGET

1.1 Introduction.

Evapotranspiration, the process by which water is evaporated from the soil and through vegetation, plays a major role in the hydrologic cycle. The process is of particular interest to hydrologists because it represents a loss of moisture that might otherwise appear as streamflow. The magnitudes of this loss are indicated in a summary of available data expressing evapotranspiration as a percentage of the annual precipitation (Baumgartner, 1965). The percentages range from 30 percent for bare soil, 40-45 percent for non-irrigated cereals and vegetables, 70 percent for forests, and 75 percent for lakes, to greater than 100 percent for irrigated crops.

These figures emphasize the importance of vegetation in the evapotranspiration process. Our Pacific Northwest region is both well-vegetated and well-watered, with high volumes of timber and streamflow. Such a combination suggests that evapotranspiration might be significantly reduced through modification of vegetation during timber harvesting operations (U. S. Senate, 1960). For example, the watershed studies of Rothacher (1970) have revealed that the water yield may increase 460 mm (18 inches) following clear-cut logging in the Oregon Cascades.

A reduction in evapotranspiration should augment discharge during lowflow periods in the summer. However, Rothacher (1970) reported that 80 percent of the increased yield occurred during the October to March rainy season, partly as a result of greater soil moisture storage in the cutover areas at the end of the dry summer. Thus far, few studies have sought to determine basic evapotranspiration information for this region. Knowledge of how the evapotranspiration process operates over a range of conditions is essential if water yield considerations are to affect decisions on land management.

During the past two decades, there has been confirmation that water and the latent energy that it represents may be considered as interchangeable entities. A growing awareness of this interchangeability has contributed to acceptance of the concept that evaporation is simply a form of energy conversion. Indeed, in many cases it has been found easier to measure the energy converted in the evaporation process than to measure the water loss directly.

More recently, investigators have begun to consider the importance of meteorological transfer processes in the establishment of a characteristic microclimate. Many of these studies of dynamic processes that control the transfer of heat, water vapor, and momentum between plant canopies and the atmosphere are reviewed by Miller (1965), who places the contributions of the surface properties and of the processes into perspective.

Widespread practical interest in the evaluation of evapotranspiration is thus complemented by fundamental considerations of the processes of energy transfer at the surface of the earth.

1.2 Objectives.

The School of Forestry initiated a five-year study of wildland evapotranspiration in 1966 as part of its program in forest hydrology. The Water Resources Research Institute has provided the major financial support of this study. It comprised

one aspect of the Institute sponsored project A-001-OREG, entitled "The Hydrology of Water Yield Prediction".

The goal of the evapotranspiration study is an evaluation of water use by different classes of watershed vegetation within Oregon. This will provide a basis for determining the feasibility of water supply augmentation by vegetation manipulation. The objectives of the study are to:

1. Evaluate evapotranspiration under different climatic regimes, using energy balance techniques.

2. Test and revise models now used to estimate the energy components that comprise the surface energy balance.

3. Develop and improve instruments and observational techniques used to measure the parameters needed for evaluation of the energy balance.

The purpose of this discussion is to show the means, methods, and direction of our research in contributing to the above goals.

The energy balance concept provides the basic research tool for this work. Energy balance methods offer advantages in sensitivity; they are non-destructive and thus permit repeated sampling at a given site (Federer, 1970).

We shall now examine how the evapotranspiration process fits into the fundamental concept of a balance of energy at the earth's surface. In subsequent chapters, the specific methods used in this study will next be discussed with respect to theory and to the design of experiments undertaken. Finally, the application of the method will be illustrated with the analysis of data obtained over four surfaces with contrasting energy balance regimes: a non-vegetated pumice desert; a lush, wet meadow; a young lodgepole pine forest; and a large, shallow, fresh-water marsh.

1.3 Energy Budget Concepts.

Let us examine the energy budget concept. Energy must be available in order for water to change phase from liquid to vapor in the evaporation process. An equivalent amount of energy will be released when the vapor condenses back into the liquid phase. A specific amount of "latent energy of vaporization" is required for the phase change. The value is precisely known as a function of temperature and pressure; 585 calories per gm is an approximation that will be suitable for our discussion.

Energy balance theory links energy to evapotranspiration. "Energy balance" is a descriptive term that simply refers to an accounting of the energy that is gained and lost to the surface of interest. Such an analysis is derived from the widely accepted principle of conservation of energy. Simply stated, this says that the sum of incoming energy will balance the outgoing energy, plus any changes in energy storage at the site.

The application of this principle to measurements of energy budgets over natural surfaces requires that the forms and quantities of energy crossing the boundaries of the experimental site be identified. Let us now examine a basic model of the energy fluxes that are normally encountered over natural surfaces.

1.3.1 Basic Model.

The model can be written for forests and other natural surfaces as

$$Q^* + H + \lambda E + G = 0 \qquad [1\text{-}1]$$

where Q^* represents the net exchange of radiation, H and λE are respectively the net turbulent exchanges of sensible and latent heat between the surface and the atmosphere, and G is the net change of stored sensible heat in the soil and biomass. The storage term, G, in Equation [1-1] is positive when energy is conducted to the exchange surface; the other terms will be positive when their "sense" is directed downward toward the exchange surface.

Some minor components of the surface energy balance have been omitted from Equation [1-1] for simplicity. Probably the most important of these is photosynthesis. It is generally acknowledged that in vegetation the photochemical fixation of energy by photosynthesis is usually less than a few percent with respect to Q^* (Baumgartner, 1965). Thus it may be neglected in our treatment. Several other smaller components are discussed by Budyko (1956, p. 6-7); these are primarily of theoretical interest and need not be considered here.

Net radiation is the residual of four radiation fluxes at a surface. It is equal to the incoming shortwave and longwave minus the reflected short- and longwave, and the emitted longwave. However, the residual net radiation term also represents the net transformation of energy from radiative to non-radiative forms. This concept is basic to formulation of the surface energy balance.

The partitioning of net radiation into the three fluxes of convective, latent, and stored energy poses the basic problem in the energy budget. This partition can be estimated by a variety of methods. Those used here include the Bowen ratio and an aerodynamic model.

1.3.2 The Bowen Ratio.

The Bowen ratio method is frequently used to estimate H and λE. It assumes a similarity exists in the exchange processes that control the diffusion of heat and the diffusion of vapor from the surface into the atmosphere. Because of this similarity, measurements of wind above the surface need not enter into the analysis. Instead, the estimates are based upon measurements of temperature and vapor concentration gradients. The basic method was proposed by Bowen (1926). The following derivation is similar to those available in many review articles (Webb, 1965).

The flux of sensible heat into the air is proportional to the temperature gradient above the surface. Likewise, the flux of vapor is proportional to the vapor concentration gradient above the surface. This can be expressed in Equations [1-2a and 1-2b] as

$$H = -K' \, \partial\theta/\partial z \qquad [1\text{-}2a]$$

$$\lambda E = -K'' \, \partial e/\partial z \qquad [1\text{-}2b]$$

where K' and K" are the respective proportionality coefficients for convection and for water vapor transfer, and $\partial\theta/\partial z$ and $\partial e/\partial z$ are the respective gradients of potential temperature and of vapor pressure with height above the surface. The negative sign is conventional heat transfer notation that insures positive transfer proceeds in the upward direction.

Potential temperature is used to eliminate the effects of pressure on air temperature. The potential temperature gradient can easily be approximated, if each observed air temperature (T) is first transformed by addition of the product of the adiabatic lapse rate (-0.01°C/m) and the height of that sensor above a common reference plane.

Additional constants can be factored out of the coefficients of proportionality to yield

$$K' = \rho C_p \cdot K_H \qquad [1\text{-}3a]$$

$$K'' = \frac{.622\rho}{p} \lambda \cdot K_E \qquad [1\text{-}3b]$$

where ρ (gm/cm^3) is the density of the air, C_p (cal/gm°C) is the specific heat of the air, p (mb) is the pressure of the atmosphere, and λ (cal/gm) is the latent energy of vaporization of water. The "transfer" coefficients K_H and K_E apply respectively to sensible and latent energy; written in the form of Equations [1-3a and 1-3b], both coefficients have units of cm^2/sec.

With two exceptions, all of the quantities in Equation [1-1] are either known constants, can be measured directly in the case of net radiation and the soil heat storage, or they can be estimated from measured temperature and vapor pressures as shown in Equations [1-2] and [1-3]. The exceptions are the two transfer coefficients K_H and K_E. These coefficients can be determined if they are numerically equal. Although this is a point of speculation among micrometeorologists, the coefficients are generally considered to be equal if the exchange surface is homogeneous, i.e., there is not a patchy distribution of wet and dry spots (Tanner, 1963). Confirmation of this view is given by Dyer (1967), Swinbank and Dyer (1967), and Denmead and McIlroy (1970).

When appropriate conditions prevail, and $K_H = K_E = K$, then Equations [1-1], [1-2], and [1-3] can be combined to yield

$$-\lambda E = (Q^* + G) \,/\, [1 + (C_p p/.622\lambda)(K_H/K_E)\Delta\theta/\Delta e]$$

$$= (Q^* + G)/\,(1 + \beta) \qquad [1\text{-}4]$$

where $\Delta\theta/\Delta e$ is the ratio of the difference in potential temperature and in vapor pressure over the same distance Δz near the surface, and β is the Bowen ratio of sensible to latent energy over the surface (Tanner, 1960).

The energy balance components may thus be evaluated from periodic measurements of Q*, G, T, and e, using the Bowen ratio analysis as a simplification. The periodic evaluations of the components can then be integrated into hourly and daily totals. If the instrumentation used for the necessary measurements is sufficiently portable to permit sampling different sites, the energy balance response of various surfaces can be deduced from repeated measurements of relatively short duration.

1.3.3 Aerodynamic Approach.

The Bowen ratio method assumes equality of the transfer coefficients K_H and K_E. In a different approach, a number of aerodynamic models have been developed from consideration of the gradients of temperature (or vapor) and wind speed. We shall consider the form discussed by Holbo (1971).

The gradient of wind speed near the surface can be incorporated into the basic transfer models (Eqs. [1-2] and [1-3]) in a form summarized in Sellers (1965):

$$H = -\rho C_p k^2 (\Delta\theta\ \Delta u/(\Delta \ln z)^2)\phi \qquad [1\text{-}5a]$$

$$\lambda E = -\rho \frac{.622}{p}\ \lambda k^2\ (\Delta e\ \Delta u/(\Delta \ln z)^2)\phi \qquad [1\text{-}5b]$$

where k is Von Karman's constant ($k \approx 0.4$) and the gradients of potential temperature, windspeed and vapor with height are represented by the respective incremental approximations of $\Delta\theta/\Delta \ln z$, $\Delta u/\Delta \ln z$ and $\Delta e/\Delta \ln z$.

The factor ϕ is a function of the stability of the atmosphere near the surface. It represents the ratio of the transfer coefficient for heat (or vapor) to an analogus transfer coefficient for momentum, K_M. When the temperature stratification in the atmosphere is adiabatic or neutral, the value of this ratio (and of ϕ) is unity. This condition is often met over freely evaporating surfaces. When a temperature gradient exists, however, the transfer of momentum will be enhanced in unstable (lapse) conditions, and suppressed in stable (inversion) conditions and the ratio will depart from unity.

A correction for these circumstances in provided by the model

$$\phi = (1 - \alpha Ri)^{\gamma} \qquad [1\text{-}6]$$

where α and γ are constants, and Ri is the Richardson number (Richardson, 1920). The Richardson number expresses the relative contributions to transfer of the bouyancy effects due to heating, and of the frictional effects due to wind. It is approximated by

$$Ri = (g/\theta)(\Delta\theta/\Delta z)/(\Delta u/\Delta z)^2 \qquad [1\text{-}7]$$

where g is the acceleration due to gravity, θ is the mean potential temperature of the air layer, $\Delta\theta/\Delta z$ approximates the vertical gradient of potential temperature with height, and $\Delta u/\Delta z$ approximates the vertical gradient of horizontal wind speed.

A range of values have been reported in the literature for α and γ. The values appropriate for a given experiment appear to be related to the heights chosen for measurement, and to the roughness of the exchanging surface. Holbo (1971), for example, estimated $\alpha = 34$ and $\gamma = 0.55$ for a relatively smooth, pumice desert site.

1.4 Discussion.

Energy balance research into the processes that affect the hydrologic cycle has a bearing on many questions of water supply, consumption, and conservation. With respect to evaluation techniques for water supplies, energy balance studies should be involved in determining the effects of land and forest management practices

on water quantity and quality; the definition of water requirements and consumptive use of various agricultural crops and trees under varying conditions, including proper rate and timing of irrigation; the development of low-flow prediction techniques; and the development of simulation models for water yield characteristics and prediction. Energy balance theory could play an important role in determining the potential of forest land irrigation. Such studies have fundamental relevance to the role of plants in the water cycle, and to the effects of conservation practices upon yield from agricultural watersheds. Further, in contrast to empirical techniques, energy balance theory allows the generalization of research results to areas other than those where the experiments have been carried out.

Measurement of the latent energy term has been the goal of most of the past energy balance research (Tanner, 1960, Rosenberg, et al., 1968). There is also a growing awareness that the relationships among the components of the energy budget are important in defining the microclimate of plant communities. Previous research, reviewed by Miller (1965) and by Reifsnyder (1967), has identified gross differences in energy budgets for diverse classes of surfaces (bare soil, low crops, high crops, forest) with different water availability (arid, water limiting, irrigated, free water), and in areas with different climatic regimes.

There are good reasons for the energy balance differences that have been reported. The absorption of radiation depends upon physical properties (such as albedo) of surfaces as different as water, soil, and vegetation. Absorption depends also upon the geometrical considerations of slope, aspect, and latitude. The net conversion of absorbed radiation into other energy forms depends upon such surface properties as heat capacity, conductivity, diffusivity, and roughness with respect to air movement.

The conversion is also affected by environmental characteristics such as the availability of water and the geographical proximity of area with different energy absorption and conversion efficiencies (de Vries, 1963). For example, forests are found to have a high potential for converting net radiation into latent energy (Baumgartner, 1956; Denmead, 1964; Dzerdzeevski, 1963; Rauner, 1960, 1966).

The basic problem in evaluating the surface energy balance is therefore twofold: the first problem is to determine the amount of net radiation converted into latent energy and into sensible energy in the soil, plants, and air; the second is to interpret the relation among characteristics of the surface and the observed energy budget.

We have defined the models that are to be used in the energy balance evaluation. We shall next describe the field instrumentation, and then examine the contrasts that are apparent among four experimental sites with different surface characteristics: a pumice desert, a wet meadow, a lodgepole pine forest, and a marsh.

1.5 Literature Cited.

Baumgartner, A. 1956. Investigations on the heat- and water economy of a young forest. Translated by E. Pichler from: Untersuchungen über den Wärme- und Wasserhaushalt eines jungen Waldes. Ber. Deut. Wetterdienst. 5:4-53. CSIRO Translation 3760, Melbourne, Australia. 1958.

Baumgartner, A. 1965. The heat, water, and carbon dioxide budget of plant cover: methods and measurements. Methodology of Plant Eco-physiology: Proceedings of the Montpellier Symposium. UNESCO, Paris, Pp. 495-512.

Budyko, M. I. 1956. The heat balance of the earth's surface. Trans. from Russian. U.S. Weather Bureau, Washington, D.C. 1958. 259 pp.

Bowen, I. S. 1926. The ratio of heat losses by conduction and by evaporation from any water surface. Phys. Rev. 27:779-787.

Denmead, O. T. 1964. Evaporation sources and apparent diffusivities in a forest canopy. J. Appl. Meteorol. 3:383-389.

Denmead, O. T. and I. C. McIlroy. 1970. Measurements of non-potential evaporation from wheat. Agr. Meteorol. 7:285-302.

de Vries, D. A. 1963. The physics of plant environments. In: Evans, L. T. (ed.). Environmental control of plant growth. Pp. 5-22. Academic Press, N. Y.

Dzerdzeevskii, B. L. 1963. Study of the heat balance of the forest. Silva Fenn. 113:1-17.

Dyer, A. J. 1967. The turbulent transport of heat and water vapor in an unstable atmosphere. Quart. J. Roy. Meteor. Soc. 93: 501-508.

Federer, C. A. 1970. Measuring forest evapotranspiration - theory and problems. U.S.D.A. Forest Service Research Paper NE-165. Upper Darby, Pa. 25 pp.

Holbo, H. R. 1971. Development of a stability correction for estimating convective transfer. OSU Dept. Atmos. Science Tech. Rep. No. 71-7, 8 June 1971. 10 pp.

Miller, D. H. 1965. The heat and water budget of the earth's surface. Advan. Geophys. 11:176-277.

Rauner, Ju. L. 1960. The heat balance of forests. Izvestiya Akademii Nauk SSSR, Seriya Geograficheskaya. 1:49-59. Translated by Israel Prog. Sci. Transl., No. 1342. U.S. Dept. Commerce, Washington, D. C. 1965.

Rauner, Ju. L. 1966. Methodik und einige Ergebnisse der experimentellen Erforschung des Wärmehaushaultes der Waldbestände. Angewandte Meteorol. 5:157-165.

Reifsnyder, W. E. 1967. Forest meteorology: the forest energy balance. Inter. Review Forestry Res. 2:127-179.

Richardson, L. F. 1920. The supply of energy to and from atmospheric eddies. Proc. Royal Soc. London, A, 97:354-373.

Rosenberg, N. J., H. E. Hart and K. W. Brown. 1968. Evapotranspiration, review of research. Bulletin MP20, Nebraska Agric. Expt. Station, Lincoln. 80 pp.

Rothacher, J. 1970. Increases in water yield following clear-cut logging in the Pacific Northwest. Water Resour. Res. 6:653-658.

Sellers, W. D. 1965. Physical Climatology. Univ. of Chicago Press.

Swinbank, W. C., and A. J. Dyer. 1967. An experimental study in micrometeorology. Quart. J. Roy. Meteor. Soc. 93:494-500.

Tanner, C. B. 1960. Energy balance approach to evapotranspiration from crops. Proceedings, Soil Sci. Soc. Amer. 24:1-9.

Tanner, C. B. 1963. Basic instrumentation and measurements for plant environment and micrometeorology. Soils Bull. 6, Univ. Wisconsin, Madison.

U.S. Senate, Select Committee on National Water Resources. 1960. Water resources activities in the United States. Evapo-transpiration reduction. Committee Print No. 21, U.S. Govt. Print. Off., Washington, D.C.

Webb, E. K. 1965. Aerial microclimate. In: Waggoner, P. (ed.). Agricultural Meteorology. Chapter 2. Meteorol. Monographs, Vol. 5, Amer. Meteorol. Soc., Boston.

2. ENVIRONMENTAL INSTRUMENTATION

Virtually all energy budget studies are involved to some degree in the development of specialized instrumentation. The work undertaken here has proven to be no exception in this regard. However, we have endeavored to use standard equipment and components where ever possible in order to minimize the time required for development.

The results of studies such as this must be interpreted with regard to the instrumentation and data techniques that are used. Since our solutions to certain measurement problems may prove useful to other workers elsewhere, it appears appropriate to describe our environmental instrumentation. This is most easily accomplished by grouping the material into three categories. The first is a general description of the environmental data acquisition system used in this work. The second is a discussion of the design of the psychrometer sensors used to measure the parameters of air temperature and vapor concentration. The third deals with our solution for the problem of accumulating and recording the pulses generated by cup anemometers.

2.1 The Data Acquisition System.*

A number of environmental data acquisition systems have been described in recent years. Some of these systems have been mobile (Clayton and Merryman, 1960; Valli, 1966), but most have been fixed installations (Allen, 1970; Backlund and Perttu, 1971; Fritschen and Van Bavel, 1963; Reifsnyder, 1962). Fritschen (1970) has reviewed specific requirements for data systems employed in microclimate research. These systems have sought to combine the attributes of precision, convenience in application, and ease in data processing. The performance of these and similar systems has continued to improve with the development of new instruments and increased experience in field operation.

This section describes an environmental data collection system that has been developed at Oregon State University for energy budget research. The configuration of this mobile, self-contained system will be described, and the performance evaluated. The system is designed for flexibility in order to meet the needs of a variety of environmental studies.

The data acquisition system includes a laboratory, recorder, sensors, signal cables and instrument supports. The system is mobile, self-contained, and capable of a high degree of precision. It has been tested during several field seasons in different types of environmental studies (Gay, 1970; Gay, Stebbins, and Black, 1971). However, the primary use has been for energy balance studies over different natural surfaces.

2.1.1 The Mobile Laboratory.

The mobile laboratory houses the recorder, provides office space in the field, and storage space for the transportation of sensors, cables, and instrument supports. The 8x12-foot truck-mounted van in Figure 2-1 is insulated and air conditione to maintain a stable environment for recording. The air conditioner must be equipped with an "easy start" compressor for satisfactory operation with a generator in the field. An Onan 2500 watt generator[1] in a weather-tight housing and equipped

*Based on a paper by L. W. Gay, presented to the National Conference on the Forest, Weather, and Associated Environment, Atlanta, Georgia, May 18-20, 1971.

Fig. 2-1. Mobile laboratory, OSU Environmental Data Acquisition System. The 8X12 ft air conditioned van is truck mounted for mobility.

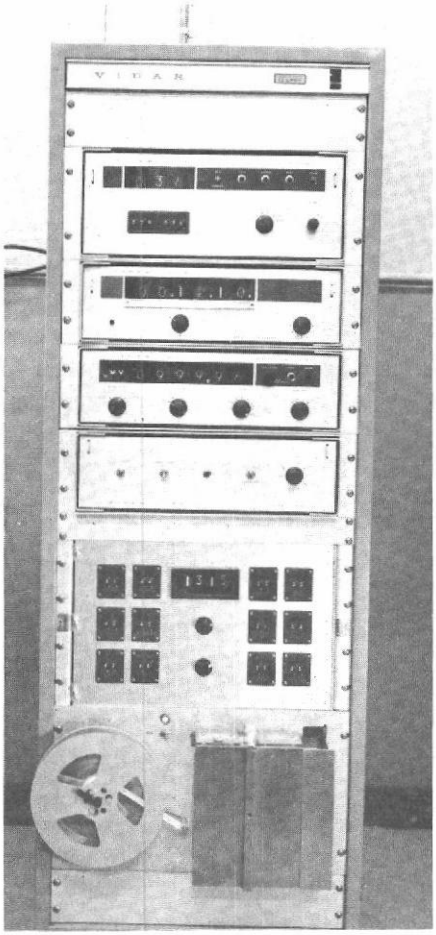

Fig. 2-2 (above, right). Digital data logger used in the OSU System. The capacity is 90 analog and 12 digital channels. The resolution is 0.1 microvolt and the maximum scan rate is 5 channels per second. Output is by paper-tape punch and strip printer.

Fig. 2-3. Energy balance research site. Parameters measured include net and total allwave radiation, incoming and reflected global radiation, soil heat flux, and 6 levels of wind speed, air temperature and humidity.

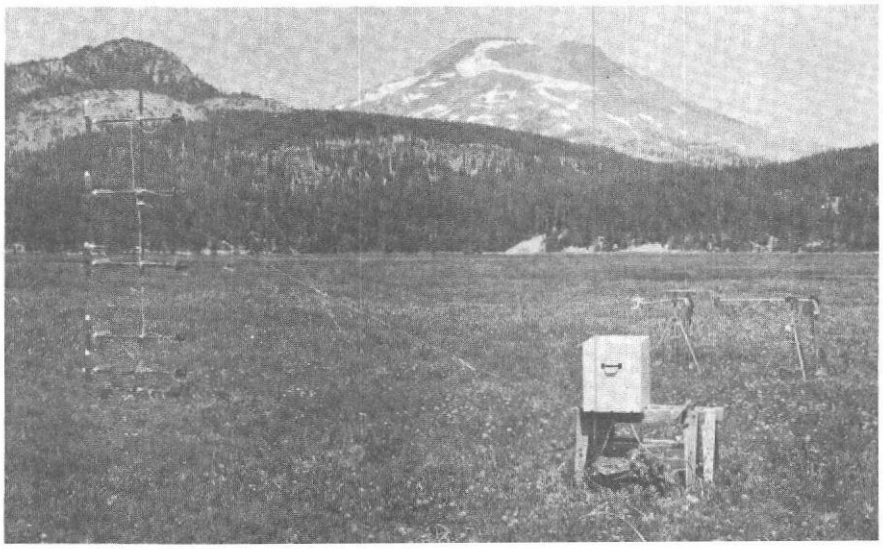

to operate with LPG fuel has proven very satisfactory in our use.

2.1.2 The Digital Recorder.

Some considerations in the selection of digital recorders are outlined by Buckley (1969). The recorder in our system is shown in Figure 2-2; it is a Vidar 5202 unit[2] with both punched and printed tape output. The integrating voltmeter has a resolution approaching 0.001 percent (0.1 microvolt), an input impedance in excess of 10 megohms on all ranges, an overall effective common-mode rejection in excess of 150 dB for all frequencies with up to 1,000 ohms source imbalance, and an auto-ranging accessory to select among the six decade ranges that span $\pm$10 mV to $\pm$1000 V. The maximum scan rate is 5 channels per second, with a 166-2/3 millisecond integration period. The crystal oscillator timebase clock will initiate scans at selectable intervals from 1 min to 10 days.

The present system capacity includes 100 channels for analog, and 12 channels for digital inputs. The digital inputs are continually recorded on an electronic counter that totalizes 4 decades of BCD data (up to 9,999 counts) from each of 12 anemometers. The electronic counter is interfaced to the digital recorder so that the pulse totals can be recorded and the counters reset during each data scan. The details of construction and operation of the counter and interface will be presented in detail in section 2.3 of this chapter.

2.1.3 Sensors.

The sensors used with the system respond to the common environmental parameters of radiation, temperature, water vapor concentration, windspeed and wind direction, and soil heat flux. The sensors are deployed in Figure 2-3 in a typical energy balance study of mean temperature, vapor, and windspeed profiles over a wet meadow.

Upright and inverted Kipp pyranometers[3] are used to measure incoming and reflected shortwave radiation. Total incoming and net allwave radiation is measured with polyethylene-shielded, CSIRO[4] pyrradiometers and net pyrradiometers.

Temperatures are measured with copper-constantan thermocouples, referenced against a heated (65°C) Pace reference junction[5] with a capacity of 48 circuits. Soil and pyrradiometer reference temperatures are measured with individual thermocouples Air temperatures are measured with two series-connected thermocouple junctions in aspirated psychrometers that were constructed after the basic design of Lourence and Pruitt (1969), as modified by Gay (1972). The psychrometers utilize four-junction thermopiles and a ceramic-wick wet-bulb element in the evaluation of the water vapor concentration in the atmosphere. The design will be discussed in detail in section 2.2. The rate of change of soil heat storage values are measured with small NIL heat flux disks[6], connected 5 in series to yield an output of about 2.5 mV per cal/ cm^2min.

The wind speed measurements are made with standard Thornthwaite sensitive anemometers[7], connected to the recorder through the electronic counter and interface (Gay and Holbo, 1970) described in detail in section 2.3. The Thornthwaite amplifier, power supply, and electromechanical counters are replaced in this application by the counter and interface. Wind direction is indicated by an analog signal derived from a simple, rotary, voltage divider.

2.1.4 Cables and Connectors.

The cables and connectors must provide flexibility for a variety of experimental setups, be easy to lay out, be weatherproof and yet not degrade the signal quality. The connectors should provide continuity of the individual shields, and the connector pins should be gold- or silver-plated to minimize thermal offsets.

The basic cabling design provides for multiconductor cables to run from the recorder to the vicinity of the instruments. From that point, twisted, shielded pairs of wires run to each instrument. Small connectors[8] link the signal cables to the recorder, and large connectors[9] link the multiconductor cables to the bundle of individual signal pairs which then plug into small connectors[9] at each instrument. The multiconductor cables are made up in 75 m (250 ft) lengths for convenience; additional extension cables may be added as needed. The basic design groups six instruments per set of cables for convenience, so that one cable can handle a group of radiometers, or a six-level psychrometer or wind profile mast. Actually, any number of instruments can be deployed within the capacity of the cable system.

The thermocouple cable system shown in Figure 2-4 contains 12 shielded, twisted pairs of copper-constantan that link the two-junction thermopiles in six psychrometers to the heated reference junction. Interconnection to the individual pairs is made with a copper-constantan terminal strip in a weather resistant junction box[10]. Copper-constantan jack plugs are used to connect the individual pairs to the dry-bulb thermopile at each psychrometer. These simple connectors are not waterproof, but can be made so with vinyl tape.

The main cables are easily spooled in and out with a simple cable winding drum.

2.1.5 Instrument Supports.

The instrument support system must also provide for a variety of instrument configurations. The 6-unit mast at the meadow site in Figure 2-3 is a typical configuration for measurements over bare soil or low vegetation. The light, guyed mast of 1-inch pipe is similar to that described by Lourence (1967). The key feature is an inexpensive, "split-rail cross" clamp[11] that grips the psychrometers at right angles to the mast at any desired level.

The psychrometers can be readily deployed for measurements of temperature and vapor concentration at only two levels, as required for Bowen ratio estimates of evapotranspiration, with the aid of inexpensive, roof-top antenna tripods[12] pictured in Figure 2-5. The temperature and vapor profiles over a forest, however, must be sampled at a scale quite different from that of bare soil or low vegetation. The support mast shown in Figure 2-6 over a lodgepole pine forest in central Oregon is a standard TV tower[12] that is erected in 10-foot sections. Two of the "split-rail cross" clamps are used to hold each of the psychrometers and the anemometer support arms to one face of the triangular tower.

2.1.6 System Operation.

The use of the system in the field is enhanced by the compatibility of the components, especially the cables, connectors, and instrument supports. Two men can set up the system for an energy balance study as pictured in Figure 2-3 in about half a day. Additional time is required for more complex surfaces,

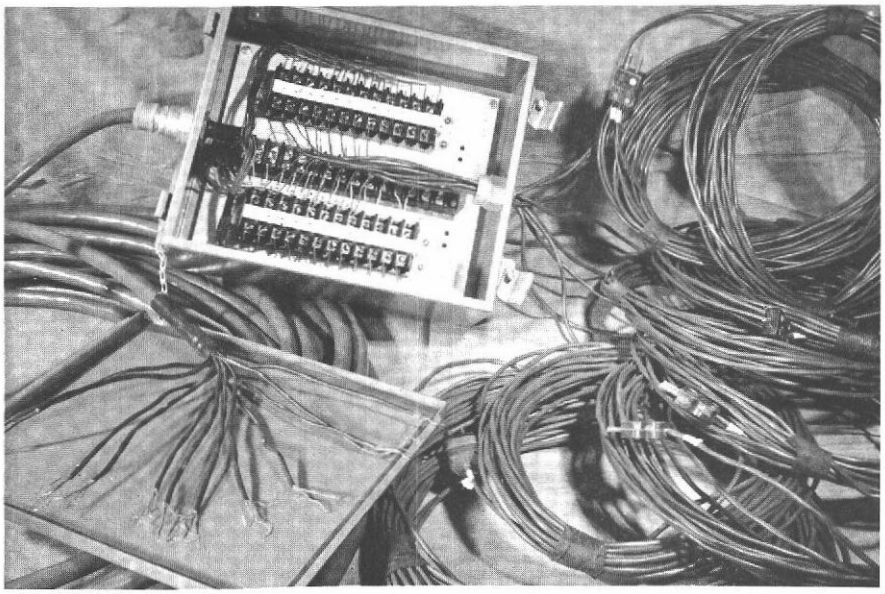

Fig. 2-4. (right) Thermocouple cable and connector system. Copper and constantan terminal strips are used to connect the individual signal pairs to a 12-pair, multiple-conductor cable that is 75 m long. All circuits are shielded.

Fig. 2-5. (below, left). Psychrometers deployed for Bowen ratio estimates of evapotranspiration. Measurement heights are at 40 and 80 cm.

Fig. 2-6. (below, right). Energy balance instrumentation above a young Pinus contorta forest 7 m in height. The tower supports instruments for measurement of wind direction, the radiation exchange components, and 6 levels of temperature and humidity.

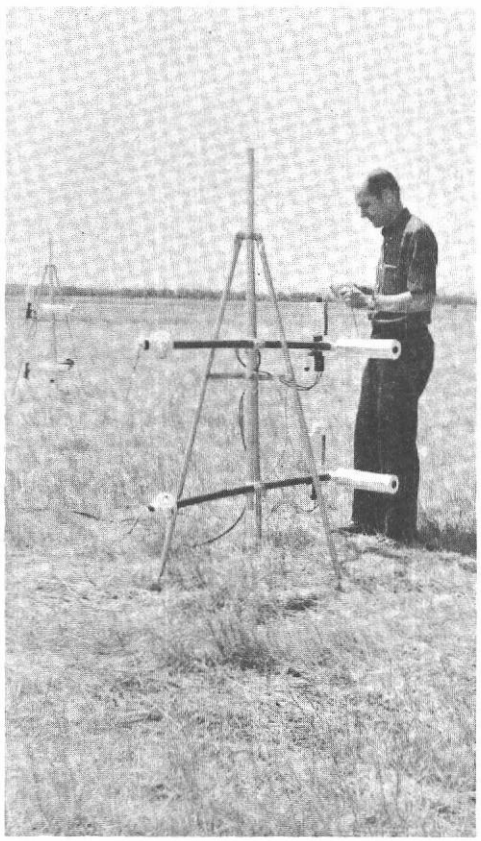

such as forest, or a marsh.

The equipment has generally operated well in the field measurement program. Our use has emphasized high precision measurements over short periods that extend to perhaps 10 days in length, with maintenance taking place as needed between sampling periods. The paper-tape punch has given difficulties in the field, and broken solder joints in the electronic equipment have also given periodic problems. This latter problem appears related to movement of the laboratory from one site to another. It has also proven prudent to monitor a known input, such as from an ice-bath, to provide a continual check on the stability of both the temperature measuring system and the digital recorder.

No particular difficulties have been encountered in operating from portable generators in the field. The recorder used here is rather insensitive to fluctuations in line voltage and/or frequency. However, the performance is noticeably improved if the entire system is grounded at one point, usually near the generator for convenience, in accordance with standard low-level circuit practice.

Ease in data handling is one of the major advantages offered by digital data recording equipment and most computer centers can routinely process the output of the recorders. However, we have found it necessary to edit the data to insure an error-free record before applying transformations. The errors encountered have generally been related to performance of the sensors rather than to problems in the recorder. A visual inspection of the transformed data is also made before the integration and analysis programs are applied. Digital recorders do offer many advantages in speed, accuracy, and data handling convenience. However, continued care and attention has been found to be essential in both the collection and the processing of the environmental data.

2.1.7 Summary.

An environmental data acquisition system developed at Oregon State University includes a recorder, a mobile laboratory, a power source, sensors, signal cables, and instrument supports. The operation and configuration of the system is described.

The self-contained system combines mobility with an exceptionally high degree of precision. The heart of the system is a digital recorder with up to 100 analog inputs at a maximum rate of 5 per second; the maximum resolution is 0.1 microvolt. The recorder also contains a unique, expandable, 12-channel digital scanner that is designed for anemometers and other sensors that have a pulse output.

The sensors measure radiation, temperature, water vapor concentration, conductive heat flux, and wind run. The system cables, connectors, towers and instrument supports are designed for use in adverse weather, and for ease and flexibility in installation. Two men can set up the system in half a day for a typical energy balance study. The system is truck-mounted in an 8x12-foot, insulated van.

The design of this particular system is well-adapted for environmental studies that require high resolution measurements over the relatively short period of 5 to 10 days. The components and their configuration have been intensively field tested over several field seasons in studies of radiation exchange, seedling environment and the forest energy budget. The present form of our system should be of interest to others concerned with the collection of environmental data.

2.1.8 Equipment Source Footnotes

Note: Sources are cited for reader's convenience and no endorsement is implied.

1. Onan Series LK. Onan Corp., 2315 University Ave. S. E., Minneapolis, Minnesota 55414.

2. Vidar 5202 D-DAS. Vidar Corp., 77 Ortega Ave., Mountain View, California 94040.

3. Model CM-2. Kipp and Zonen, Delft, Holland.

4. Model E-1. Swisstecco, Pty, Ltd., 26 Miami St., Hawthorne, Victoria, Australia.

5. Pace Engineering Co., 13035 Saticoy St., North Hollywood, California 96105.

6. NIL HFIC Disk. National Instrument Laboratories, 12300 Parklawn Drive, Rockville, Maryland 20852.

7. Wind Profile System. Thornthwaite Associates, Route 1, Centerton, Elmer, New Jersey 08318.

8. Miniature Side-mounting Connectors JF-2P-2S-AB. Winchester Electronics, Main and Hillside Aves., Oakville, Connecticut 06779.

9. Amphenol Connector Division, Amphenol-Borg Electronics Corporation, 1830 South 54th Ave., Chicago, Illinois 60650.

10. Thermo-electric Corporation, Saddlebrook, New Jersey 07662.

11. Hoellander Mfg. Co., 3841 Spring Grove Ave., Cincinnati, Ohio 45223.

12. Rohn Mfg. Co., 310 Quincy St., Reno, Nevada 89502.

2.1.9 Literature Cited.

Allen, L. H. 1970. An operational system for (1) sampling and sensing micrometeorological elements, and (2) logging and processing micrometeorological data. In: Powell, J.M., and C. F. Nolasco (Eds.), Proceedings, Third Forest Microclimate Symposium, Canadian Forestry Service, Calgary, Alberta. Pp. 91-116, March 1970.

Backlund, B. and K. Perttu. 1971. System for data logging at short intervals and processing of data about plant growth and climate. Royal College of Forestry, Stockholm. 47 pp.

Buckley, D. J. 1969. Digital data acquisition systems. Engineering Spec. 6901. Engineering Research Service, Canada Dept. Agriculture, Ottawa.

Clayton, W. H., and J. D. Merryman. 1960. Design of the mobile micrometeorological stations employed on Project Greenglow. Final Report AF19(604)-04562. Dept. Oceanography and Meteorology, A & M College of Texas, College Station, Jan. 1960. 83 pp.

Fritschen, L. J. 1970. Particular problems of instrument design and overall development of systems for agricultural and climatological stations. Meteor. Monogr. 11:346-351. October 1970.

Fritschen, L. J. and C. H. M. van Bavel. 1963. Micrometeorological data handling system. J. Appl. Meteor. 2:151-155.

Gay, L. W. 1970. Energy balance estimates of evapotranspiration. In: Water Studies in Oregon. SEMN WR 012.69, pp. 17-39. Oregon Water Resources Research Institute, Corvallis, January 1970.

Gay, L. W. 1972. On the construction and use of ceramic wick thermocouple psychrometers. In: Brown, R. W., and B. P. Van Haveren, (Eds.). Psychrometry in Water Relations Research. Utah Agric. Expt. Station, Logan. (In Press).

Gay, L. W., and H. R. Holbo. 1970. A counter and interface for use with digital data acquisition systems. Proceedings: Conference on Electronic Instrumentation. Pp. 91-115. Departments of Physics and Electrical Engineering, University of Idaho, Moscow, Idaho. May 22-23, 1970.

Gay, L. W., R. L. Stebbins, and R. M. Black. 1971. The effect of spray irrigation on plum temperatures. Northwest Sci. 45: 200-208.

Lourence, F. J. 1967. Instrumentation development and calibration. Chapter II, Part III, Final Report, USAEC Contract No. DA-02-086-AMC-0447(E), pp. 15-27. University of California, Davis.

Lourence, F. J., and W. O. Pruitt. 1969. A psychrometer system for micrometeorology profile determination. Jour. Appl. Meteor. 8:492-498. August, 1969.

Reifsnyder, W. E. 1963. Techniques of measuring, recording and processing micro-meteorological variables in forest energy-budget studies. Symposia on Water Balance of the Soil and forest Meteorology. Pp. 115-120. Meteorological Branch, Dept. Transport, Canada. Toronto, July 13, 1962.

Valli, V. J. 1966. A biometeorological data logging system for agricultural research. Ga. Ag. Expt. Sta., Univ. Ga., Mimeo. Series N.S. 244. January 1966. 18 pp.

2.2 The Ceramic-Wick Psychrometer*

The temperature and the concentration of water vapor are two parameters that define the state of the atmosphere at a point. Measurements may be crude for climatological purposes, but they must necessarily be precise for micrometeorological profile analyses that seek to evaluate the transfer of energy at the earth-atmosphere interface.

Wet-bulb psychrometry has remained the most common technique for evaluating atmospheric moisture under the conditions normally encountered in micrometeorology. A variety of designs has proven useful in the field. In 1967, Fred J. Lourence described a new thermocouple psychrometer that combines to an unusual degree the attributes of precision, simplicity, ruggedness, and portability (Lourence, 1967; Lourence and Pruitt, 1969). A unique feature of this psychrometer is a porous ceramic wick as the wet-bulb element. The simplicity of construction of this design also enhances its application in micrometeorological studies. Surprisingly, despite its many attractive features, confirming reports on the use of the Lourence psychrometer have not appeared elsewhere.

The objectives of this section are to describe my experience in the construction of the Lourence psychrometer, along with observations on its use in the field. Some modifications have been made in the original design. These, however, are primarily for convenience and to provide flexibility in use.

2.2.1 The Psychrometer Design.

The specific design and construction details of the Lourence psychrometer have been described elsewhere by Lourence (1967), Lourence and Pruitt (1969) and Gay (1972), so only a summary need be given here to point out modifications introduced in my construction.

The basic structure is of standard, 1-inch, polyvinyl chloride (PVC) pipe. This material is light and strong, and the fittings that are available make friction joints that can easily be disassembled for servicing. The PVC pipe that connects the psychrometer and the aspiration fan also serves as the main support arm for the instrument. Figures 2-3, 2-5, and 2-6 show a number of psychrometers deployed in the field. The water reservoirs are mounted vertically, and the dry- and wet-bulb elements are contained within a cylindrical sunshield, oriented horizontally.

The dry- and wet-bulb design is straightforward. The arrangement and dimensions of Lourence's thermopile are shown in Figure 2-7. The thermopiles in our unit are made of 36-gauge, copper-constantan thermocouple wire with nylon insulation on each wire, and an over-all nylon sheath. The two-junction, dry-bulb thermopile is referenced against a heated (65°C) junction that may be located some distance from the psychrometer. A second thermopile, but containing four junctions, is wound between the dry bulb and the wet bulb, so that the wet-bulb depression can be read directly. All thermocouple wires run within the tubes that support the dry bulb and the wet bulb. The cables leading from each psychrometer thus include two copper-constantan pairs to connect the dry-bulb junctions with the reference junction, and one copper-copper pair to carry the output signal from the wet- and dry-bulb thermopile. The signal cables have been described in paragraph 2.1.4, and pictured in Figure 2-4.

*Based on a paper by L. W. Gay, presented to the Symposium on Psychrometry in Water Relations Research, Utah State University, Logan, Utah, March 17-19, 1971.

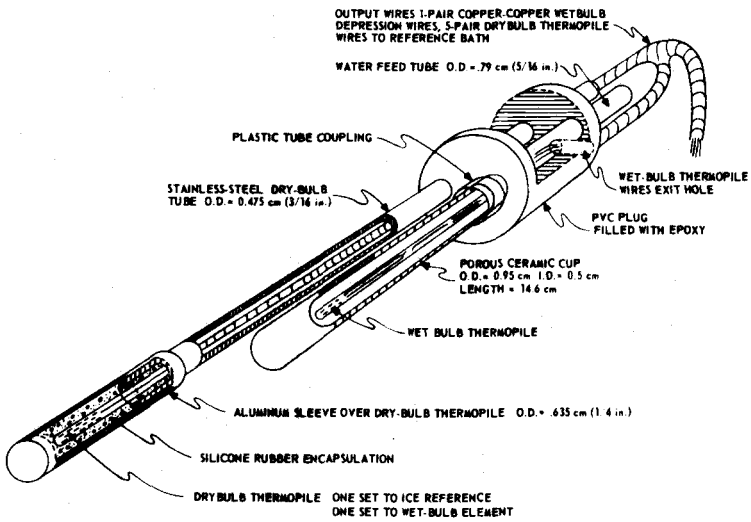

Figure 2-7. A cutaway view of Lourence's ceramic-wick design (from Lourence, 1967).

The respective outputs of my dry bulb and wet bulb are about 80 and 160 microvolts per degree Celsius, as compared with Lourence's output of 200 microvolts per degree Celsius. This reduced output is a factor to be considered when selecting a recorder for the psychrometers. The reduction in junctions in my psychrometers is not intended to make construction easier, but rather to facilitate interconnection between the dry-bulb thermocouples and the system reference junction.

The thermocouple junctions must be carefully insulated from each other. This sometimes becomes a problem in the wet-bulb element. The most satisfactory technique is to insulate each junction separately with a short length of the nylon insulation sheath; this sheath is then fused with a match (Tanner, 1963) to give a water-resistant seal. The junctions can be bundled into one compact mass using an overall sheath of shrinkable tubing. We prefer not to use silastic sealing compounds on the wet-bulb thermopile because of possible contamination of the porous ceramic wick. The dry-bulb junctions are encapsulated with epoxy within a 0.79 cm (5/16 in.) stainless steel sleeve.

The porous ceramic wet-bulb element is connected directly to the water reservoir by tubing. The water reservoir is an integral part of the psychrometer in our construction and its 150 ml capacity is adequate for daily operation in the field. Because it is mounted above the element, a positive head is applied at all times. The ceramic wicks are easily removed for cleaning or replacement; they are inexpensive and readily available.[1]

The dry-bulb time constant (time to achieve about 63 percent of a step-change in temperature) averaged 58 seconds. This compares with a wet-bulb time constant of 72 seconds. Surprisingly, these constants are only about 1/3 as large as those reported by Lourence and Pruitt (1969) despite our larger (0.79 cm) dry-bulb sleeve. The phase relation between the dry and wet elements was judged satisfactory for the evaluation of time-averaged temperature and vapor profiles.

The entire psychrometer unit can be removed from the main support pipe. The thermocouple elements also unplug from the horizontal radiation shield to expose the ceramic wick for inspection or replacement. The simple but effective radiation shield is constructed of polystyrene foam, 2.54 cm (1 in.) in thickness; the outer surface is covered with aluminized mylar tape for maximum rejection of radiant energy (Fuchs and Tanner, 1965). The cylindrical shield is mounted on a 30.5 cm (12 in.) length of PVC tubing that has been lined with aluminum foil tape to minimize radiative transfer to the cooled wet-bulb element. A similar foam shield also reduced heating and cooling of the water reservoir. Connectors for the signal cables are mounted beneath the water reservoir.

Aspiration can be achieved with a variety of suitable blowers. I used surplus 28 VAC squirrel-cage blowers with a #2 housing, cemented to a PVC pipe flange which serves as a convenient connector. Twenty volts maintains an aspiration velocity of 6 m/s which is well above the required minimum of about 4 m/s. Voltage drop along the blower power cable must be considered with long cable runs. The low voltage reduces the shock hazard to personnel working with the psychrometers in the field.

In summary, the psychrometer construction described here differs from Lourence's

[1]R&J Ceramics, 2552 Cottage Way, Sacramento, California 95825. Approximate cost in 1970: $8 per dozen.

design in the following respects: use of a lightweight, foam, radiation shield; an integral water supply with a positive head; connectors for the dry-bulb and wet-bulb circuits; fewer circuits in each thermopile (a qualified disadvantage); and a larger dry bulb for a longer time constant.

2.2.2 Reference Junction Considerations

An electrically heated reference junction offers several advantages over the traditional ice-bath reference. The major advantages are: the ability to operate for extended periods in a field environment where an ice supply and requisite cleanliness may not be available; and the ease with which thermocouple circuits may be combined, terminated, and changed, by the gold-plated screw terminals provided on the heated junction. The disadvantages include the need for power, and possibly some reduction in reference temperature stability.

The Pace reference junction with a capacity of 48 separate, shielded copper-constantan thermocouple circuits will accomodate up to 12 psychrometers. The cost of such a junction is about $500. The nominal operating temperature of 150°F can be set down to 149°F, which is conveniently equal to 65°C. The junction heater draws a maximum of 180 watts at 120 VAC. The specifications are $\pm$0.05°C for long-term stability and for the spatial variability on the terminal board. Our experience verifies this value for long-term stability, but suggests that the spatial variability is no more than 0.01°C.

Such a heated junction can be enclosed in an insulated, weather-proof case and operated near the psychrometers, with only copper-copper lines necessary to carry the signal back to the recorder. However, the reference temperature has achieved maximum stability when housed in the air-conditioned laboratory near the recorder. This sometimes requires a long run with the thermocouple cable and therefore special attention must be given to the thermocouple cables and connectors.

2.2.3 Temperature and Vapor Pressure Calculations

The dry-bulb temperature (T_d) and the wet-bulb temperature (T_w) must be determined to evaluate the vapor pressure of the air (e) with the psychrometer.

The dry bulb is referenced to a heated (65°C) junction, so the resulting signal is negative for all dry-bulb temperatures below 65°C. The electrical output of the dry-bulb thermopile (E_d), expressed in millivolts, can be converted to temperature (in °C) by the following cubic equation:

$$T_d = [(0.0438E_d/n_d - 0.4377)\ E_d/n_d + 22.7]\ E_d/n_d + T_r \qquad [2\text{-}1]$$

where n_d is the number of thermocouple circuits in the dry-bulb thermopile, and T_r is the temperature (in °C) of the reference junction. In my system, $n_d = 2$ and $T_r = 65$°C. Equation [2-1] is a regression relation derived from the standard copper-constantan output tables, but based on a reference temperature of 65°C instead of 0°C.

The wet bulb is referenced against the dry bulb, and, because the wet bulb is ordinarily at a lower temperature than the dry bulb, the output of this thermopile is negative. The electrical output of the wet-bulb thermopile (E_w), expressed in millivolts, can be combined with the dry-bulb output to evaluate wet-bulb

temperature (°C) by a modification of Equation [2-1]

$$T_w = [(0.0438\ (E_d/n_d + E_w/n_w) - 0.4377)\ (E_d/n_d + E_w/n_w + 22.7]$$
$$(E_d/n_d + E_w/n_w) + T_r \qquad [2\text{-}2]$$

where n_w is the number of circuits in the wet-bulb thermopile. In my system, $n_w = 4$.

The dry-bulb and wet-bulb temperature may thus be calculated for a system of copper-constantan thermopiles with a heated reference junction, if the number of thermocouples is known for each thermopile, an electrical output is measured, and the reference temperature is known or measured. Before applying Equation [2-1], however, one should confirm that the copper-constantan wire conforms to the standard output tables.

The vapor pressure of the air (in mb) can be calculated from T_d and T_w (in °C), using the empirical psychrometric equation

$$e = e_s - Ap(T_d - T_w) \qquad [2\text{-}3]$$

where e_s is the saturation vapor pressure (mb) at the wet-bulb temperature T_w (°C), A is a psychrometric constant, and p is the atmospheric pressure (mb). The psychrometric constant varies with temperature, aspiration speed, and radiation load. Lourence and Pruitt (1969) present convincing experimental evidence that an appropriate expression for this constant in their psychrometer is

$$A = 6.97 \times 10^{-4}\ (1 + 0.00115\ T_w). \qquad [2\text{-}4]$$

Equation [2-4] is of the same form as the generally accepted constant for mercury thermometers when the aspiration velocity is between 4 and 10 m/s (List, 1966, p. 365), but it is about 5.5 percent greater. Examination of Lourence and Pruitt's experimental data indicates that the measured gradients of vapor pressure above a surface are little affected by the choice of either psychrometric constant. The absolute values are shifted somewhat, however.

Standard tables can be used for evaluation of the temperatures, and the vapor pressure as linear interpolation will be adequate for many purposes. An adjustment must be made with standard psychrometric tables (List, 1966) to account for the psychrometric constant in Equation [2-4]. The reduction of a large number of observations, however, is most easily done in the computer.

The value of e_s (in mb) in Equation [2-3] can be calculated conveniently by Murray's (1967) formulation of Teten's approximation

$$e_s = 6.1078 \exp\ (17.2693882\ T_w/\ (T_w + 237.30)) \qquad [2\text{-}5]$$

for all $T_w > 0$°C. Equation [2-5] is within 0.1 percent agreement of the internationally accepted Goff-Gratch formulation for temperature above freezing. The constants in Equation [2-5] change if frozen wet bulbs are to be considered, but such modification is not appropriate for the Lourence psychrometer because freezing destroys the ceramic wicks.

The vapor concentration of the air (e), expressed as partial pressure of the water vapor in mb, is thus calculated from a combination of Equations [2-3],

[2-4], and [2-5], once T_d and T_w are known in °C.

2.2.4 Calibration

The philosophy adopted here in calibration is that the differences between instruments are more important than the absolute values. In other words, sensitivity is of more importance than is absolute accuracy. This is important because such factors as the connectors, amplifier drift, and reference junction offsets introduce bias into the data. The measured differences between instruments will not be affected, however, if the same bias is applied to each of them.

The relative accuracy of the dry-bulb sensors can be determined easily with a stirred bath and a temperature standard. The absolute differences among twelve dry-bulb sensors, as measured with the digital recorder, were around 0.01°C.

Vapor pressure calibration is not as convenient, for observations must be made with the psychrometers under aspiration. The aspiration requirement makes it difficult to obtain a suitable source of air with uniform temperature and moisture properties, to make relative comparisons of one instrument against another. Further, standard instruments required to assess absolute accuracy are lacking.

Absolute comparisons were made in the laboratory between the Lourence psychrometer and the "standard" Assmann psychrometer. The Assmann psychrometer is rather crude; its general acceptance as a standard appears related more to the ease in standardizing construction than to the accuracy of its readings. The comparisons established that absolute values determined with the ceramic wick psychrometer agreed with the Assmann measurements, but with substantial scatter.

Next, comparisons were made of three psychrometers, operated as a closed system within a climate-controlled growth chamber. Over a range of temperature between 6°C and 25°C, dry-bulb sensors that were within 0.01°C of each other in the stirred bath tests, diverged as much as 0.1°C. With vapor pressures ranging from 6 to 15 mb, the differences among Lourence psychrometers in this chamber were as large as 0.1 mb. These differences, however, appear to result from insufficient mixing within the chamber rather than from differences among instruments. Other available evidence suggests that the accuracy of the instrument is greater than indicated by these tests.

Let us examine indirect evidence of the precision in the psychrometers under the conditions of our pumice test site on September 4, 1969. The mean air temperature and vapor pressure profiles are plotted in Figure 2-8 for the hour 1030-1130, Pacific Daylight Time, as measured at 20, 40, 80, 160, 240 and 320 cm above the surface. The hourly means are based on 12 samples made at 5-minute intervals. Both profiles show a linear decrease with the logarithm of height, and the wet-bulb depressions were about 7°C under the conditions of measurement. The linearity and similarity of the temperature and vapor profiles indicate precision of around 0.05°C and 0.05 mb.

The necessity of replicating humidity observations is well illustrated in similar data collected at the same site on August 13, 1969 and plotted in Figure 2-9. The mean air temperature profiles for the 1730-1830 hour are much warmer than in the previous example, although the decrease with the logarithm of height again approaches linearity. The wet-bulb depressions were also greater, and averaged some 15°C during this hour.

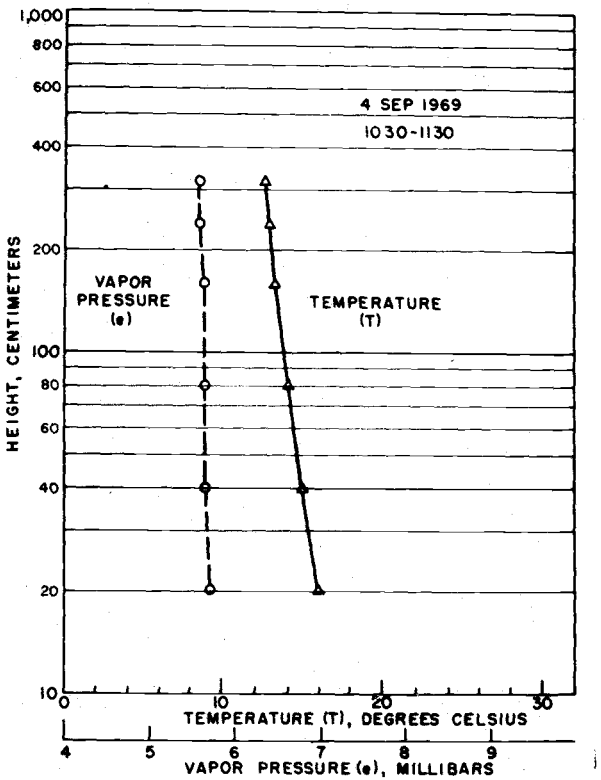

Figure 2-8. Mean temperature and vapor profiles at the pumice test site. Heights of measurement are 20, 40, 80, 160, 240 and 320 cm.

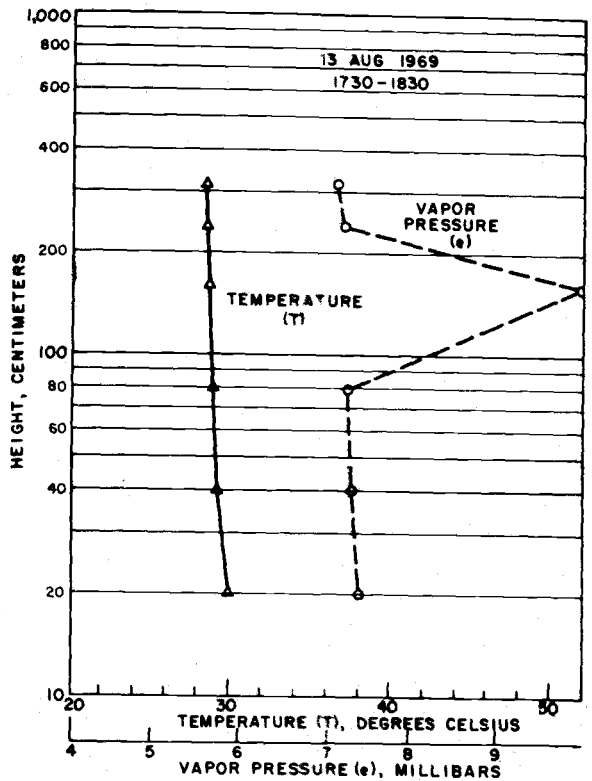

Figure 2-9. Mean temperature and vapor profiles at the pumice test site. Heights of measurement are 20, 40, 80, 160, 240 and 320 cm.

Examination of the vapor pressure profile, however, clearly reveals that the 160 cm psychrometer is in error. In practice, readings from this malfunctioning instrument would be deleted before an analysis was begun.

Figure 2-9 confirms that psychrometer measurements must be replicated to assure that the vapor measurements are valid. Precision operation of a wet-bulb psychrometer is not routine, even with a good system and the best of intentions. Profile measurements at three or more heights do provide a basis for acceptance or rejection of a given vapor measurement. If measurements are made at only two levels, as required in a Bowen ratio analysis, then several replications should be made.

Our concern is with biased readings, rather than random errors of measurement. The bias normally encountered in wet-bulb psychrometry tends to increase the estimate of vapor concentration, and in general, the instruments with the lowest vapor concentrations may be presumed to be operating the most satisfactorily.

2.2.5 Field Use

Bubbles will sometimes develop for no apparent reason in the water supply tube leading to the porous ceramic wick; this is probably what caused the error evident in Figure 2-9. Boiling the distilled water to remove gas has helped minimize this problem. Some of the ceramic tubes appeared to be less porous than others; the wall thickness, for example, varied from lot to lot. We simply discard ceramic elements that appear to have excessively thick walls.

Although no gradual deterioration of the ceramic wicks has been apparent, we ordinarily change the elements about every 3 days. Catastrophic failures can occur in operation. Because of the high elevation of the experimental sites in central Oregon, the wet-bulb temperature often dropped below 0°C on clear summer nights, and the ceramic elements froze and cracked. Our experience confirms that this design, despite its other advantages, is not suitable when wet-bulb temperatures fall below 0°C.

2.2.6 Summary

Psychrometers for micrometeorological research should be sensitive, durable, portable and simple to operate. In 1967, Fred J. Lourence of the University of California-Davis reported on his development of a thermocouple psychrometer that possessed these characteristics to an unusual degree. The unique feature of Lourence' design was a ceramic wet-bulb element that showed promise of eliminating the wick-feed problems not explicitly brought out that are commonly encountered in wet-bulb psychrometry.

This paper described our construction and tests of the Lourence psychrometer, along with observations on performance during two field seasons. Our minor modificatio of Lourence's original design include the addition of an integral water supply and a new sunshield. Also, our construction has fewer thermocouple junctions and a heated reference, to enhance the ease with which the psychrometers can be combined into a measurement system handling up to 12 psychrometers. The system components include the psychrometers, the heated reference junction, cables and connectors, instrument supports and the recorder.

Our experience confirms that the ceramic wet bulb design of Lourence offers

advantages of simplicity in construction and reliability in use. When used with care and appropriate recording equipment, the psychrometer can define the gradients of temperature and water vapor concentration in the atmosphere with precision approaching 0.05°C and 0.05 mb. This is adequate performance for the evaluation and analysis of mean profiles within the atmospheric boundary layer.

2.2.7 Literature Cited.

Fuchs, M., and C. B. Tanner. 1965. Radiation shields for air temperature thermometers. J. Appl. Meteor. 4:544-547.

Gay, L. W. 1972. On the construction and use of ceramic-wick psychrometers. In: Brown, W. R., and B. P. Van Haveren, (Eds.). Psychrometry in Water Relations Research. Utah Agric. Expt. Station, Logan. (In Press).

List, R. J. 1966. Smithsonian Meteorological Tables. 6th rev. ed. Smithsonian Misc. Coll.: 114, Publ. 4014, Smithsonian Institution, Washington, D. C. 527 p.

Lourence, F. J. 1967. Instrumentation development and calibration, p. 15-27, Chapter II, Part III, Final Report, USAEC Contract No. DA-02-086-AMC-0447(E). University of California, Davis.

Lourence, F. J., and W. O. Pruitt. 1969. A psychrometer system for micrometeorology profile determination. J. Appl. Meteor. 8:492-498.

Murray, F. W. 1967. On the computation of saturation vapor pressure. J. Appl. Meteor. 6:203-204.

Tanner, C. B. 1963. Basic instrumentation and measurements for plant environment and micrometeorology. Soils Bull. 6. Univ. Wisconsin, Madison.

2.3 A Counter With Interface For Use With Digital Data Acquisition Systems

Digital data loggers are now commonly used for periodic recording of analog data from a variety of transducers. However, the less expensive data loggers are not designed to handle inputs that are already coded in digital form. This limitation may pose vexing problems. For example, in meteorological studies it is often necessary to record data both from digital transducers, such as pulse-generating cup anemometers, and from analog transducers such as bridges and thermopiles.

The pulses generated by a digital transducer can be accumulated and recorded periodically. However, custom interfacing of available counters to the data system is expensive. We have therefore designed and constructed a suitable counter unit for this purpose, using TTL integrated circuit modules and printed circuits of our own design (Gay and Holbo, 1970). The counter consists of a signal conditioner, an accumulator unit, and an interface that allows the data to be recorded with a standard digital data acquisition system. The signal conditioning and interfacing circuits adapt the accumulators to our specific transducers and data system. Though the counter design is oriented to our requirements, its principles can readily be applied to similar problems involving other digital transducers and data acquisition systems.

The development of integrated circuits and their use as building blocks has greatly simplified the problem of designing digital equipment. We hope that our experience will encourage others to undertake construction of their own specialized instruments, particularly when they are not available commercially. In many cases, the favorable price differential between "shop-built" and commercial instruments will also enter into the decision of whether to build or to buy.

2.3.1 Digital Transducers.

Anemometers commonly used in micrometeorology yield a pulse train, rather than an analog, output. There are two reasons for the popularity of pulse output anemometers. The first is sensitivity. Friction of the pulse generator can be made appreciably less than that of analog signal generators and thus the accuracy will be enhanced at low wind velocities. The second is that a count of pulses over a time interval will provide an average wind velocity for the interval. This integrated average has important sampling advantages for measuring a parameter as variable as that of wind velocity.

The anemometer[2] in our system uses a photoresistor to minimize friction in the pulse generator. The anemometer support arm contains a small light bulb arranged so that a shutter connected to the anemometer shaft will alternately make and break the light beam incident upon the photoresistor. Several different circuits can be used to develop a pulse as the photoresistor cycles from low resistance in the light stage to high resistance in the dark stage. The shutter is arranged so that one revolution of the cups completes one light-dark cycle. The calibration of the cups is such that 10 Hz is the maximum pulse frequency expected; this corresponds to a wind velocity of 1455 cm sec^{-1}.

The characteristic of the anemometer that is important for our design is the relatively low frequency of 10 Hz or less. At these frequencies, four decades, or 9,999 pulses, would be ample capacity for 10 minute sampling periods. Another factor to be considered is the number of anemometers to be employed in a specific

study. Our experiments require as many as 12 anemometers.

Let us pause briefly at this point to consider alternatives to the electronic counter unit that we have constructed. We used electromechanical counters to totalize anemometer pulses in the past, and recorded the data on photographs. This is unsatisfactory in the long run because of data handling and collation problems. Another possibility is to use one of a variety of digital-to-analog converters in order to convert the pulse totals into an analog form acceptable to the standard data logger. However, our experimental measurements seek to distinguish small differences in wind velocity when the average may be quite large. The small percentage errors associated with analog-to-digital conversion may in such cases exceed loss of precision associated with the initial conversion to analog and the subsequent conversion back to digital form in the voltmeter. Our efforts have thus been directed toward accumulating the pulses and adapting the data logger to serve as the recorder.

There are several possible choices in type of counter. The maximum pulse frequency is well within the capability of stepping switches or other electromechanical counters. However, because of the advantages of size and versatility, we decided to construct electronic accumulators. The electronic accumulators were easily made compatible with our data logger.

2.3.2 The Counter and Interface Design.

Design of the counter unit took into account the relatively simple and inexpensive circuits available in TTL integrated circuit modules[3]. In addition, the counter was designed to be an external unit so that direct modifications would not be needed on the data logger.

Basically, the counter is placed between the data logger's digital voltmeter and the coupler. Upon command, the interfacing circuits "gate" the accumulator output into the coupler in place of the digital voltmeter output. The problem is primarily one of securing adequate control signals for the data gate in the interface and of organizing the appropriate accumulator, interface, and control circuits.

The operation of the counter unit can be explained with the assistance of the flow diagram in Figure 2-10. For simplification, the flow diagram shows the circuitry needed to accumulate and record one decade (0 to 9 counts) of pulse data. Additional decades could be cascaded onto the decade shown in the diagram; our accumulators actually have a capacity of four decades (up to 9,999 counts). Additional accumulators and their associated components can also be added. For simplicity, this will be discussed in the section on construction. Figure 2-10 also omits the level shift circuits that make the positive 5 volt logic of the integrated circuits compatible with the negative 15 volt logic of the data logger.

The pulse output from an anemometer is brought to its accumulator through an input board that uses a monostable multivibrator to shape the pulse. The monostable multivibrator is triggered by a high gain amplifier across a simple voltage divider circuit that utilizes the light (low) and dark (high) resistance of the photoresister in the anemometer to generate a shift in voltage sufficient to activate the accumulator. Since the pulse frequency is slow (less than 10hz), the time constant of the multivibrator can be made long, effectively filtering high frequency noise that would otherwise be a problem because of the fast response of the integrated circuit counting modules.

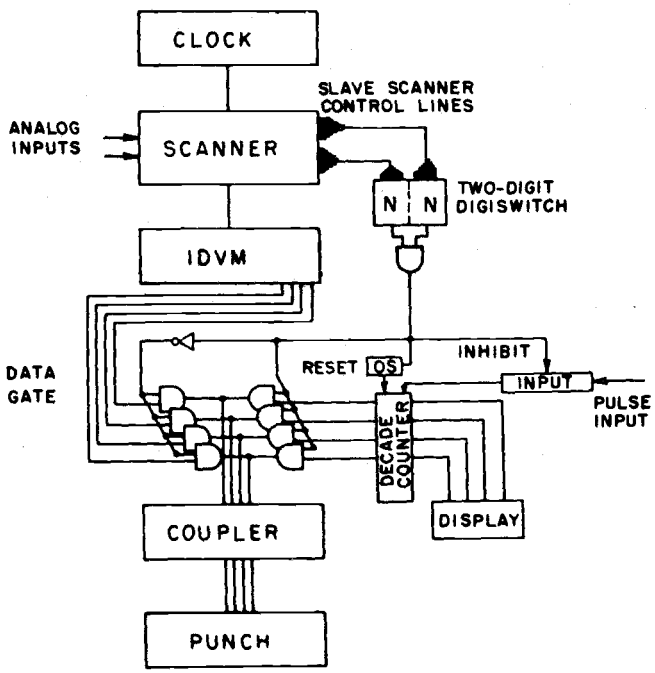

Figure 2-10. The basic circuit of the counter and interface, illustrated for one 1-decade accumulator. Circuit functions are described in the text.

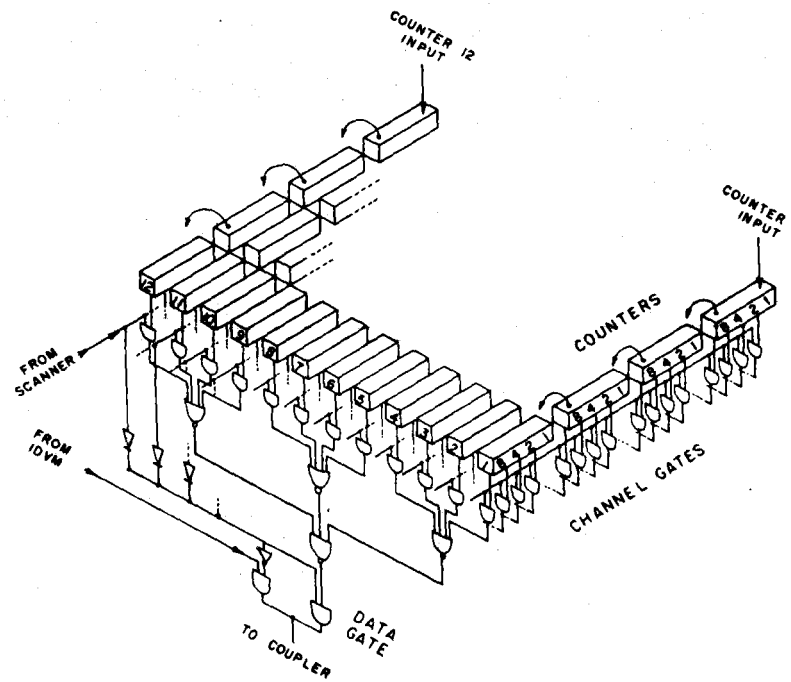

Figure 2-11. Block diagram of the counter and interface, arranged to totalize 4-decades of data from each of 12 anemometers. Circuit functions are described in the text.

The pulse totals are stored in the accumulator in binary-coded-decimal (BCD) form. Four lines must now be switched in order to transfer one digit of data. Thus the interface data gate consists of the four identical gates needed to pass a single digit representing one decade of data.

Let us now examine the control signals that are used to gate the accumulated pulse totals into the coupler of the data logger in place of the totals from the digital voltmeter. The main control signal is readily derived from the data logger's scanner. The reed relay scanner used in this system can handle up to 200 channels of analog data, providing sufficient relay modules are installed in the scanner. The relays in our recorder utilize 90 channels of this capacity, a number greater than is needed in our studies. In addition, this scanner could eventually be expanded to a maximum of 1000 channels if used with four slave scanners containing 200 channels each.

The timing logic and drive circuitry in the master scanner is transmitted to the slave scanners through three control cables, each containing 10 lines. The control cables represent units, tens, and hundreds in selecting the reed relay for a specific channel between 000 and 999. Since the slave scanners are not used, and will not be needed, on our logger, the slave scanner control lines provide an easily accessible signal for controlling the data gate in the interface of the counter unit.

The control signals are derived by feeding the units and tens control lines into the two-decade Digiswitch[4] and then into an AND gate. When the signal on the drive lines is coincident with the numbers set into the Digiswitch, the AND gate is activated. This change in state simultaneously "inhibits" the input circuit to block out pulses from the anemometer, "disables" the gate that has up to now passed output of the digital voltmeter, and "enables" the gate that passes the output of the decade counter. At this point we have effectively substituted the accumulated pulse total for the output of the digital voltmeter. This is fed into the coupler and recorded on tape. The timing logic of the data logger remains in command and advances the scanner to another channel after the coupler has processed the data. The slave scanner drive lines are then no longer coincident with the number preset into the Digiswitch so the inhibit signal is removed from the accumulator, the gate that passes the accumulator totals is disabled, and the gate that passes the digital voltmeter totals is enabled. At this time also, the delay circuit in the reset ONE SHOT fires, and the decade counter is reset to zero in preparation for totalizing counts until interrogated again during the next scan cycle.

The setting on the Digiswitch associated with each accumulator specifies when the data gate will be opened. It therefore addresses the channel in which the contents of a specific accumulator will be recorded. This feature provides for flexibility in recording. It is not necessary to record the different accumulators in sequence; each can be addressed to any channel in any order. The only requirement is that no two accumulators be addressed to the same channel.

Since the decades in each accumulator are substituted for those of the voltmeter, decade-by-decade, it is evident that there is a limit to the number of decades that can be cascaded in each accumulator. Our voltmeter transfers six decades of voltage data, and one decade each of polarity and decimal place. Thus our accumulators could be expanded to totalize 8 decades of data (up to 99,999,999 pulses) if we had interest in recording either for longer periods, or from a digital transducer with a higher frequency output.

The interface section of the counter thus functions as a digital scanner that scans among the various accumulator sections. Simplicity is achieved in this design by allowing the analog scanner to remain in control of the timing and channel selection logic. Use of the slave scanner drive logic and the Digiswitch gate allows flexibility in addressing the contents of a given accumulator to any specific channel for recording. Further, the unit is completely external to the data logger and so no modifications are needed on the standard logger components.

2.3.3 Construction.

A description of the counter unit construction must elaborate on the simplified operating principles described in the preceding section. We will attempt to discuss organization and construction without going into excessive detail on the individual circuits.

We simplified assembly of our counter by use of printed circuit boards. The boards are all 4.5 inches in width, of 1/16 inch glass epoxy, and fit a standard 44-pin edge connector. Forty circuit boards were produced locally[5] at a cost of about $2.75 each. Layout and photographic services were also provided by the board manufacturer; these services added an additional $200 to the cost of the boards. The prices given here and later are intended to serve as guides, as current prices may be somewhat higher or lower.

The accumulator is the heart of the counter unit. The 4-decade, BCD accumulator circuit board consists of four, decade-counter modules[6], cascaded to provide 4-decades of counting capacity (up to 9,999 counts). The decade counter modules are mounted in plug-in sockets to facilitate replacement. The 20 lines needed on each accumulator circuit board include the power supply (5 V), the count input, the reset line, ground, and 16 lines (4 per decade) that output the contents of the 4-decade BCD accumulator.

The price of the components varies somewhat according to quantity. However, the cost of one complete printed circuit board with 4 integrated circuit modules was about $27, excluding the connectors and amortization of the layout work. The cost of a commercial counter[7] with lower performance specifications was $27 per decade, or $108 total, in 1968 when we began our construction.

We decided not to display the contents of each accumulator separately. Cost of the necessary decoder and display modules is about $25 per decade, or $100 per 4-decade accumulator. In addition, the display panel would require more rack space than was conveniently available to us. We therefore used only one display module in our counter unit. The contents of any given accumulator can be displayed as desired through a rotary switch. A 4-decade cold-cathode neon tube display assembly cost about $130[8] complete with decoders. This unit will operate at integrated circuit logic levels.

The "stacking" of other accumulators into the basic circuit described in Figure 2-10 requires additional control circuitry in order to select the accumulator that is being interrogated. Let us refer back to Figure 2-10. The data gate drawn in the Figure must switch 4 lines between the 1-decade accumulator and one of the digits in the voltmeter. If the accumulator is cascaded to four decades, then as explained earlier, the data gate must switch 16 lines between the accumulator and the voltmeter. The inclusion of additional 4-decade accumulators means that the 16 output lines of each accumulator must be gated together, line for line.

These output line gates must be controlled so that only the contents of the desired accumulator will be presented to the data gate for transfer during interrogation.

The required gating among the accumulators can be achieved by inserting a "channel gate" between the accumulators and the data gate. The function of the channel gate can be seen in Figure 2-11, which depicts 12 4-decade BCD counters in a simplified schematic. The data gate is drawn just as it was in the flow diagram in Figure 2-10, except there are 16 data gates to handle the 16 output lines of the 4-decade accumulators instead of four to handle the four lines of the 1-decade accumulator. The added channel gates in Figure 2-11 are shown between the accumulators and the data gates. Though Figure 2-11 represents the counter that we have constructed, the same general scheme could be applied to counters containing other numbers of accumulators.

Let us now consider the operation of the channel gates. The scanner signal that passed through the Digiswitch to enable the data gate in Figure 2-10 must now perform an additional function: control of the channel gates. The "From Scanner" control line in Figure 2-11 comes from the Digiswitch that is associated with a particular accumulator. When one of these control lines is turned on, then not only is the data gate enabled, as before, but the channel gates will pass only the contents of the addressed accumulator.

The channel gates utilize AND-OR-INVERT gates to feed a POSITIVE NAND gate in order to achieve the desired gating among accumulators. Several configurations are possible. With 12 accumulators it is convenient to use three 4-wide 2-input AND-OR-INVERT gates[9] to feed one 3-input POSITIVE NAND gate[10].

The channel gate boards are separate from the accumulator boards. Each gate required in the counter configuration that we constructed cost about $1.50, so the total cost of the gates on one channel gate board is about $9. Note that one channel gate board is required for each line of data to be transferred, so sixteen channel gate boards are needed for four decades of accumulator capacity. The exact configuration of the gates on the board depends upon the number of accumulators to be installed in the counter.

The function of the channel gates is to select among the accumulators on each of the 16 data lines. Therefore, the channel gate boards are in effect oriented perpendicular to the plane of the accumulator boards as shown schematically in Figure 2-11.

The data gates make up the third type of printed circuit board. The data gates combine several functions: they serve as AND gates; they involve an inversion of the scanner control signal; and they must shift the logic of the channel gate output to a level compatible with that of the data logger. Consequently, the data gates incorporate a number of discrete components with some integrated circuit modules in order to function as shown in Figure 2-10 and 2-11. The data gates for our counter were wired on a printed circuit breadboard; the circuit diagram is available upon request.

The necessary level shift from +5 V in the integrated circuits to -15 V in the data logger was conveniently accomplished with a commercially made printed circuit board[11], costing $62.40 with connector. This level converter provides 16 circuits on one board. Thus only one converter is needed to handle the 16 lines that must be switched between the 4-decade accumulators and the digital

voltmeter.

We selected a well-regulated yet inexpensive 5 amp power supply[12] to provide the 5 volts needed for the integrated circuit modules. This supply cost $168, including a fast response crow bar for over-voltage protection. A simple 200 VDC power supply was constructed to provide the filtered, unregulated 10 milliamp current needed to operate the anodes of the neon tubes in the display module. In addition, we built a regulated, remotely sensing, 3 VDC power supply to provide the current needed to operate the lightbulbs in the anemometers' photoresistor chopper circuit.

2.3.4 Assembly.

The completed circuit boards and power supplies were assembled in a two-tier printed circuit board enclosure that took up 10.5 inches of rack space, with the power supplies mounted behind the printed circuit boards.

The upper tier of circuit boards contains the 12 accumulators, plus six additional boards with the signal conditioning and the level shifting circuits. The lower tier holds the 16 channel gate boards, plus four additional boards that make up the data gate. Thus 38 printed circuit boards are required in our counter design.

Each of the 12 Digiswitches on the front panel is associated with an accumulator. When the preset value on a Digiswitch is coincident with the number of the channel being scanned by the scanner unit of the data logger, that Digiswitch will pass a signal that causes the contents of the associated accumulator to be substituted in place of data from the digital voltmeter.

A 4-decade display module is also mounted on the front panel. The contents of any of the 12 accumulators can be examined by use of the rotary selector switch, which is the lower of the two switches below the display module. The other knob is the off-on switch.

There is no provision in our design for insertion of a dummy number directly into the accumulators for test purposes. We can, however, substitute an oscillator for the pulse inputs from the anemometers and fill all of the accumulators simultaneously. The performance can then be checked by inspecting to see that all accumulators contain the same number of counts.

The completed counter is shown mounted in the rack of the data logger in Figure 2-2. The configuration of the data logger is the scanner at the top, followed by the clock, digital voltmeter, coupler, counter and interface, and paper tape punch. The assembled logger is compact enough to readily transport to field experimental sites as part of the environmental data acquisition system. It now has the flexibility needed to record from the variety of transducers used in environmental measurement work. The basic counter design could be adapted to other data loggers and to other digital transducers.

2.3.5 Summary.

Our problems concerned the inability of standard data logging systems to record signals from both analog and digital transducers. We have designed

and constructed a simple counter that will accumulate pulses from a number of transducer The accumulators in the counter are interfaced to the data logger for recording. Though the design is adapted to our specific data logger and transducers, the principles could be applied to a solution of the same problem in other data logging systems.

Our counter unit was constructed primarily from TTL integrated circuit modules and our own printed circuit boards. The accumulator portion of the counter is organized to totalize four decades of data (up to 9,999 pulses) from each of 12 cup-anemometers. The pulse frequency of the anemometers is slow, 10Hz or less, compared to the 10MHz specifications of the IC counter modules. The contents of any 4-decade accumulator can be displayed on a cold cathode, neon tube display module.

The interface portion of the counter keeps the entire unit external to the data logger. The contents of each accumulator can be addressed to any channel of the data logger. The interface functions as a simple digital scanner so that accumulated pulse totals are transferred, recorded, and the appropriate accumulator reset to zero whenever the data logger scanner samples an addressed channel. For simplicity, the interface is controlled by the timing logic of the data logger's analog scanner.

The total cost of components in the completed counter and interface unit, including integrated circuits, boards, power supplies, display module, chassis, etc., was about $1600. This corresponds to $33 per decade and represents a considerable saving over a commercially manufactured unit. No allowance is made for labor in these costs, however. Despite the advantages of integrated circuits, a considerable amount of wiring is required to handle the transfer of digital information that is needed here. Thus a decision to manufacture a similar unit elsewhere would have to consider, in addition to cost, the availability of labor and the possibility of delays in completion while working out modifications in our design. An important but frequently overlooked advantage is often gained, however, by constructing instruments such as the one described here. This advantage is the increased competence that one obtains in electronic instrumentation, a competence that will pay dividends in the future, whether in the maintenance of old equipment or in the specification, design or construction of new equipment.

2.3.6 Equipment Source Footnotes.

1. Vidar Corporation, 77 Ortega Street, Mountain View, California 94040.

2. Thornthwaite Associates, Centerton, New Jersey.

3. Texas Instruments, Inc., P. O. Box 5012, Dallas, Texas 75222.

4. Digitran Co., Div. Becton-Dickinson & Co., 855 S. Arroyo Pkwy., Pasadena, Cal., 91105, Series 13000, Type 13031.

5. Custom Systems Associates, Inc., 1427 N. W. Davis Street, Portland, Oregon.

6. Texas Instrument SN7490N Decade Counter.

7. Digital Equipment Corporation Model K210 Counter.

8. Integrated Circuit Electronics, Inc., P. O. Box 647, Waltham, Mass. 02154

9. Texas Instrument SN7454N 4-wide 2-input AND-OR-INVERT gate.

10. Texas Instrument SN7410N Triple 3-input POSITIVE NAND gate.

11. Cambridge Thermionic Corp., 8703 La Tijera Blvd., Los Angeles, Calif. 90045 Cambion Type A 780-5704 Output Logic Level Converter, with connector 706-7029-01.

12. RO Associates, Inc., 917 Terminal Way, San Carlos, Calif. 94070. Model M605 Integrated Circuit Power Supply.

2.3.7 Literature Cited.

Gay, L. W., and H. R. Holbo. 1970. A counter and interface for use with digital data acquisition systems. Proceedings: Conference on Electronic Instrumentation. Div. Continuing Education, Univ. Idaho, Moscow. August, 1970, pp. 91-115.

3. DATA HANDLING AND PROCESSING

Digital data acquisition systems are now commonly used to collect environmental data in a form that is conducive to rapid, efficient handling and processing. A variety of techniques can be used to achieve this purpose, but the final choice is often dictated by factors beyond the control of an individual investigator. These factors include such things as the availability of specialized equipment and services in the university computer center.

Despite these external limitations, it appears appropriate to examine the general scheme applied here to the microclimate data collected with the environmental data acquisition system that we have assembled. Other helpful information on the handling and processing of environmental data has been published by Backlund and Perttu (1971) and by Brown and Rosenberg (1969).

3.1 Data Handling Philosophy.

Our experience confirms that visual checks are essential for adequate control of data quality. It is a difficult if not impossible task to develop an error-checking routine that will eliminate all possible errors from the data. Furthermore, it is not easy to develop data handling techniques that can be applied to all of the possible measurement configurations. Our data handling procedures have therefore evolved into a multiple-pass system in which certain operations are performed on the data on each pass through the computer. Some of the more common errors can be isolated by programing, but the other errors must be detected by inspection of the output before a subsequent processing operation is attempted.

This approach can be inefficient. Yet if carefully done, a balance can be obtained between excessive man-hours spent in contemplating the data on the one hand, and excessive computation costs incurred by machine checking for certain rare errors on the other. A visual check of the data appears to be the simplest and best way of detecting general errors.

3.2 Data Handling Facilities.

The data handling facilities include both the data acquisition system, and the facility that will be processing the data. One can exercise some degree of control over the data acquisition system, but this seldom affects the development of facilities in the computer center. The two groups of facilities must, of course, be compatible.

3.2.1 Recording Equipment

Two output devices are used on our Vidar data acquisition system: a paper-tape punch and a strip printer. The main data output is by punched paper tape. The strip printer was added to provide redundancy in event of occasional failures of the punch, and also to provide a convenient readout when calibrating and checking sensors in the field.

3.2.1.1 Paper Tape Punch. Our Vidar data logger is equipped with a Talley M420 paper tape punch. The output is the standard 8-level ASCII code. The major advantage of paper tape over magnetic tape is ease in verifying data at the time of collection. Also, paper tape does not deteriorate in

storage. We use a standard, opaque, oil-free tape. There have been no apparent problems with excessive punch wear because of the lack of oil on the paper tape.

The oil-free tape does shrink and swell with changes of relative humidity in the room containing the recorder. On a number of occasions, the paper tape has wedged in the throat of the punch block mechanism, because of excessive swelling at night. We now place a small light bulb near the tape roll to keep it dry.

The basic format of the data words was established by the factory design of the data system, although minor format changes can be easily made. The format used for a standard data word in our system is

NNPEOXXXXXXW

where: NN is a two-digit channel number; P is the number representing polarity (1 is +, 2 is -), E is the exponent that locates the decimal (10^{-E}, where $2 \leq E \leq 7$) between 10.0000 mV and 1000.00 V; O is not used in voltage measurements; X is a data digit; and W is an end-of-word symbol. The standard data word contains 12 digits. The punch speed is 60 characters per second, so the system is limited by the punch to a maximum recording rate of 5 channels per second.

The first data word punched into a scan sequence is a time word from the clock. The time word also contains 12 digits, but in the form

OOOODDDHHMMW

where: OOOO is not used for the time word; DDD is the day of the year ($1 \leq$ DDD ≤ 365); HH is the hour of the day ($0 \leq$ HH ≤ 23); and MM is minutes ($0 \leq$ HH ≤ 59).

The data punched onto the paper tape thus consists of a number of scan sequences; each sequence begins with a time word and continues with a succession of data words. Each scan is identified by the time at which it was initiated and each observation by its channel identification number to facilitate data processing.

3.2.1.2. Strip Printer. The system also drives a Mohawk Data Sciences M812D-10 printer with 10 columns of data. The model used here is full rack-width, but only 13.1 cm (5 3/16 inches) high. It has a maximum speed of 12 lines (data words) per second, although the Vidar recorder used here is limited to 5 data words per second. The printed strip, much like an adding machine tape, is not convenient to read, but such a printer is generally faster than page format models which must print each digit sequentially.

3.2.2. Processing Facilities.

Data processing facilities at Oregon State University are within the Computer Center, established in 1965 as a separate organizational unit to serve as a focal point for computer-related activities on the campus.

A Control Data Corporation 3300 computer system provides the primary support for computational services. A PDP-8 satellite computer serves on-line to the CDC 3300 to facilitate operation of a time-sharing "OS-3" system of 180 remotely located online consoles. The time-sharing system provides

convenient access to the capabilities of the CDC 3300 computer. The Center also has a Calcomp plotter which has proven useful to us for inspection of data and analysis. Other facilities are described in detail in a series of Computer Center bulletins.

Paper tape is no longer commonly used in our Computer Center, and we have therefore encountered recurring problems in transforming the paper tape into a computer-compatible magnetic tape. A variety of conversion devices have been used for this purpose. At present, the PDP-8 reads the paper tape and writes onto a magnetic tape which is subsequently used as input to the CDC 3300.

3.3 Data Processing Routines.

The function of the various programs in our multiple-pass system will be described. Copies of individual programs can be supplied upon request. The normal sequence of events in our data processing includes a check and listing of the raw data, editing of errors, transformation of the raw data into engineering units, integration of transformed data, plotting of integrated data, computation of specific energy budget analyses, and plotting of analyses.

3.3.1 Checking, Listing and Editing of Raw Data

Two passes are normally used in initial processing: TAPE 1 and TAPE 2.

3.3.1.1 TAPE 1 program converts time records (time records consist of a time word followed by up to 100 instrument readings) from an original saved file into a new saved file and provides a line printer listing of this new file. The program checks for errors in the data and writes on the new file the character "x" in place of any original character which is in error or cannot be understood. A diagnostic message is given for each error found.

Input: A magnetic tape file created from the original paper tape.
Output: (1) A saved file with errors printed as "x"'s. One record in the file represents one time record.
(2) A listing of the saved file.
(3) A list of diagnostic messages.

3.3.1.2 TAPE 2 program corrects the errors found by using TAPE 1. The program reads, from a saved file specified by the user, the data which has already been processed by TAPE 1. Then a list of corrections is read from another saved file or from cards, and a new saved file with corrected data is created. A listing of this new, corrected file is also provided.

Input: (1) A saved file (data that has been processed by TAPE 1).
(2) A list of corrections to be made.

Output: (1) A saved file of corrected data.
(2) A listing of the new saved file.

3.3.2 Transformation into Engineering Units.

GAYTRAN performs calculations using time records that have been

corrected by program TAPE 2 and using input parameters that are read from a saved file or from cards. With these input parameters, the user specifies the name of the saved file of corrected time records, the instrument numbers for each calculation and the transformation equations and constants to be used in each calculation. The user may request a listing of all input parameters and also that the calculated values be saved under a specified file name for future use.

Input: (1) A saved file of corrected data (output from TAPE 2).
(2) A file or cards of parameters

Output: (1) A listing of calculated values by time record (w/input parameters if desired).
(2) A saved file of calculated values (if desired).

3.3.3. Integration of Transformed Data

The integration procedure may include several steps. The first integrates, the second lists, and the third plots the data.

3.3.3.1. INTEG1 integrates in hourly intervals from half-hour to half-hour. The program uses as input the calculated values from the GAYTRAN program. A file or card deck with input parameters which specify the input file name, output file name and the number of each type of instrument present on the input file is also required. The results are listed and a saved file of the results is created.

Input: (1) A saved file of calculated values from GAYTRAN.
(2) A file or card deck w/input parameters for each file to be integrated.

Output: (1) A listing of the hourly results.
(2) A saved file of the results.

3.3.3.2. LISTING provides a line printer listing of hourly integrated data for any number of instruments. The program requires as input a saved file of integrated data (from INTEG1) and a file of input parameters. The input parameters include the site and date of the data and the instruments and levels of these instruments desired.

Input: (1) Saved file of integrated data (output from INTEG1).
(2) File of input parameters.

Output: Line printer listing - may be several pages.

3.3.3.3 These are several plotting routines that have proven useful in interpretation of the data and the subsequent analyses. WVTPLT provides for a plot of the profiles of wind, vapor, or temperature with height. Each hourly profile of the specified parameter is plotted on the same set of axes. This provides for inspection and comparison of all profiles from similar plotting, but only one hourly profile is placed on a graph.

DIFRENCE plots the values of one set of measurements against the values of another level for level. The combinations that have been useful for similarity testing are: temperature vs. vapor pressure; and temperature vs.

wind speed. For convenience, the data are transformed before plotting by subtraction of the value measured at the bottom level. The program plots each hour throughout the day on the same set of axes.

PLOTFLUX plots the radiation budget for each hour in a given day. The variables plotted are: net radiation, global radiation, reflected global radiation, re-radiation, and atmospheric radiation.

The following input and output descriptions apply to these three plotting programs.

Input: (1) Saved file of integrated data.
(2) File or card deck of parameters, labels and scale.

Output: X-Y plot to specified scale.

3.3.4. Computation of Energy Budgets

This step in the system includes both computation and plotting of energy budget results.

3.3.4.1 COMPUTE calculates energy budget components from several different models, using the hourly integrated data files. The energy budget models include:

(1) Bowen ratio fluxes
   a. using soil heat flux from flux plates
   b. using soil heat flux calculated from soil properties and temperature profiles.

(2) Aerodynamic fluxes, based on either
   a. KEYPS diabatic profile corrections, or
   b. Empirical diabatic profile correction developed from the Richardson number.

A file or card deck of input parameters specifies the name of the saved file of data from INTEG1, the sensor levels to be used in the analyses, the models and constants to be used in the analyses, and the name of the output file to be saved. The output is listed and stored.

Input: (1) File of integrated data
(2) File or card deck of parameters

Output: (1) Listing of energy budget calculations
(2) Saved file of results.

3.3.4.2. Plots of Energy Budgets. BUDGPLOT plots the energy budget results for a 24-hour period. Up to four variables can be plotted at any one time and the choice of measurements is left to the user. The measurements we have used at various times include: net radiation, soil heat flux from discs, ground flux from temperature profiles, latent heat flux using Bowen Ratio, sensible heat flux using Bowen Ratio, latent heat flux using a corrected aerodynamic model, sensible heat flux using a corrected aerodynamic model, latent heat flux derived as a residual in the energy budget equation, and ground flux

derived as a residual in the energy budget equation.

Input: (1) Saved file of results from COMPUTE
(2) File or card deck of input parameters

Output: X-Y plot of selected variables at appropriate scale.

3.4. Data Processing Costs

The basic core charge for the OSU system is $360 per hour. The cost of computation depends upon the charge rate and efficiency of the computers available, so costs will of course vary from center to center. However, it may be of interest to examine the costs involved in the routine processing of the data collected during one day of our operation.

The experimental design for the marsh measurements at Malheur Lake is described in detail in Chapter IV. Briefly, the data collection program included: 6 types of radiation measurements; 6 measurements of air temperature, vapor pressure, and wind speed; three measurements of water temperature; 1 reference temperature; and 1 wind direction measurement. Twenty-nine environmental measurements were made every 10 minutes from 0000 to 0800 hours, and from 2000 to 2400 hours. Measurements were made every 5 minutes from 0800 to 2000 hours.

The cost of using the various programs on this data was:

TAPE 1	$7.50	(total depends upon errors found)
TAPE 2	8.50	(total depends upon errors found)
GAYTRAN	14.50	
INTEG1	1.75	
LISTING	0.60	
WVTPLT	5.00	(PLTWVT, 5.50 for 3 hours).
DIFRENCE	2.10	
PLOTFLUX	2.00	
COMPUTE	1.30	
BUDGPLOT	1.70	
Total	$44.95	

We often find it necessary to correct, rerun and replot various portions of the data in order to check for errors and inconsistancies. Our experience indicates that the computation costs for a full day as described here are more likely to approach $100 in our Computer Center instead of $44.95.

3.5. Literature Cited.

Backlund, B., and K. Perttu. 1971. System for data logging at short intervals and processing of data about plant growth and climate. Royal College of Forestry, Stockholm. 47 pp.

Brown, K. W., and N. J. Rosenberg. 1969. Computer program for plotting time-dependent meteorological data. Agri. Meteorol. 6:463-464.

4. MICROCLIMATE MEASUREMENTS

The field experiments described here were conducted over four of the natural surfaces that are found throughout the high, semi-arid plateau of central Oregon: a pumice desert, meadow, forest and marsh. The experimental sites possess surface characteristics that create contrasts in the absorption of radiant energy radiation, and in its disposition. These contrasts create different microclimates.

Since these studies were carried out with similar experimental designs, the results provide a comparison of the effects of the surface energy exchange processes for a variety of surface conditions. Such quantitative comparisons are enhanced through consideration only of measurements made under the similar weather conditions that prevail with cloudless skies. The measurements were not simultaneous at each site, but all fell within the period of mid- to late summer.

We shall first describe the characteristics of the experimental sites, and then examine the field measurements of the microclimatic variables. A variety of analyses can be applied to the data. Use of the data in energy budget studies will be discussed in a subsequent chapter.

4.1 Experimental Sites.

Certain site characteristics are important for energy budget analyses. In general, the surface must be homogenous, flat, and large in extent to permit the energy exchange processes to approach a steady-state with respect to location. The larger the expanse, the greater is the thickness of the atmospheric boundary layer, or zone of influence of the surface on the state of the atmosphere. A thicker boundary layer provides greater latitude in positioning sensors in the vicinity of the surface. The sites utilized in these experiments conform to these criteria.

The pumice desert site is about 60 km southeast of Bend, Oregon, at an elevation of about 1600 m. It is adjacent to the local landmark of Sand Springs and east of Pine Mountain and China Hat. The pumice site is flat and large, with a diameter of approximately 1500 m. The surface is uniformly covered to a depth of about 60 cm with Newberry pumice that was deposited approximately 2000 years ago. The site has remained essentially devoid of vegetation since the pumice was deposited. A low, sparse stand of ponderosa pine (Pinus ponderosa Laws.) and lodgepole pine (Pinus contorta Dougl.) is established on the pumice soils surrounding the site. The size, appearance and character of the pumice surface is evident in Figures 4-1 and 4-2.

The wet meadow lay immediately north of shallow Sparks Lake, about 30 km west of Bend. The meadow was flat, about 1500 m in diameter, and at an elevation of approximately 1600 m. The meadow vegetation consisted of rushes and sedges, interspersed with a variety of forbes. The meadow is used as a pasture for cattle during the latter part of each summer: the measurements reported here were made before grazing began. The characteristics of the wet meadow site are pictured in Figures 4-3 and 4-4.

The forest site was about 45 km southwest of Bend, on Snow Creek between Crane Prairie and Wickiup Reservoirs. The 40-year-old lodgepole pine forest

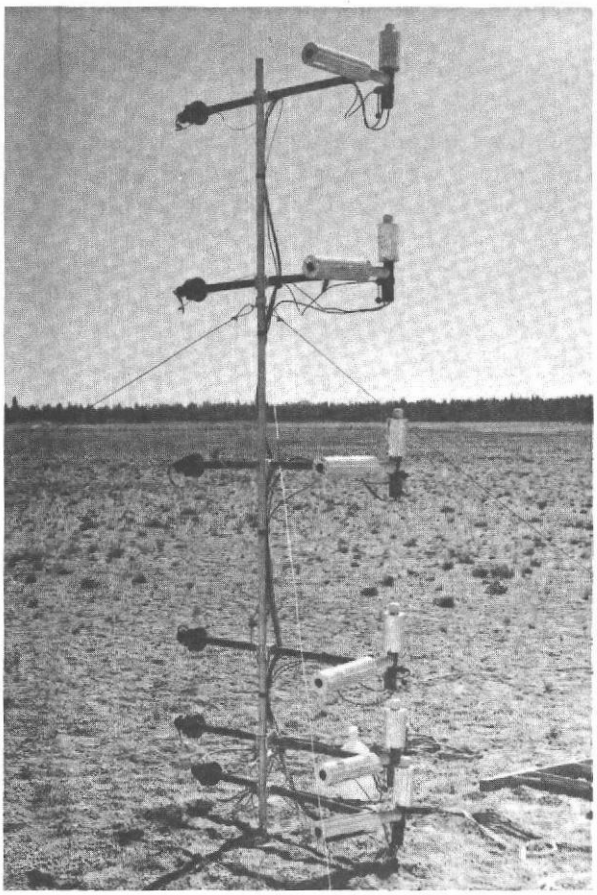

Figure 4-1. (left) Pumice site and psychrometer mast.

Figure 4-2 (below) Anemometer mast, pumice site.

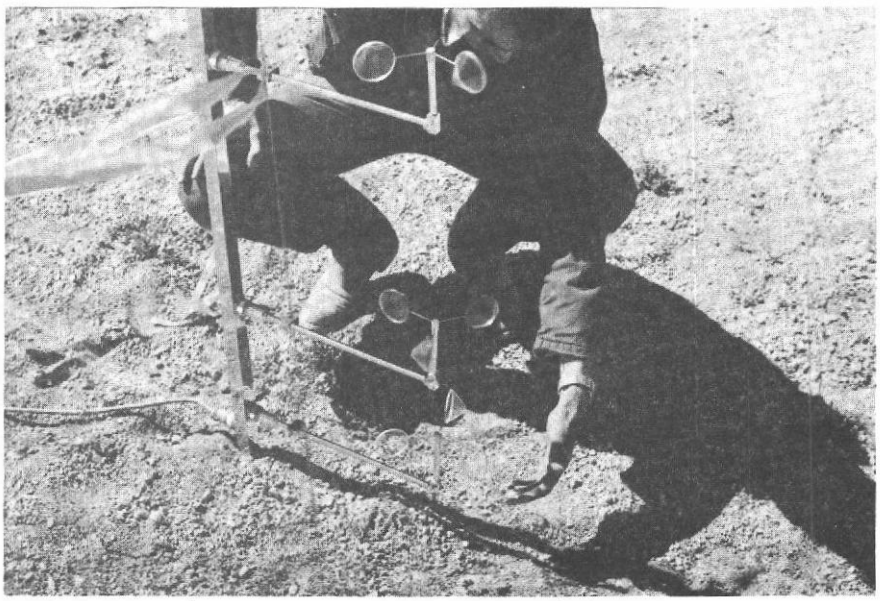

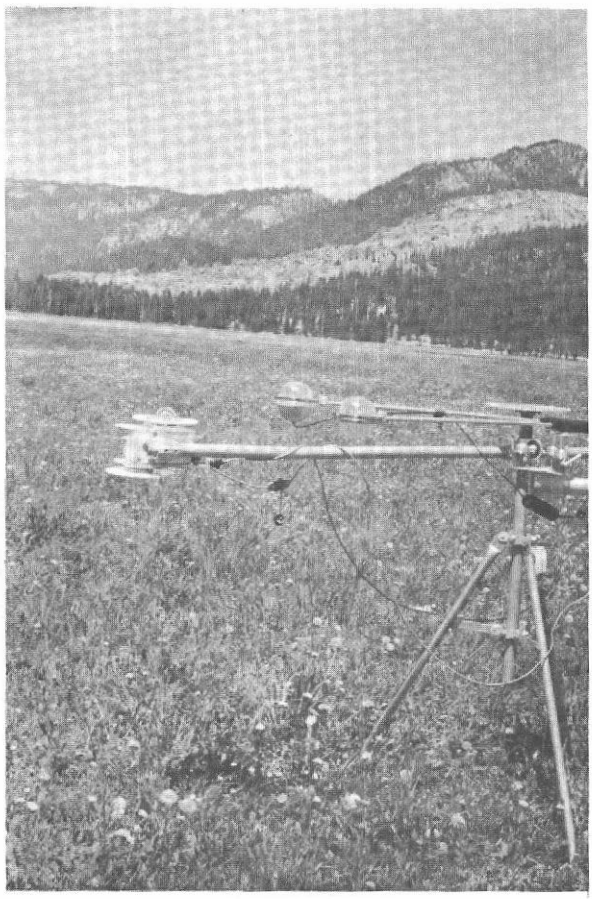

Figure 4-3. Radiometers, meadow site. A pair of Kipp pyranometers is at the left; one is upright and one inverted to measure incoming and reflected shortwave radiation. The CSIRO pyrradiometer in the center measures incoming short- plus longwave radiation. The CSIRO net pyrradiometer on the right measures net radiation, the major term in the energy balance.

Figure 4-4. (below) Energy balance instrumentation, meadow site. The psychrometer and anemometer masts are at the right of the picture. The heated thermocouple reference junction is in the weatherproof case in the foreground. The view is north, across Sparks meadow, elevation 1,650 m., toward South Sister, elevation 3,150 m.

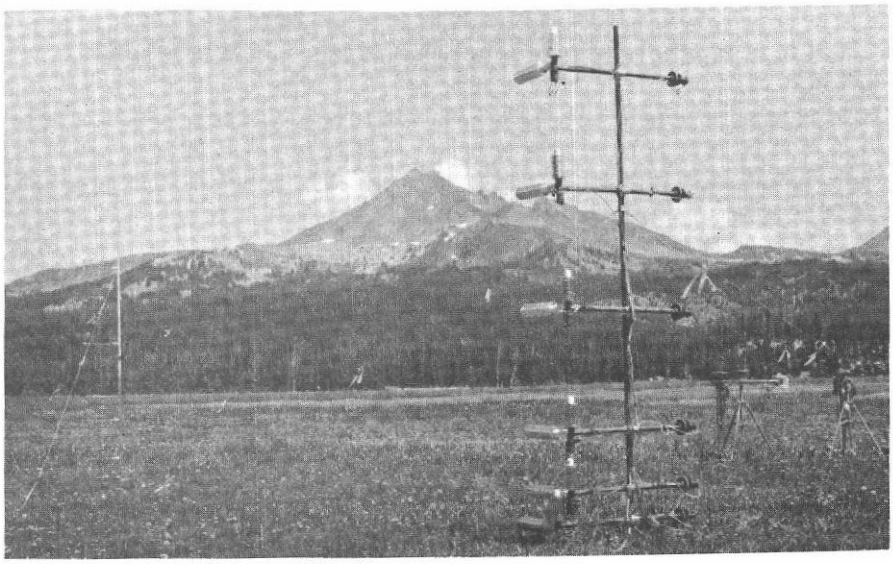

is on an old burn of about 2 square kilometers in area. Fetch toward the northwest, the direction of the prevailing wind, was nearly 1 km. The soils at this site are derived from pumice, a material characteristic of the volcanic activity that once occurred throughout the central Oregon region.

The mean height of the stand was about 7 m. The height was rather uniform but the canopy was not unbroken, as there were many gaps and openings of 5 to 15 m in diameter, scattered throughout the stand. The stand included a wide range of stem diameters. No measurements were made, but the mean diameter is estimated to be between 10 and 15 cm. The forest canopy was shown earlier in Figure 2-6.

The marsh measurements were made at Malheur Lake, a large, shallow, freshwater marsh some 20,000 ha in area. The lake, el. 1,248 m, is located 45 km southeast of Burns, Oregon, in the Silvies River drainage basin, about 200 km east-southeast of Bend. The unique ecological and physical features of Malheur Lake have been described in detail elsewhere (Dubbert, 1969; Oregon WRRI, 1971). For our purpose, the Lake represents a large, moist oasis in the midst of a vast semi-arid plateau. Very little of the marsh is open water; most of the area is covered with typical marsh vegetation of bulrushes and cattails.

The marsh measurement site was about 5 km out into the Lake on the east side, with the Cole Island dike providing accesss. The instrumentation was set up in the marsh vegetation about 80 m west of the low dike. The water depth was about 70 cm at the instrument location, and the mass of the bulrushes extended about 150 cm above the water level. Tips extended as high as 240 cm. The site of the water and mud temperatures was about 20 m east of the radiometers; water depth here was 30 cm. A small catwalk built out into the marsh provided access to the instruments.

4.2 Field Measurements

Field measurements were made at the pumice, meadow and forest sites in the summer of 1969, and at the marsh site during the summer of 1971. The measurements reported here were made during periods of fine, clear weather during mid- to late summer. They were obtained during expeditions that were usually a week in duration. This was generally a long enough time to insure that at least one 24-hour period of suitable weather coincided with satisfactory instrument performance.

The basic scheme of measurements was similar at each site. The measured parameters included temperature and vapor concentration in the air at six levels above the surface, net radiation, soil heat flux (except in the marsh) and soil (or water) temperature. Soil (or water) temperatures were measured at 5 levels at the desert and forest site, three levels at the marsh and one level at the meadow site. Further, the incoming and outgoing, short- and longwave components of net radiation were measured at each of the four sites.

The basic data obtained during the measurement program is tabulated in this section; notes indicate any discrepancies in the basic measurement scheme. The data appear suitable for a variety of analyses and tests, not all of which will be attempted in this report.

4.2.1 The Pumice Site Measurements.*

Two sets of observations are summarized in Tables 4-1 and 4-2. The first is for the 24-hour period of July 17, 1969 and the second is for the 24-hour period of September 4, 1969. The values represent hourly averages calculated with the integration program. Heights of the observations are indicated in the tables.

The surface temperature of the pumice desert is calculated from the estimate of outgoing longwave radiation. No corrections were applied for either emissivity or reflection of atmospheric radiation, so the surface temperature estimates are of the "effective" radiating temperature of the pumice as seen by the radiometers. This temperature is derived from calculations involving all of the radiometers, and thus includes any residual calibration errors among the four radiometers.

4.2.2 The Meadow Measurements.

Two sets of observations are summarized for the meadow site in Tables 4-3 and 4-4. The first represents the 24-hour period 0800-0700 hours, July 28-29, 1969, and the second is for the 13-hour period 0800-2000 hours, July 31, 1969.

As before, values represent hourly means, determined by the integration program. Note that only one soil temperature sensor was used at this site; it was at -5 cm, the depth of the soil heat flux disks. Vapor pressure is tabulated for three levels on July 28, and four levels on July 31, because some of the psychrometers malfunctioned during these data runs.

4.2.3 The Forest Measurements

Two sets of observations are summarized for the lodgepole pine site in Tables 4-5 and 4-6. They represent the respective 24-hour periods of midnight to midnight, August 21 and August 27, 1969. The values represent hourly means derived from the integration programs. The scale of the forest elements is quite different from those of the preceeding surfaces. The instrument heights begin at 707 cm, the level of the tips of the taller trees, and increase in 125 cm increments.

Soil temperatures and heat flux were sampled at one site on the forest floor. The depths of temperature measurement were the same as for the pumice desert (0, -2, -5, -10, and -20 cm). The 0 level is at the interface between the soil and the litter layer; a radiometric surface temperature is not tabulated for the forest. Only three levels of vapor pressure are tabulated on each day because of malfunctioning psychrometers.

4.2.4 The Marsh Measurements.

Observations at Malheur Lake are summarized in Tables 4-7 and 4-8 for the respective 24-hour periods from midnight to midnight, August 21 and 23,

---

*Holbo, H. R. The energy budget and soil thermal regime of a pumice desert. Final Report FS-PNW-1203. March 10, 1971. Mimeo., 26 pp. Oregon State University School of Forestry, Corvallis, Oregon

Table 4-1. Microclimate Measurements at the Pumice Site, July 17, 1969.

HR	Q* LY/MIN 100CM	SOIL TEMPERATURES DEGREES C SURFACE	2CM	5CM	10CM	20CM	AIR TEMPERATURES DEGREES C 20CM	40CM	80CM	160CM	240CM	320CM	VAPOR PRESSURE MILLIBARS 20CM	40CM	80CM	160CM	240CM	320CM	WINDSPEED CM/SEC 20	40	80	160	240	320
1	-0.090	4.43	8.59	16.35	18.60	17.35	6.41	6.67	7.35	8.06	8.49	8.91	7.34	7.37	7.41	7.48	7.48	7.47	61	77	94	116	134	146
2	-0.095	1.43	6.97	15.21	18.04	17.30	2.29	2.39	3.04	4.06	4.78	5.17	6.48	6.54	6.66	6.83	6.84	6.85	48	64	83	105	111	114
3	-0.081	.33	5.56	14.19	17.46	17.20	.61	.71	1.13	2.06	2.67	3.15	5.91	5.94	6.07	6.25	6.27	6.39	46	60	75	96	108	113
4	-0.077	-1.16	4.32	13.20	16.87	17.18	-1.34	-1.15	-0.75	.04	.65	1.10	5.33	5.38	5.51	5.69	5.86	5.96	35	45	56	68	71	70
5	-0.071	-1.21	3.19	12.28	16.29	16.92	-2.22	-2.24	-1.90	-1.43	-1.21	-0.96	5.45	5.20	5.10	5.21	5.29	5.35	28	37	44	54	61	66
6	-0.032	3.85	2.76	11.43	15.73	16.80	-1.96	-2.02	-2.02	-1.78	-1.61	-1.43	5.90	5.83	5.01	5.49	5.06	5.12	26	34	46	56	63	65
7	.043	15.82	5.47	11.80	15.12	16.70	3.47	3.16	3.03	2.95	2.82	2.76	5.15	5.46	6.52	6.04	6.43	6.49	33	36	38	39	40	38
8	.183	25.66	12.43	11.09	14.50	16.42	10.89	10.54	10.29	10.07	9.74	9.83	7.29	7.29	7.19	7.13	7.09	7.12	44	53	56	59	60	58
9	.339	35.05	20.65	12.73	14.12	16.10	16.13	15.41	14.97	14.65	14.40	14.31	6.73	6.77	6.65	6.58	6.65	6.62	74	87	87	93	96	96
10	.429	41.94	28.47	15.23	14.12	15.83	18.99	18.01	17.43	16.95	16.63	16.56	17.07	16.34	5.97	5.91	5.94	5.88	106	122	130	139	142	144
11	.523	46.47	35.15	17.99	14.51	15.56	21.47	20.54	19.77	19.02	18.60	18.78	19.95	19.49	5.26	5.12	5.03	5.17	143	167	178	193	200	205
12	.594	48.36	39.81	20.69	15.31	15.39	23.84	22.50	21.47	20.36	20.03	20.09	6.32	6.16	5.99	5.73	5.83	5.87	191	228	249	271	281	289
13	.627	49.43	42.56	23.05	16.39	15.30	24.37	23.09	22.02	21.25	20.74	20.66	6.88	6.38	6.30	6.35	6.29	6.19	209	252	275	302	315	323
14	.620	47.64	43.72	24.93	17.55	15.38	25.46	24.13	23.00	22.16	21.65	21.53	7.33	6.45	6.40	6.41	6.33	6.24	217	263	290	317	330	338
15	.585	44.79	42.67	25.25	18.70	15.56	26.21	24.93	23.79	22.93	22.38	22.27	7.48	6.29	6.15	6.18	6.09	6.02	264	326	360	397	413	423
16	.508	39.67	40.28	26.89	19.71	15.81	26.07	24.87	23.84	23.01	22.48	22.39	7.34	5.75	5.65	5.66	5.57	5.45	255	315	350	388	407	418
17	.409	33.14	36.47	26.96	20.50	16.17	25.53	24.59	23.71	23.03	22.65	22.52	7.24	5.23	5.15	5.16	5.07	4.95	294	369	416	468	491	504
18	.267	26.40	31.90	26.41	21.04	16.53	23.96	23.32	22.75	22.22	21.89	21.82	7.94	5.83	5.78	5.78	5.71	5.56	301	380	431	485	513	527
19	.113	19.15	26.77	25.41	21.34	16.87	21.83	21.57	21.34	21.11	20.90	20.89	8.54	6.54	6.48	6.50	6.43	6.30	295	376	426	483	513	531
20	-0.051	14.05	20.32	23.37	20.89	16.82	17.65	17.73	17.86	17.94	17.94	17.97	5.65	5.86	5.69	5.70	5.61	5.48	246	313	359	412	438	456
21	-0.112	11.09	15.91	21.67	20.68	17.03	13.85	14.28	14.77	15.29	15.56	15.71	5.86	6.09	5.93	5.90	5.81	5.68	133	169	199	236	254	264
22	-0.137	9.05	13.38	20.02	20.29	17.21	11.90	12.41	13.02	13.70	14.09	14.33	6.47	6.67	6.52	6.50	6.40	6.30	137	173	205	250	274	290
23	-0.103	7.84	11.81	19.61	19.77	17.32	10.56	10.96	11.40	11.81	12.06	12.25	7.21	7.38	7.31	7.33	7.27	7.19	106	135	160	193	212	225
0	-0.095	5.89	10.34	17.63	19.33	17.35	8.12	8.51	9.05	9.60	9.99	10.29	7.39	7.48	7.43	7.50	7.45	7.40	0	0	0	0	0	0

Table 4-2. Microclimate Measurements at the Pumice Site, September 4, 1969.

HR	Q* LY/MIN 100CM	SOIL TEMPERATURES DEGREES C SURFACE	2CM	5CM	10CM	20CM	AIR TEMPERATURES DEGREES C 20CM	40CM	80CM	160CM	240CM	320CM	VAPOR PRESSURE MILLIBARS 20CM	40CM	80CM	160CM	240CM	320CM	WINDSPEED CM/SEC 20	40	80	160	240	320
1	-0.072	-6.15	-3.49	10.31	14.81	15.69	-6.45	-5.96	-4.81	-3.90	-3.34	-2.90	4.66	3.77	4.29	4.49	4.57	4.60	37	44	55	58	62	68
2	-0.069	-7.88	-4.83	9.26	14.22	15.58	-7.46	-7.42	-6.89	-5.66	-4.86	-4.48	3.43	3.47	3.58	3.89	4.10	4.27	33	45	57	70	72	82
3	-0.067	-9.13	-5.75	8.33	13.62	15.44	-8.27	-8.15	-7.39	-6.34	-5.72	-5.43	3.22	3.21	3.43	3.74	3.89	4.04	32	42	46	56	53	62
4	-0.065	-9.59	-6.70	7.51	13.06	15.28	-9.82	-9.65	-8.98	-8.18	-7.30	-6.51	2.92	2.94	3.08	3.39	3.58	3.80	32	41	48	57	64	75
5	-0.058	-9.61	-7.28	6.75	12.50	15.09	-9.74	-9.67	-9.22	-8.45	-7.83	-7.31	2.93	2.96	3.07	3.33	3.44	3.55	45	56	66	78	84	90
6	-0.054	-9.30	-7.23	6.33	12.13	14.96	-9.32	-9.36	-9.05	-8.43	-8.19	-7.91	2.95	2.94	3.03	3.15	3.24	3.35	41	53	62	80	85	87
7	.033	3.61	-2.73	5.63	11.38	14.66	-6.04	-6.22	-6.27	-6.35	-6.36	-6.26	3.69	3.71	3.71	3.69	3.74	3.83	31	34	35	37	38	39
8	.122	13.35	5.62	5.84	10.97	14.53	1.73	1.29	1.20	1.03	.94	.88	4.22	4.48	4.11	4.16	4.25	4.29	50	56	58	61	63	64
9	.251	25.47	13.39	7.73	10.60	14.30	10.11	9.65	9.40	9.01	8.89	9.63	4.68	4.57	4.44	4.45	4.40	5.06	98	112	118	127	132	137
10	.383	32.31	18.09	10.72	10.56	14.05	14.26	13.41	12.81	12.14	11.91	11.67	5.93	5.84	5.79	5.82	5.77	5.78	188	221	241	264	277	290
11	.499	35.36	20.48	13.68	10.91	13.81	15.81	14.70	13.84	12.98	12.62	12.27	5.70	5.64	5.62	5.61	5.56	5.56	255	304	335	373	386	404
12	.557	37.73	23.31	16.30	11.54	13.63	17.43	16.19	15.25	14.18	13.87	13.50	5.42	5.32	5.28	5.30	5.23	5.22	235	280	306	334	350	365
13	.596	37.71	24.95	18.49	12.38	13.51	19.00	17.68	16.68	15.54	15.12	14.72	5.69	5.57	5.56	5.56	5.50	5.50	318	382	421	468	493	517
14	.565	38.48	26.46	20.02	13.36	13.49	19.72	18.40	17.41	16.41	16.03	15.70	5.68	5.57	5.58	5.54	5.49	5.51	281	336	370	417	428	447
15	.491	36.95	26.96	21.21	14.33	13.55	19.58	18.35	17.56	16.56	16.30	16.00	6.12	5.98	5.92	5.90	5.85	5.89	249	297	327	362	377	395
16	.396	31.78	25.15	21.78	15.22	13.69	19.12	18.04	17.28	16.41	16.10	15.80	6.27	6.15	6.12	6.08	6.03	6.06	293	354	393	435	456	478
17	.257	25.66	22.21	21.50	15.96	13.88	17.43	16.71	16.19	15.49	15.27	15.04	5.94	5.82	5.78	5.74	5.70	5.72	299	359	401	448	472	494
18	.090	19.33	19.64	20.57	16.46	14.10	15.81	15.44	15.21	14.79	14.66	14.47	5.63	5.52	5.49	5.43	5.41	5.39	268	323	364	409	433	460
19	-0.072	11.79	14.91	19.09	16.68	14.37	12.68	12.77	12.87	12.89	12.90	12.86	5.65	5.59	5.58	5.51	5.49	5.50	229	279	316	360	381	403
20	-0.125	7.00	9.14	17.24	16.65	14.59	9.12	9.46	9.76	10.22	10.37	10.44	5.69	5.70	5.75	5.67	5.66	5.68	138	164	187	220	226	265
21	-0.115	3.21	6.10	15.47	16.36	14.77	5.79	6.27	6.80	7.44	7.89	8.15	5.76	5.73	5.74	5.73	5.74	5.72	91	121	141	179	199	213
22	-0.099	-1.31	2.12	13.80	15.90	14.89	1.06	1.61	2.45	3.62	4.31	4.86	5.06	5.13	5.22	5.27	5.33	5.41	52	66	79	88	100	85
23	-0.093	-2.19	.41	12.63	15.93	15.72	-0.37	.14	1.15	2.94	3.95	4.55	4.87	5.43	5.03	5.25	5.59	5.58	78	104	135	175	195	212
0	-0.085	-3.57	-1.07	11.75	15.54	15.77	-2.83	-2.45	-1.56	-0.70	-0.05	.30	4.24	5.62	4.39	4.54	4.68	4.74	0	0	0	0	0	0

Table 4-3. Microclimate Measurements at the Meadow Site, July 28, 1969.

HR	Q* LY/MIN 100CM	G LY/MIN 5CM	SOIL T DEG C 5CM	AIR TEMPERATURE DEGREES C 20CM	80CM	240CM	VAPOR PRESSURE MILLIBARS 20CM	80CM	240CM	WINDSPEED CM/SEC 20	40	80	160	240	320
8	.217	.020	8.96	9.26	7.98	7.62	9.08	7.99	7.65	0	0	0	0	0	0
9	.402	-0.015	13.30	15.82	15.19	14.91	10.74	8.14	7.44	62	76	84	92	98	99
10	.593	-0.054	18.20	17.62	17.87	17.64	11.15	7.97	6.61	117	145	168	194	209	216
11	.745	-0.083	22.47	18.62	18.97	18.64	11.17	7.73	6.26	142	176	205	238	254	263
12	.846	-0.097	25.84	19.89	19.96	19.55	11.88	8.41	6.86	144	180	212	248	266	278
13	.899	-0.099	27.86	20.71	20.45	20.09	11.84	8.77	7.25	149	188	224	265	285	299
14	.872	-0.098	28.09	20.96	20.86	20.44	11.01	8.60	6.99	191	241	294	351	382	402
15	.796	-0.091	26.84	21.23	21.01	20.64	10.96	8.34	6.68	187	239	290	346	376	395
16	.667	-0.055	25.42	21.15	20.92	20.57	11.68	9.40	7.99	152	192	233	274	298	315
17	.499	-0.037	23.90	20.15	20.00	19.73	11.83	9.93	8.67	146	185	227	272	295	311
18	.310	-0.021	22.01	18.69	18.85	18.83	11.06	9.65	8.66	148	188	232	279	306	326
19	.115	-0.006	19.96	16.63	17.26	17.65	8.93	7.94	7.26	137	175	217	263	291	310
20	-0.064	.003	17.90	11.54	14.13	15.61	9.32	8.35	7.95	52	72	91	114	127	133
21	-0.132	.023	15.46	5.44	8.77	11.04	8.45	8.44	8.37	0	0	0	0	0	0
22	-0.163	.033	13.27	3.09	5.41	7.38	7.30	7.56	7.74	0	0	0	0	0	0
23	-0.186	.039	11.67	.35	2.61	5.00	6.11	6.31	6.46	0	0	0	0	0	0
0	-0.119	.042	10.20	-1.11	.67	2.79	5.87	5.44	5.46	0	0	0	0	0	0
1	-0.199	.043	9.11	-2.01	-0.72	1.04	5.83	4.84	5.02	0	0	0	0	0	0
2	-0.193	.044	8.10	-3.09	-1.89	.16	4.66	4.54	4.53	0	0	0	0	0	0
3	-0.190	.045	7.19	-4.13	-2.75	-0.79	4.37	4.50	4.42	0	0	0	0	0	0
4	-0.095	.046	6.37	-4.91	-3.59	-1.57	4.12	5.40	4.15	0	0	0	0	0	0
5	-0.091	.047	5.66	-5.53	-4.18	-2.24	3.97	3.99	5.15	0	0	0	0	0	0
6	-0.079	.046	5.07	-5.65	-4.38	-2.46	3.93	3.98	4.31	0	0	0	0	0	0
7	.020	.043	5.05	-2.94	-2.56	-1.67	4.56	4.32	4.29	0	0	0	0	0	0

Table 4-4. Microclimate Measurements at the Meadow Site, July 31, 1969.

HR	Q* LY/MIN 100CM	G LY/MIN 5CM	SOIL T DEG C 5CM	AIR TEMPERATURE DEGREES C 20CM	80CM	160CM	320CM	VAPOR PRESSURE MILLIBARS 20CM	80CM	160CM	320CM	WIND SPEED CM/SEC 20	40	80	160	240	320
8	.248	.019	8.68	7.24	6.33	6.14	6.10	6.82	8.16	6.08	6.81	46	60	68	73	76	77
9	.387	-0.015	13.85	15.59	14.85	14.37	14.56	10.24	7.87	7.75	7.33	49	61	67	73	77	77
10	.569	-0.053	19.82	18.56	18.27	17.67	17.98	9.70	6.75	6.81	5.85	74	89	99	112	119	121
11	.716	-0.080	24.60	21.28	19.78	19.23	19.46	10.66	7.07	6.89	5.92	85	109	127	145	152	156
12	.830	-0.096	27.93	21.36	21.11	20.57	20.81	10.67	7.48	7.37	6.21	117	146	172	199	212	219
13	.879	-0.100	30.10	22.21	21.78	21.26	21.56	10.70	7.77	7.79	6.46	141	177	210	244	263	274
14	.893	-0.094	31.37	22.52	22.01	21.45	21.72	11.45	9.30	9.45	8.10	178	226	277	332	360	379
15	.784	-0.080	31.90	22.30	21.89	21.34	21.63	10.98	8.88	9.30	7.87	173	218	268	318	345	363
16	.656	-0.063	29.33	21.77	21.45	20.93	21.20	11.25	9.35	10.05	8.49	169	212	259	311	339	357
17	.486	-0.042	26.53	21.65	21.47	20.83	20.28	11.43	9.70	10.54	9.05	157	200	248	298	325	344
18	.293	-0.023	23.60	19.30	19.26	18.93	19.14	11.34	10.02	10.96	9.58	134	169	206	245	268	285
19	.093	-0.006	21.00	16.87	17.36	17.32	17.65	9.44	8.66	9.78	8.37	128	163	203	255	273	290
20	-0.085	.004	18.20	11.59	14.29	15.15	15.90	7.36	6.35	7.70	6.27	63	85	110	132	157	166

Table 4-5. Microclimate Measurements at the Forest Site, August 21, 1969.

HR	Q* LY/MIN 1300CM	G LY/MIN 5CM	SOIL TEMPERATURE DEGREES C 0CM	2CM	5CM	10CM	20CM	AIR TEMPERATURE DEGREES C 707CM	832CM	957CM	1082CM	1207CM	1332CM	VAPOR PRESSURE MILLIBARS 707CM	957CM	1207CM	WINDSPEED CM/SEC 707	832	957	1082	1207	1332
1	-0.100	.009	8.37	13.18	14.16	14.91	13.86	8.61	9.06	9.38	9.66	9.90	10.13	10.05	10.33	10.52	0	0	0	0	0	0
2	-0.087	.011	6.17	11.95	13.28	14.58	13.81	6.17	6.75	7.22	7.70	8.03	8.29	8.92	9.41	9.68	0	0	0	0	0	0
3	-0.090	.013	4.76	10.83	12.40	14.22	13.74	4.65	5.32	5.99	6.52	7.04	7.54	8.10	8.86	9.29	0	0	0	0	0	0
4	-0.074	.013	3.65	9.85	11.58	13.84	13.65	3.99	4.38	4.81	5.32	5.84	6.34	7.88	8.34	8.76	0	0	0	0	0	0
5	-0.062	.013	2.77	9.01	10.84	13.46	13.54	3.07	3.58	4.20	4.88	5.37	5.71	7.24	7.89	8.46	0	0	0	0	0	0
6	-0.049	.013	2.02	8.27	10.18	13.08	13.41	2.18	2.52	2.89	3.48	4.04	4.54	6.98	7.31	7.87	0	0	0	0	0	0
7	.037	.012	2.75	7.84	9.64	12.72	13.30	3.09	3.26	3.60	4.03	4.52	5.04	7.21	7.46	7.99	39	51	65	78	94	111
8	.216	-1.031	9.58	9.13	9.68	12.36	13.13	9.96	9.92	9.99	10.00	9.94	9.89	9.28	9.28	9.30	50	59	66	71	77	84
9	.441	-1.113	18.52	12.60	11.10	12.08	12.91	14.86	14.78	14.82	14.79	14.72	14.63	10.22	10.12	10.12	65	70	75	76	79	81
10	.655	-1.025	25.32	16.27	13.40	12.04	12.70	19.17	19.06	19.03	19.01	18.92	18.80	11.30	11.22	11.20	88	96	101	106	109	114
11	.812	-1.030	27.83	17.78	15.00	12.31	12.66	22.12	22.02	21.85	21.84	21.73	21.60	10.26	10.11	10.06	116	128	136	140	143	149
12	.919	-1.026	30.91	19.36	16.04	12.73	12.48	23.80	23.71	23.49	23.43	23.34	23.23	8.76	8.61	8.56	142	160	172	180	184	191
13	.960	-1.051	34.35	21.75	17.50	13.15	12.44	25.33	25.23	24.99	24.90	24.79	24.66	9.00	8.84	8.79	153	170	186	196	204	216
14	.937	-1.040	39.82	23.34	18.59	13.64	12.47	26.19	25.97	25.72	25.63	25.48	25.35	9.79	9.63	9.50	201	228	248	264	279	295
15	.847	-1.053	38.76	24.56	19.83	14.19	12.54	27.13	26.84	26.61	26.55	26.33	26.22	9.65	9.46	9.30	180	209	231	245	258	276
16	.711	-1.022	31.59	24.72	20.53	14.74	12.69	27.05	26.81	26.61	26.53	26.39	26.25	9.04	8.84	8.68	241	282	315	337	360	385
17	.522	-1.022	33.56	24.80	20.68	15.20	12.85	26.26	26.07	25.95	25.88	25.78	25.67	9.85	9.67	9.55	228	268	301	323	345	369
18	.293	-1.012	26.06	23.58	20.67	15.60	13.05	24.55	24.41	24.33	24.28	24.20	24.09	11.62	11.45	11.34	226	267	299	324	346	372
19	.056	-1.006	21.96	21.79	19.95	15.84	13.24	22.36	22.33	22.31	22.32	22.28	22.22	12.37	12.22	12.13	163	194	220	238	253	273
20	-0.115	-1.000	18.18	19.98	19.01	15.91	13.41	19.39	19.56	19.66	19.72	19.75	19.81	12.14	12.01	11.95	0	0	0	0	0	0
21	-0.113	.005	14.60	18.08	17.89	15.86	13.58	16.11	16.58	16.90	17.16	17.36	17.58	11.93	11.89	11.90	0	0	0	0	0	0
22	-0.104	.007	12.18	16.45	16.77	15.71	13.70	13.17	13.78	14.17	14.48	14.75	15.05	11.14	11.32	11.47	0	0	0	0	0	0
23	-0.096	.010	9.92	14.96	15.70	15.45	13.77	10.03	10.47	10.93	11.41	11.81	12.24	9.95	10.21	10.58	0	0	0	0	0	0
0	-0.092	.011	8.54	13.93	14.93	15.23	13.80	9.28	9.80	10.42	10.81	11.18	11.39	9.61	10.09	10.50	0	0	0	0	0	0

Table 4-6. Microclimate Measurements at the Forest Site, August 27, 1969.

HR	Q* LY/MIN 1300CM	G LY/MIN 5CM	SOIL TEMPERATURE DEGREES C 0CM	2CM	5CM	10CM	20CM	AIR TEMPERATURE DEGREES C 707CM	832CM	957CM	1082CM	1207CM	1332CM	VAPOR PRESSURE MILLIBARS 707CM	832CM	957CM	WINDSPEED CM/SEC 707	832	957	1082	1207	1332
1	-0.064	.014	1.38	7.84	9.73	12.14	12.21	1.00	1.50	2.10	2.59	3.18	3.79	6.06	6.29	6.62	65	85	99	109	117	127
2	-0.065	.013	1.59	7.40	9.13	11.78	12.15	1.36	1.75	2.13	2.46	2.76	3.13	6.50	6.68	6.83	65	81	94	106	116	126
3	-0.020	.010	3.31	7.29	8.73	11.44	12.06	1.93	2.10	2.33	2.54	2.78	2.96	6.57	6.67	6.79	65	82	91	99	107	114
4	-0.032	.011	2.67	7.23	8.57	11.15	11.95	1.36	1.50	1.68	1.89	2.13	2.36	6.36	6.46	6.53	50	68	85	99	109	118
5	-0.053	.010	1.93	6.92	8.32	10.90	11.84	.92	1.04	1.21	1.41	1.65	1.92	6.27	6.36	6.43	55	75	92	109	123	137
6	-0.049	.013	.39	6.09	7.88	10.67	11.74	-0.67	-0.32	.00	.33	.68	.95	5.68	5.88	6.01	45	71	94	115	129	139
7	.039	.012	.59	5.66	7.39	10.44	11.62	.02	.06	.18	.28	.38	.49	5.69	5.79	5.87	49	67	84	102	118	136
8	.206	.032	7.15	6.59	7.34	10.15	11.45	7.05	7.05	7.02	6.98	6.96	6.89	7.67	7.70	7.75	79	98	110	121	131	143
9	.454	-0.008	15.06	9.47	8.59	9.94	11.29	9.89	9.95	9.65	9.52	9.47	9.32	7.75	7.70	7.69	146	165	182	196	207	221
10	.657	-0.019	18.33	11.56	10.14	9.94	11.15	11.36	11.15	10.98	10.93	10.75	10.45	7.58	7.51	7.49	137	169	182	193	201	212
11	.817	-0.023	20.05	12.16	11.34	10.15	11.08	13.55	13.32	13.13	13.03	12.92	12.55	7.44	7.37	7.33	132	157	169	179	185	193
12	.917	-0.028	27.67	15.17	12.32	10.39	10.98	15.58	15.42	15.19	15.05	14.93	14.55	6.81	6.80	6.74	178	209	229	242	252	266
13	.955	-0.043	24.86	17.72	14.16	10.74	10.95	16.52	16.31	16.12	15.99	15.86	15.52	6.64	6.59	6.54	214	252	276	296	310	328
14	.930	-0.031	30.63	18.27	14.74	11.18	10.95	17.64	17.41	17.23	17.07	16.94	16.55	5.80	5.74	5.72	238	282	310	332	349	373
15	.836	-0.095	28.83	19.33	15.63	11.61	11.00	17.68	17.47	17.31	17.17	17.02	16.87	5.34	5.27	5.29	281	333	365	394	415	444
16	.685	-0.012	27.10	19.11	16.20	12.10	11.14	17.62	17.40	17.26	17.11	16.98	16.82	6.11	6.03	6.06	239	287	314	338	356	380
17	.498	-0.009	21.73	18.19	15.98	12.47	11.28	16.63	16.43	16.33	16.22	16.09	15.97	6.96	6.89	6.91	259	308	340	368	388	415
18	.247	-0.003	17.27	17.33	15.76	12.73	11.43	15.36	15.25	15.15	15.08	15.03	14.86	7.71	7.61	7.64	206	245	271	293	309	331
19	.002	.002	13.52	15.54	15.02	12.88	11.57	13.54	13.50	13.49	13.50	13.44	13.39	7.96	7.87	7.88	184	223	252	273	291	313
20	-0.130	.036	9.92	12.85	14.08	12.89	11.70	10.63	10.70	10.78	10.86	10.85	10.89	8.20	8.15	8.17	108	138	158	174	189	207
21	-0.129	.009	7.47	12.24	13.03	12.80	11.80	8.65	8.82	8.99	9.11	9.14	9.20	8.27	8.27	8.29	89	115	136	153	166	182
22	-0.123	.009	6.14	11.08	12.09	12.61	11.85	7.23	7.52	7.75	7.92	8.00	8.11	8.19	8.24	8.27	0	0	0	0	0	0
23	-0.108	.012	3.72	9.81	11.23	12.38	11.90	5.03	5.41	5.75	6.03	6.21	6.39	7.70	7.82	7.89	0	0	0	0	0	0
0	-0.086	.013	3.08	8.96	10.55	12.18	11.90	4.26	4.78	5.28	5.66	5.80	5.99	7.45	7.62	7.77	0	0	0	0	0	0

Table 4-7. Microclimate Measurements at the Marsh Site, August 21, 1971.

HR	Q* LY/MIN 300CM	GROUND TEMPERATURE DEGREES C SURFACE	01CM	2CM	30CM	AIR TEMPERATURE DEGREES C 220CM	240CM	280CM	360CM	440CM	520CM	VAPOR PRESSURE MILLIBARS 220CM	240CM	280CM	360CM	440CM	520CM	WINDSPEED CM/SEC 220	240	280	360	440	520
1	-0.119	15.10	18.75	20.25	20.35	14.66	14.68	14.76	14.96	15.11	15.24	10.87	10.82	10.75	10.63	10.39	10.27	123	134	152	193	227	252
2	-0.117	14.45	18.02	19.85	20.37	13.65	13.65	13.73	13.95	14.11	14.26	10.80	10.75	10.68	10.57	10.34	10.19	115	127	146	180	215	243
3	-0.119	14.72	17.84	19.62	20.35	14.15	14.16	14.23	14.39	14.52	14.60	10.77	10.75	10.69	10.62	10.43	10.33	136	150	171	212	249	277
4	-0.114	13.58	17.09	19.34	20.33	12.52	12.52	12.59	12.76	12.89	13.02	10.74	10.72	10.65	10.55	10.34	10.22	112	123	142	178	209	235
5	-0.115	13.39	17.00	19.08	20.31	12.32	12.34	12.39	12.54	12.66	12.74	11.02	11.01	10.93	10.84	10.65	10.55	110	122	137	165	198	219
6	-0.109	13.77	16.78	18.79	20.27	12.45	12.43	12.53	12.68	12.81	12.89	11.53	11.48	11.37	11.28	11.08	11.01	84	89	98	120	140	155
7	-0.031	13.10	16.63	18.60	20.22	13.27	13.18	13.26	13.41	13.51	13.55	11.26	11.17	11.04	10.93	10.70	10.56	99	108	124	150	179	194
8	.139	20.86	17.22	18.55	20.14	15.63	15.51	15.54	15.65	15.65	15.62	12.06	11.92	11.77	11.60	11.34	11.14	109	119	132	155	182	198
9	.365	22.64	17.71	18.55	20.04	17.03	16.96	16.94	17.03	16.97	16.93	12.92	12.76	12.58	12.43	12.18	11.96	108	119	129	152	176	191
10	.630	25.06	18.10	18.63	19.96	18.18	18.14	18.08	18.12	18.07	18.01	13.67	13.43	13.12	12.95	12.74	12.53	117	129	142	160	182	194
11	.784	25.85	20.01	20.21	19.88	19.30	19.30	19.21	19.22	19.19	19.13	13.96	13.66	13.32	13.06	12.73	12.51	100	104	112	128	140	147
12	.892	25.94	22.42	22.75	19.84	20.63	20.65	20.60	20.66	20.66	20.63	14.15	13.85	13.39	12.96	12.65	12.40	121	133	146	168	187	198
13	.938	25.60	24.39	24.53	19.75	21.84	21.95	21.94	22.03	22.06	22.06	14.15	13.97	13.59	13.25	12.87	12.56	143	159	177	208	234	250
14	.913	25.53	25.87	25.86	19.69	22.86	23.01	22.99	23.10	23.15	23.16	14.67	14.52	14.11	13.70	13.25	12.94	151	169	189	220	252	268
15	.817	25.13	25.41	26.04	19.72	23.85	24.04	24.04	24.17	24.24	24.27	15.03	14.85	14.39	13.96	13.50	13.16	139	156	175	205	232	249
16	.672	24.76	24.60	25.64	19.77	24.34	24.52	24.53	24.71	24.81	24.85	15.62	15.41	14.94	14.49	14.02	13.64	134	152	169	203	232	250
17	.464	24.48	24.14	24.98	19.78	25.06	25.30	25.40	25.65	25.79	25.84	15.25	14.95	14.44	13.95	13.50	13.18	111	125	138	160	182	194
18	.234	23.28	23.24	24.14	19.81	24.65	24.74	24.92	25.22	25.45	25.61	14.18	14.00	13.63	13.26	12.74	12.36	126	141	166	200	232	252
19	.005	22.30	22.06	23.24	19.85	22.80	22.87	23.05	23.40	23.67	23.83	13.59	13.48	13.29	13.06	12.62	12.37	119	133	151	187	224	247
20	-0.106	19.30	20.46	22.51	19.87	20.15	20.21	20.42	20.88	21.28	21.60	13.68	13.61	13.42	13.11	12.61	12.27	92	101	118	150	190	216
21	-0.111	18.29	19.44	21.97	19.91	18.95	19.03	19.24	19.65	19.99	20.28	12.80	12.70	12.52	12.30	11.87	11.59	98	109	128	160	200	227
22	-0.116	18.16	18.97	21.46	19.94	18.42	18.47	18.64	18.94	19.19	19.34	12.64	12.60	12.44	12.31	12.00	11.84	102	114	128	155	195	217
23	-0.118	17.47	17.74	21.07	19.98	17.68	17.71	17.83	18.12	18.34	18.50	11.96	11.93	11.83	11.71	11.42	11.26	125	129	149	184	225	250
0	-0.115	15.82	16.84	20.58	20.01	15.52	15.55	15.66	15.95	16.18	16.38	11.54	11.50	11.39	11.23	10.96	10.80	119	138	165	213	252	280

Table 4-8. Microclimate Measurements at the Marsh Site, August 23, 1971.

HR	Q* LY/MIN 330CM	GROUND TEMPERATURE DEGREES C SURFACE	0.1CM	2CM	30CM	AIR TEMPERATURE DEGREES C 220CM	240CM	280CM	360CM	440CM	520CM	VAPOR PRESSURE MILLIBARS 220CM	240CM	280CM	360CM	440CM	520CM	WINDSPEED CM/SEC 220	240	280	360	440	520
1	-0.151	11.37	12.30	16.17	19.38	10.38	10.45	10.54	10.69	10.77	10.78	8.95	8.90	8.83	8.80	8.63	8.56	123	140	154	185	207	224
2	-0.150	11.13	12.04	15.96	19.32	10.29	10.34	10.40	10.52	10.55	10.57	8.51	8.46	8.41	8.41	8.28	8.24	168	186	207	247	278	301
3	-0.143	8.44	10.24	15.68	19.24	6.95	6.93	6.97	7.02	7.02	7.02	8.89	8.84	8.77	8.69	8.53	8.51	83	90	100	121	139	152
4	-0.139	7.53	8.46	15.35	19.16	5.49	5.46	5.48	5.51	5.50	5.50	8.27	8.25	8.19	8.11	7.95	7.88	81	92	102	142	144	156
5	-0.134	7.47	8.57	15.07	19.08	5.44	5.40	5.43	5.49	5.52	5.56	8.52	8.48	8.43	8.36	8.24	8.24	81	89	100	124	143	155
6	-0.125	7.62	8.22	14.82	18.99	4.88	4.85	4.89	4.95	4.95	4.97	7.92	7.89	7.83	7.77	7.65	7.60	94	106	119	144	168	181
7	-0.063	14.27	8.62	14.51	18.89	6.04	5.79	5.84	5.90	5.89	5.82	7.83	7.79	7.73	7.70	7.56	7.55	73	77	91	97	106	112
8	.166	16.03	10.13	14.41	18.78	8.13	7.77	7.71	7.72	7.69	7.56	8.67	8.62	8.54	8.53	8.39	8.37	81	90	99	114	122	129
9	.415	18.45	12.57	14.42	18.64	9.95	9.68	9.52	9.49	9.37	9.28	9.34	9.22	9.10	9.05	8.89	8.85	70	77	83	94	99	102
10	.628	20.11	14.68	14.73	18.54	11.73	11.58	11.44	11.43	11.31	11.22	9.44	9.26	9.09	9.00	8.88	8.74	89	97	105	117	126	131
11	.793	21.03	15.75	15.73	18.43	13.40	13.34	13.21	13.17	13.09	13.01	9.58	9.40	9.15	8.97	8.77	8.62	149	168	185	213	234	248
12	.904	21.25	16.42	18.22	18.33	14.71	14.73	14.64	14.64	14.60	14.54	9.12	8.93	8.69	8.53	8.28	8.09	152	169	185	204	231	245
13	.944	21.10	20.96	20.40	18.21	16.51	16.57	16.50	16.51	16.49	16.45	9.23	9.06	8.74	8.49	8.19	7.99	154	173	192	219	240	254
14	.915	20.63	22.27	21.61	18.13	17.83	17.95	17.92	17.95	17.95	17.93	8.63	8.50	8.19	7.91	7.52	7.28	186	207	228	266	295	313
15	.817	20.42	21.47	21.76	18.13	18.85	18.97	18.96	19.03	19.06	19.06	8.91	8.76	8.43	8.16	7.76	7.52	204	227	251	296	328	349
16	.658	19.93	20.77	21.19	18.13	19.47	19.61	19.64	19.77	19.82	19.84	8.75	8.60	8.26	8.03	7.60	7.36	214	241	268	317	352	376
17	.453	19.39	19.77	20.23	18.12	19.69	19.86	19.96	20.16	20.26	20.31	8.51	8.35	8.02	7.79	7.29	7.06	182	203	228	267	301	321
18	.209	19.01	19.19	19.57	18.12	19.55	19.76	19.92	20.17	20.31	20.38	9.64	9.43	9.11	8.91	8.41	8.12	126	142	159	191	213	228
19	-0.029	19.08	18.84	19.32	18.12	18.41	18.68	18.91	19.22	19.41	19.55	12.24	12.01	11.73	11.48	11.01	10.72	82	93	104	131	150	166
20	-0.146	16.28	18.74	18.86	18.17	16.55	16.84	17.20	17.68	17.97	18.21	11.95	11.76	11.56	11.35	10.96	10.70	67	77	90	114	136	152
21	-0.144	13.74	18.36	18.38	18.20	13.62	13.84	14.26	14.93	15.31	15.63	10.98	10.78	10.41	9.91	9.43	9.06	60	71	87	119	143	159
22	-0.133	11.92	17.85	17.86	18.25	11.42	11.65	12.07	12.84	13.25	13.62	8.34	8.00	7.47	6.72	6.08	5.66	60	71	87	118	142	158
23	-0.133	11.04	17.11	17.28	18.27	9.84	9.97	10.22	10.80	11.38	12.00	8.40	8.23	7.92	7.40	6.76	6.20	61	72	88	120	153	175
0	-0.140	10.76	16.59	16.84	18.31	9.79	10.15	10.53	10.93	11.24	11.53	8.85	8.54	8.09	7.67	7.01	6.53	49	58	65	78	90	100

1971. The values represent hourly means derived from the integration program. The instrument heights begin at 220 cm, the approximate height of the tips of the reeds, and then continue with increments of +20, +40, +80, +160, +240, and +320 cm. The heights of the instruments above the reeds are thus comparable with the spacing above the pumice and the meadow surfaces.

The surface temperature of the marsh is calculated from the estimate of outgoing longwave radiation in the same manner as for the pumice site. No corrections were applied for emissivity and reflection of atmospheric radiation, so the surface temperature estimates are of the "effective" radiating temperature of the reeds and water as seen by the radiometers. This temperature is derived from calculations involving all of the radiometers, and thus includes any residual calibration errors among the four radiometers.

The other tabulated marsh temperatures were made approximately at -0.1, -2, and -30 cm depths. The site of the water temperature measurements was about 20 m east of the radiometers and the water was shallower. Thus the -30 cm depth was at the water/mud interface.

4.3 Measurement Accuracy

The accuracy of measurement enters into the analysis of microclimate data in two ways. The first is through the accuracy with which the recorded values represent the desired environmental variables; this involves an evaluation of the design and performance of the environmental data acquisition system. The second consideration in whether the experimental design insures that the measured data will meet the assumptions inherent in the particular model selected for analysis. It is quite possible that the environmental variables could be measured with an exceedingly high degree of accuracy, and yet the analyses could fail if the instruments were poorly sited, so that their measurements did not indicate the influence of the desired exchange surface. The problems of accuracy have received some attention in micrometeorological studies, while problems of experimental design have generally been overlooked. However, most studies have been deficient in their consideration of these problems.

4.3.1 Accuracy of Recorded Values.

Each measurement can contain both bias and random error. The distinction is important, since biases can be subtracted, but not averaged, out of the signal, while random errors can be removed or minimized by averaging.

Bias may be introduced by improper calibration, or by poor instrument response. For example, temperatures derived from thermocouples may contain a bias error if a standard calibration is assumed when it does not in fact apply. A biased temperature may also result if the sensor is improperly shielded against solar radiation. Random errors are most commonly associated with the recorder performance in rejection of noise, or in the design of the voltmeter. The recorders can also contribute bias to the readings through amplifier problems of drift or zero offset.

The recorder specifications are important in any estimate of system errors. The accuracy specifications for our Vidar recorder are $\pm$ 0.007% of scale, $\pm$ 0.004% of reading, and $\pm$ 4 microvolts, if the recorder is calibrated daily, if the ambient temperature remains between 24 and 26°C, and if the voltmeter

integration period extends for 166 2/3 milliseconds. Accuracy means the closeness with which the reading represents the true value. Precision, or the ability to reproduce a given reading for a constant signal, is also of interest to us. Under the conditions stated above, the precision of the Vidar recorder is ± 0.001% of scale.

The magnitude of error introduced by the recorder can be monitored if a known calibration signal is recorded. Our field measurements include the routine sampling of the temperature of an ice bath. This provides a check on the combined performance of the recorder, the heated reference junction, and the calibration of the thermocouples at one temperature. From these readings, and from the recorder specifications, an error estimate can be derived for the temperatures in the system. The recorder specifications alone can be used to estimate the accuracy of the radiation and soil heat fluxes. However, it is necessary to assume that the calibration errors are zero for radiometers and soil heat fluxmeters. In the final analysis, the judgement of the investigator must play a large role in the establishment of accuracy limits.

Based upon these considerations, values of the uncertainties in our measurements are calculated after Scarborough (1966) and are tabulated in Table 4-9. For convenience, the uncertainties are calculated and tabulated for typical values of the measured environmental variables. Holbo (1972) gives details.

The uncertainties of the differential measurements of temperature (± 0.017°C), vapor pressure (±0.052 mb), and wind speed (± 1 cm/sec) are critical factors in the use of energy budget analyses. The uncertainties given for these differential measurements in Table 4-9 are small enough to suggest that a variety of analyses can be applied to the data. The absolute values of these variables are measured with less accuracy, but, fortunately, the majority of the analyses require high accuracy only in the differential measurements.

Table 4-9. Estimate of Data Errors for Typical Values. Holbo, 1972.

Variable	Typical Value	Uncertainty
Soil or Dry Bulb Temperature	288°K (15°C)	± 0.256°C
Soil or Dry Bulb Differential	2.5°C	± 0.017°C
Vapor Pressure	8.75 mb	± 0.218 mb
Net Radiation	0.5 cal/cm^2/min	± 0.001 cal/cm^2/min
Surface Temperature (ε = 1.0)	308°K (35°C)	± 0.156°C
Windspeed	200 cm/sec	± 10 cm/sec
Wind Speed Differential	100 cm/sec	± 1 cm/sec

The recording errors for radiation (± 0.001 cal/cm^2/min) are very small. It must be noted that the calibration and sensor response errors may be quite large for net radiation. In actual practice, the accuracy of net radiometers is generally thought to be about ± 10 percent (IGY Instruction Manual, 1958). The instrumental errors are felt to be less than this in this study, but no precise estimate can be developed. The estimate of surface temperature does provide an indirect check since it is based upon measurements among four

radiometers, and contains the residual of all of the calibration errors. The surface temperatures calculated from the radiation measurements are well-behaved. They compare well with thermocouple measurements in the pumice desert, and with air temperature measurements near the surface at the meadow, forest and marsh sites. This comparison, though difficult to quantify, does give confidence in the radiation measurements.

4.3.2 Tests of the Experimental Design.

The gradient measurements must be accurate to be useful. In addition, the instruments must be placed so that their measurements reflect the influence of the exchanging surface on the state of the atmosphere near the surface. In other words, the gradient measurements must be made within the surface boundary layer.

There are several guidelines in use that relate the maximum height of useful measurement to the area of the exchange surface. Tanner (1963) has summarized these and it appears that the ratio of measurement height to fetch over the surface should be in the range of 1:100 or 1:200. The ratios for our studies do not exceed 1:250, and thus are well within the guidelines. Further, it is possible that the ratio could decrease (fetch requirements diminish) over aerodynamically rough surfaces such as the lodgepole forest studied here. However, no work yet appears to have evaluated this possibility.

Properties of the surface are known to affect the similarity between the profiles of temperature, vapor, and wind. For example, a surface could appear uniform, while in reality it might be a checkerboard of dry and moist areas. Tanner (1963) has pointed out that in such a situation the sensors may be responding to different sources of vapor and heat. This problem may be intensified when sensors are placed too close to a vegetated surface.

A related problem may be present if the various properties of the atmosphere are measured at different heights in the boundary layer. Such height differences are minimized for temperature and vapor measurements by the design of psychrometers which place the wet- and dry-bulb elements within the same air stream. The most serious problem is associated with matching the measurement heights between the psychrometers and the anemometers. Further, it is possible that the sources of heat and vapor and the sink for momentum may occur at different levels in a vegetation canopy, making height matching even more difficult to accomplish.

When these problems exist, it is inappropriate to apply energy budget analyses that assume similarity in gradients, e.g., equality of transfer coefficients.

Tanner (1963) has suggested that these problems will be revealed if the appropriate profiles are plotted against each other. If, for example, temperature is plotted against vapor pressure, a straight line will result whenever the instruments are performing properly and the experimental design is adequate, and whenever the surface conditions are such as to insure that similarity exists in the transfer of heat and vapor. This test is important, but is not commonly included in energy budget studies. It requires that the profiles be measured at a number of levels. However, the plots clearly test the adequacy of the experimental data.

Similarity was tested for the data in Tables [4-1] through [4-8] by plotting of the appropriate temperature, vapor, and wind profiles. The plots were helpful

in selection of appropriate instrument levels for subsequent analyses, and in the detection of malfunctioning instruments.

These similarity plots are reproduced in Figures 4-5 through 4-12. Part A in each Figure is a plot of θ vs. e; part B is a plot of θ vs. u. For convenience and ease in plotting, the bottom instrument value was subtracted from each reading in a given profile. The scale was originally either 0.5°C, 1°C, 1 mb, or 100 cm/sec, per inch, making it easy to detect deviations from linearity of 1 percent.

As an example of interpretation of the similarity plots, Figure 4-5A shows drift in the vapor pressure reading at the first level after 1200 hours. Also, levels 1 and 2 were not operating at 1000 and 1100 and the data for these two hours is omitted from Figure 4-5A. It is also evident that all psychrometers were operating improperly at hour 0600 and 0700. Comparison with Figure 4-5B at these hours confirms that the problem is associated with the vapor pressure measurements. Inspection of the air temperature records in Table 4-1 suggests that the wicks had frozen, and were probably thawing during this period.

In addition to linearity checks, other helpful information can be deduced from the plots. In particular, the slope of the θ vs. e profile is merely the Bowen ratio, divided by the psychrometric constant. For the majority of these high elevation sites, the psychrometric constant was slightly greater than 0.5. The diurnal change in the Bowen ratio is clearly revealed in examination of the hourly profiles of θ vs. e. For example, the shift from a positive to a negative Bowen ratio is apparent over the marsh in Figure 4-11 and 4-12, as advection begins to develop during the late morning hours and convection begins to transfer sensible energy downward to the marsh.

Small temperature offsets are evident in the plots of the marsh observations (Figure 4-11, 4-12). These offsets are apparent on both days and are most evident when the temperature gradient is near zero. We are not certain whether these irregularities are the result of instrumental errors, or whether they indicate that the lower levels of measurement are influenced by a position too close to the tops of the reeds. The temperature scale on the ordinate of the marsh plots was drawn in the ratio of 0.5°C per inch, while all other plots were drawn at 1°C per inch, so offsets are more evident for the marsh. The upper three levels approach linearity for nearly all marsh profiles, so these were the levels selected for energy budget analysis.

4.4 Summary.

The experimental design is described for measurements made at four contrasting study sites in central Oregon. The sites were flat expanses covered by pumice, wet meadow, lodgepole pine, and marsh. Measurements of the mean hourly values of net radiation, soil heat flux, and the gradients of temperature, vapor pressure, and wind speed are tabulated for two 24-hour periods of clear weather over the pumice, forest and marsh sites. The meadow data includes one 24-hour period and a 13-hour period from dawn to dark on a second day. In addition, the wind data is incomplete over the meadow. Despite these omissions, the uniformity of the sites, the prevailing weather conditions, and the experimental design permits quantitative comparisons to be drawn between the microclimates of these four surfaces.

The accuracy of the tabulated data is discussed, and projections made for

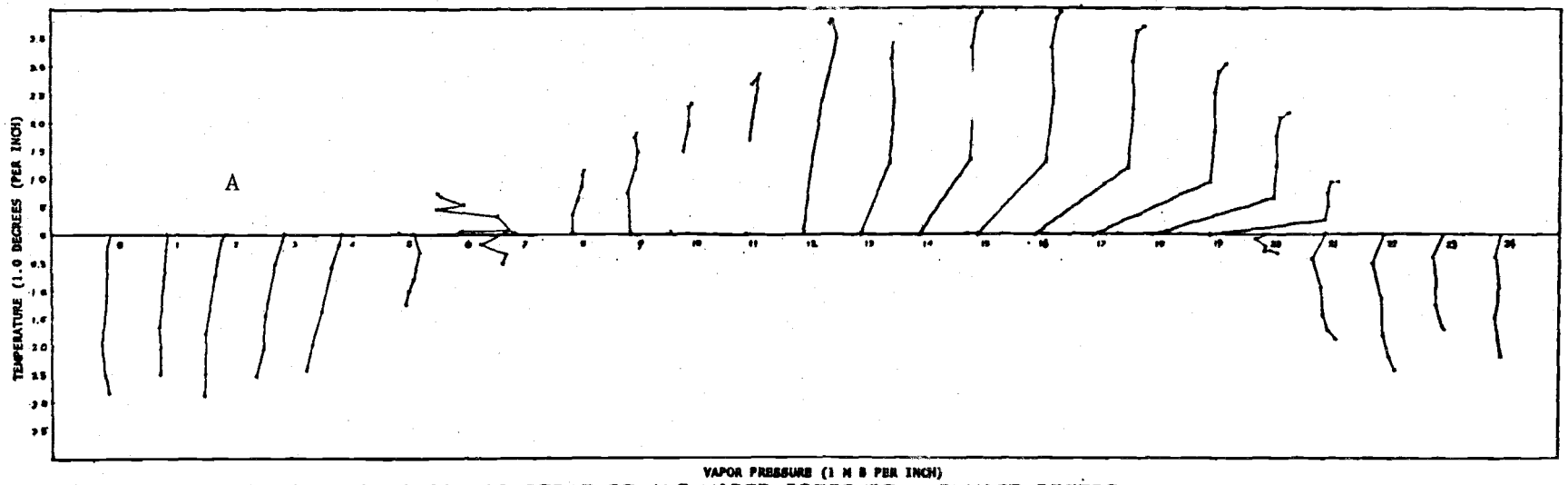

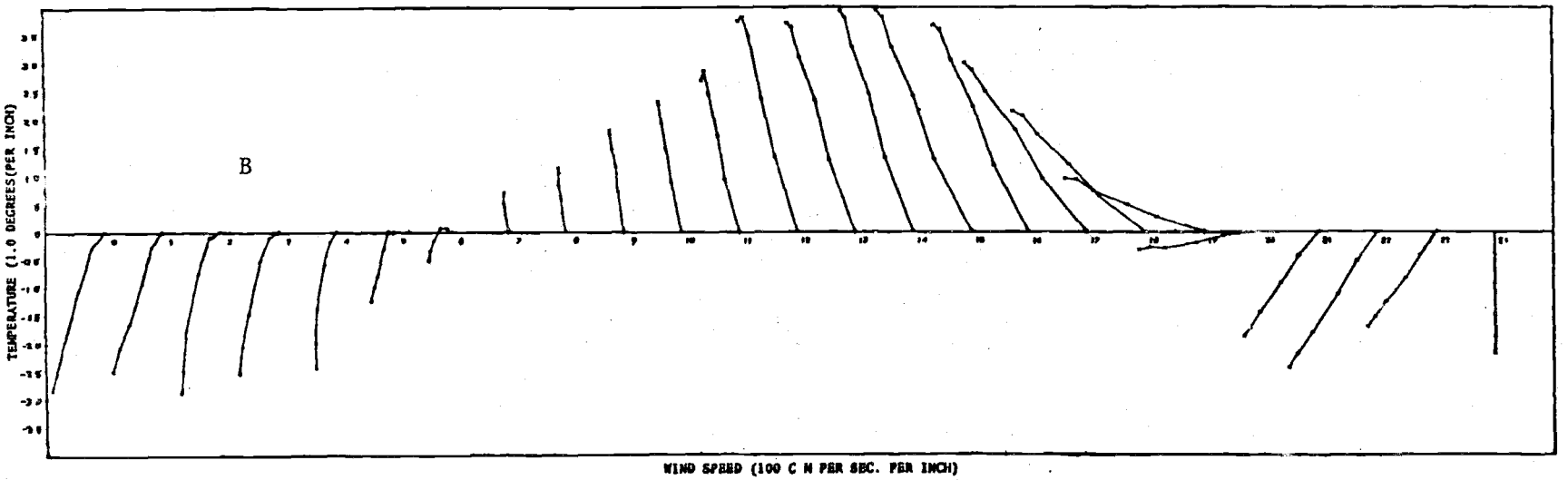

Figure 4-5. Similarity tests of the pumice desert data, July 17, 1969. A. Temperature and vapor pressure. B. Temperature and wind. The value at the first level of measurement was subtracted from each reading to facilitate plotting. The plots begin at hour 0 and continue through hour 24.

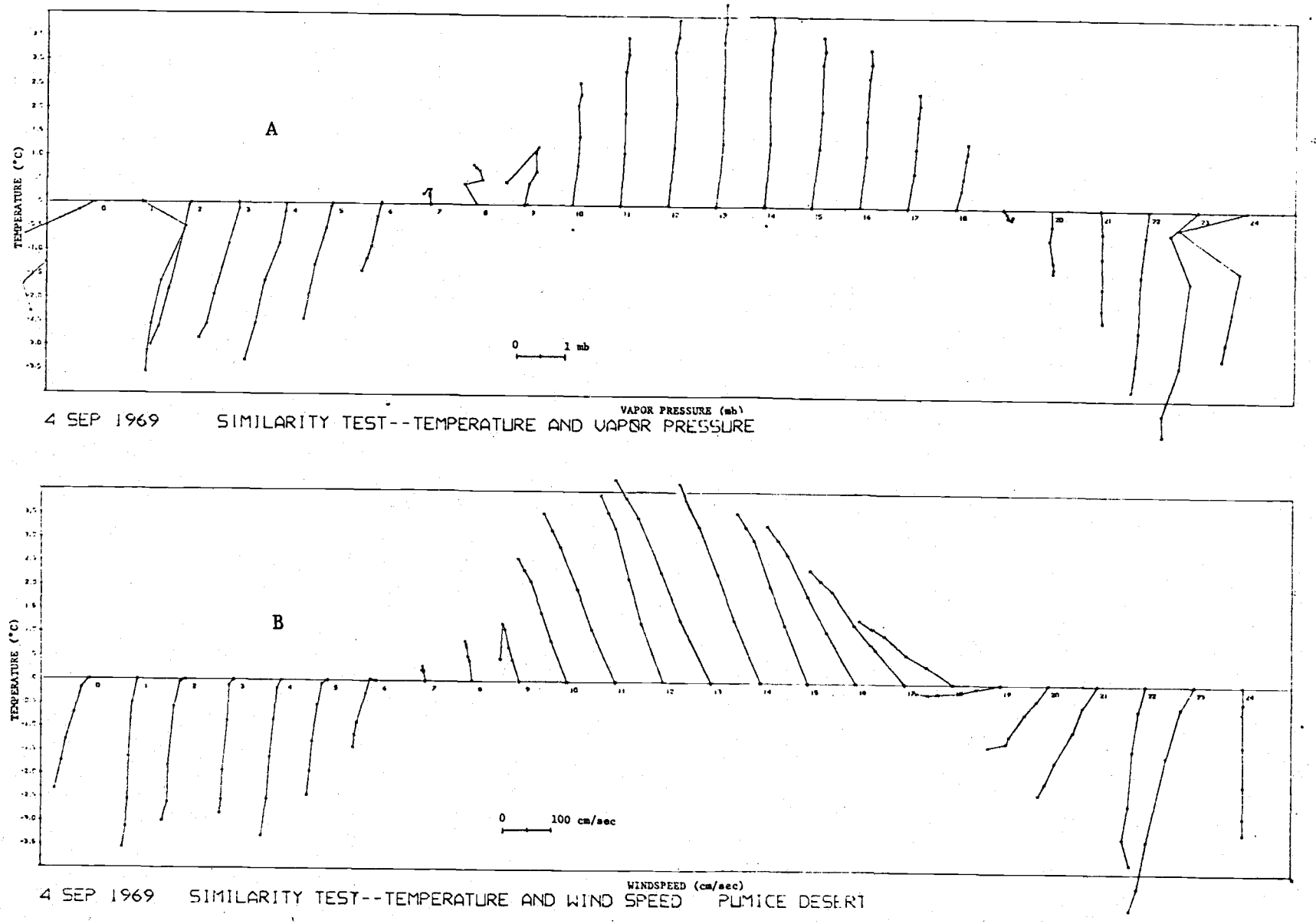

Figure 4-6. Similarity tests of the pumice desert data, Sept. 4, 1969. A. Temperature and vapor pressure. B. Temperature and wind. The value at the first level of measurement was subtracted from each reading to facilitate plotting. The plots begin at hour 0 and continue through hour 24.

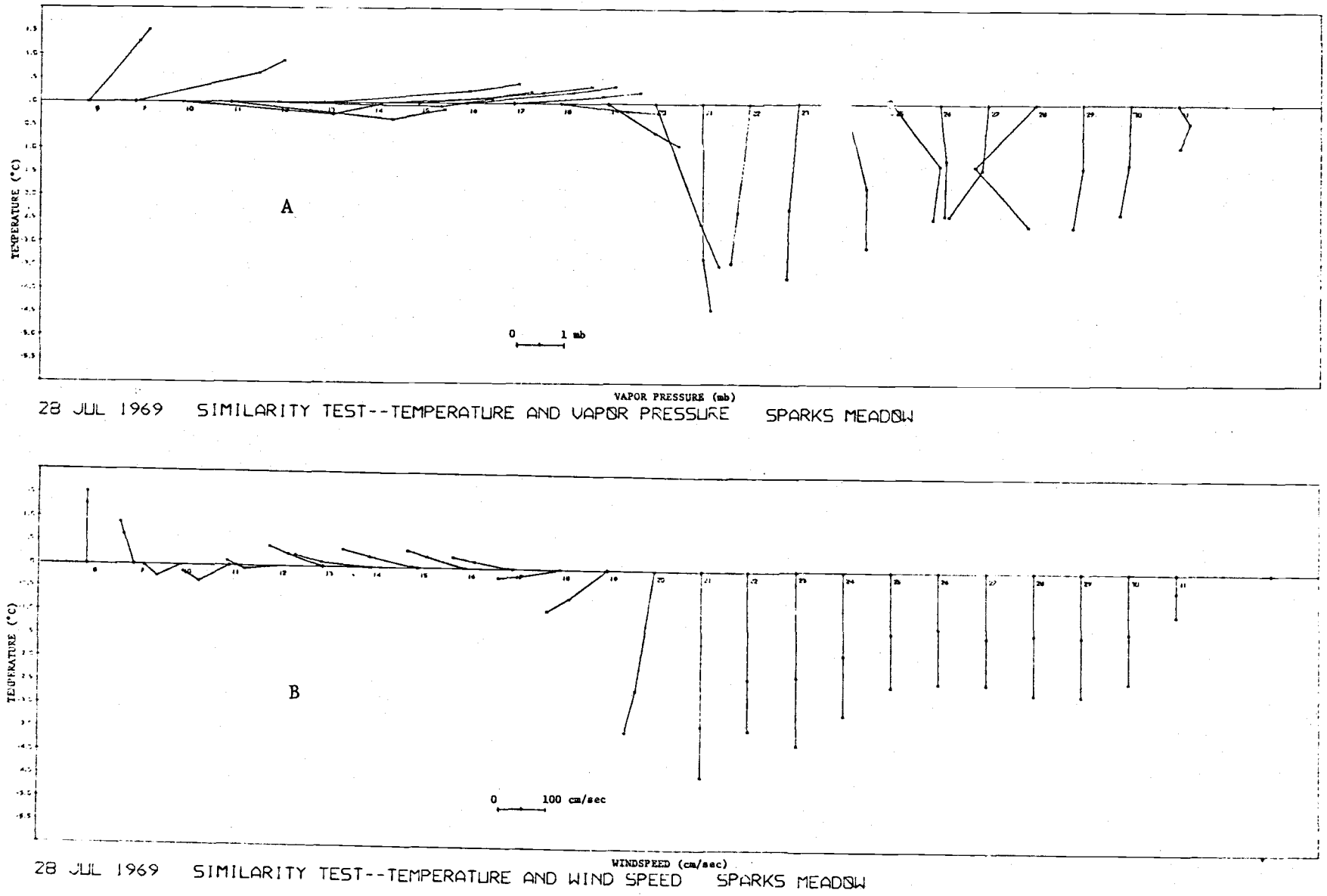

Figure 4-7. Similarity tests of the meadow data, July 28, 1969. A. Temperature and vapor pressure. B. Temperature and wind. The value at the first level of measurement was subtracted from each reading to facilitate plotting. The plots begin at hour 8 and continue through hour 31.

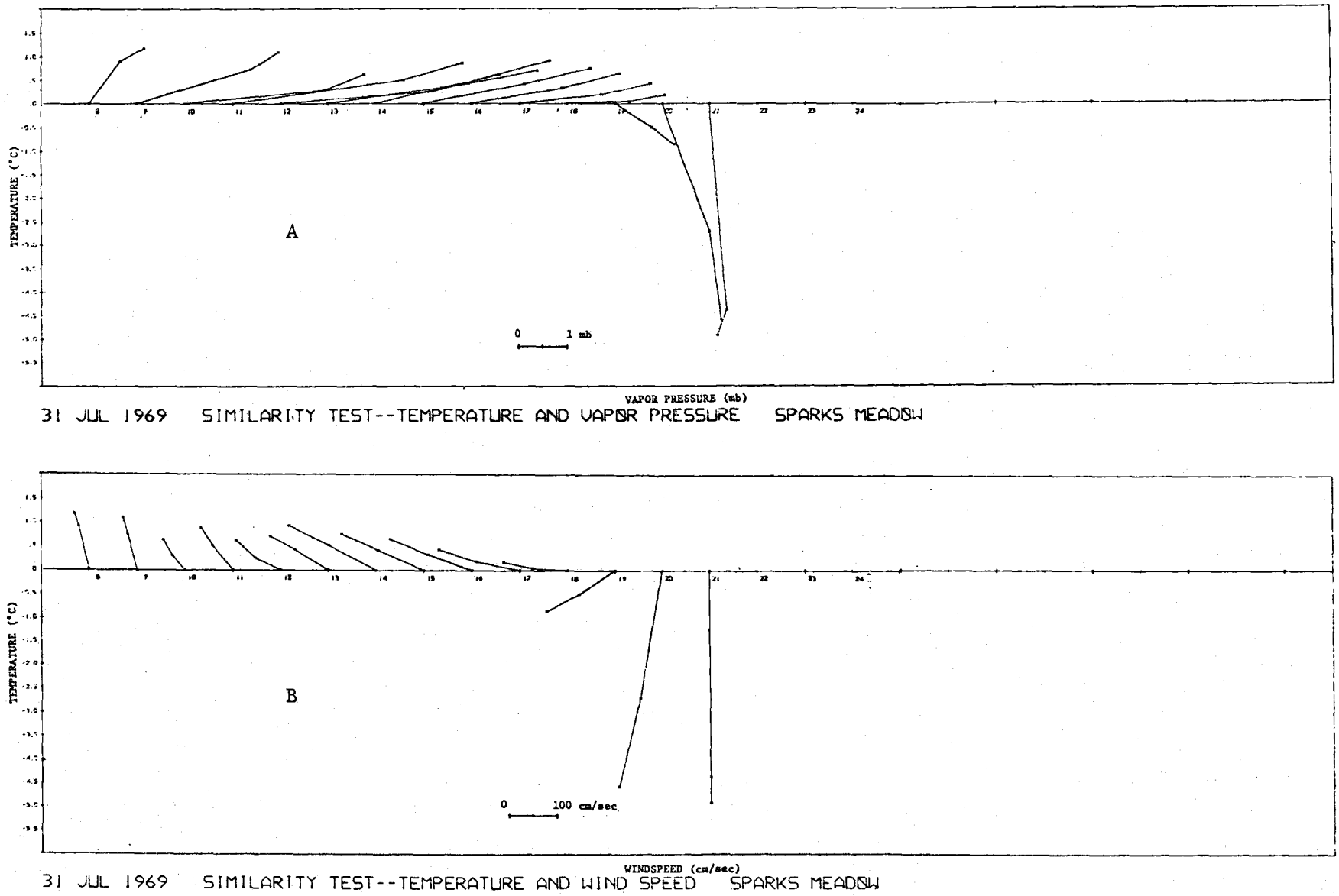

Figure 4-8. Similarity tests of the meadow data, July 31, 1969. A. Temperature and vapor pressure. B. Temperature and wind. The value at the first level of measurement was subtracted from each reading to facilitate plotting. The plots begin at hour 8 and continue through hour 21.

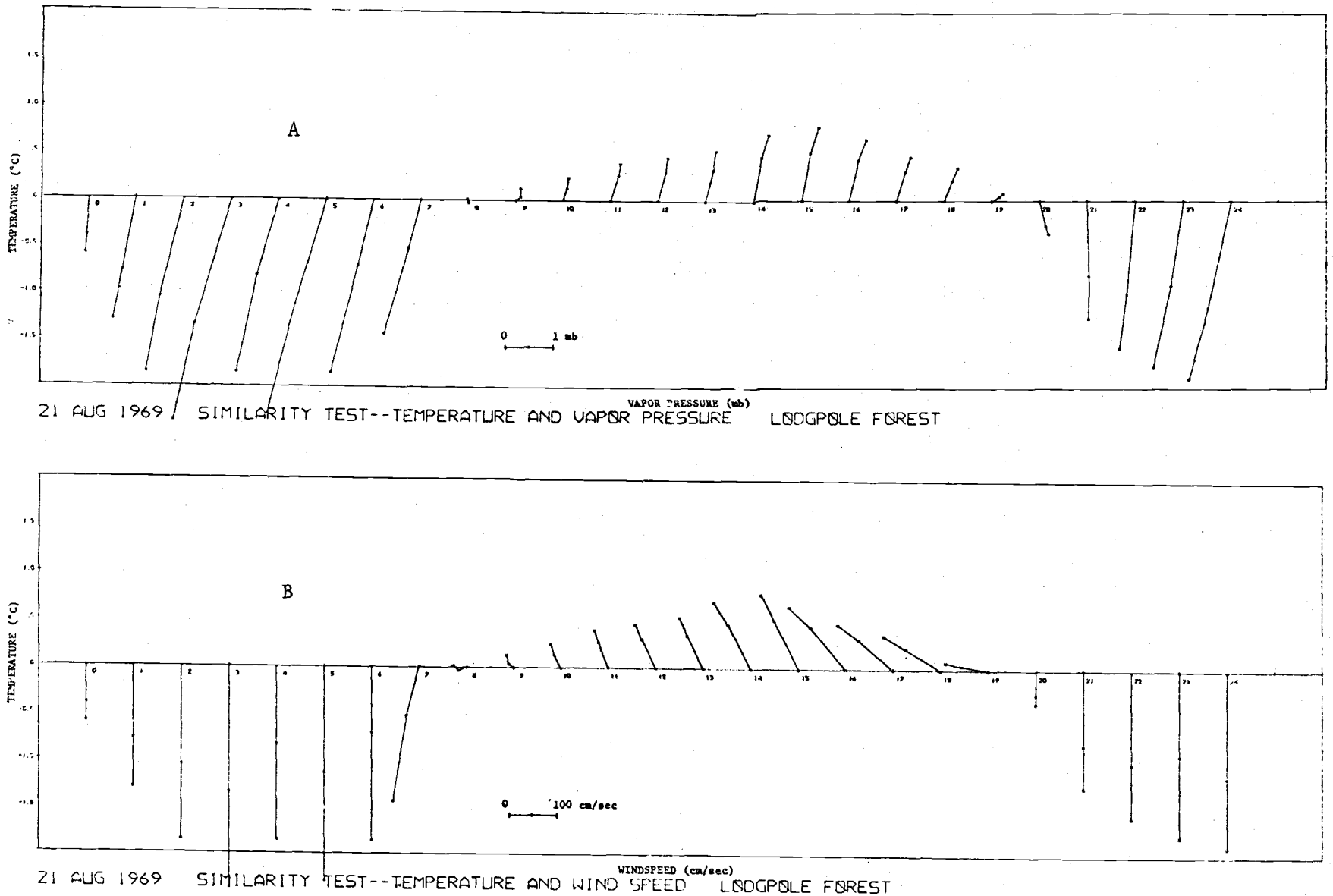

Figure 4-9. Similarity plots at the forest site, August 21, 1969. A. Temperature and vapor pressure. B. Temperature and wind. The value at the first level of measurement was subtracted from each reading to facilitate plotting. The plots begin at hour 0 and continue through hour 24.

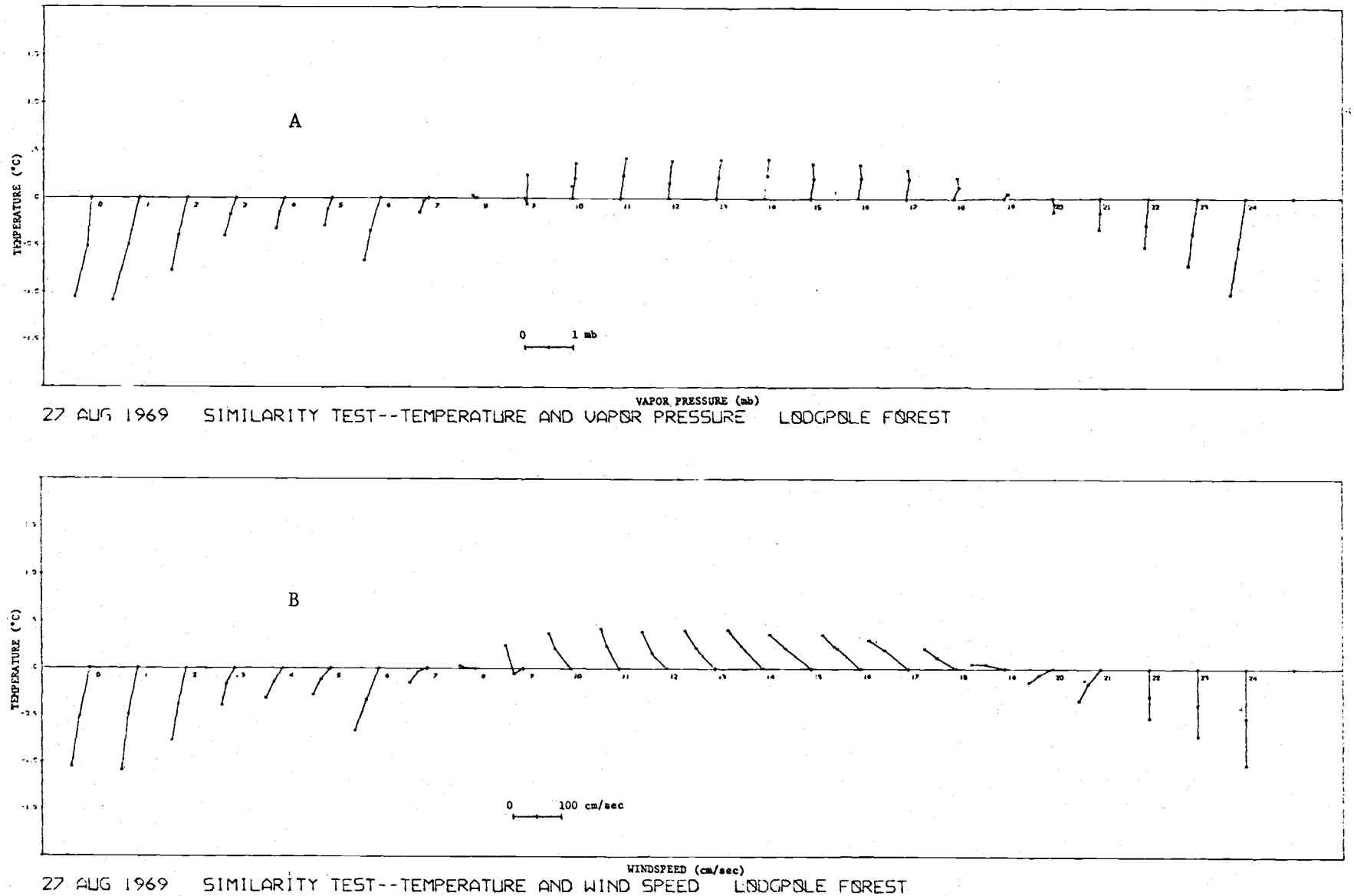

Figure 4-10. Similarity plots at the forest site, August 27, 1969. A. Temperature and vapor pressure. B. Temperature and wind. The value at the first level of measurement was subtracted from each reading to facilitate plotting. The plots begin at hour 0 and continue through hour 24.

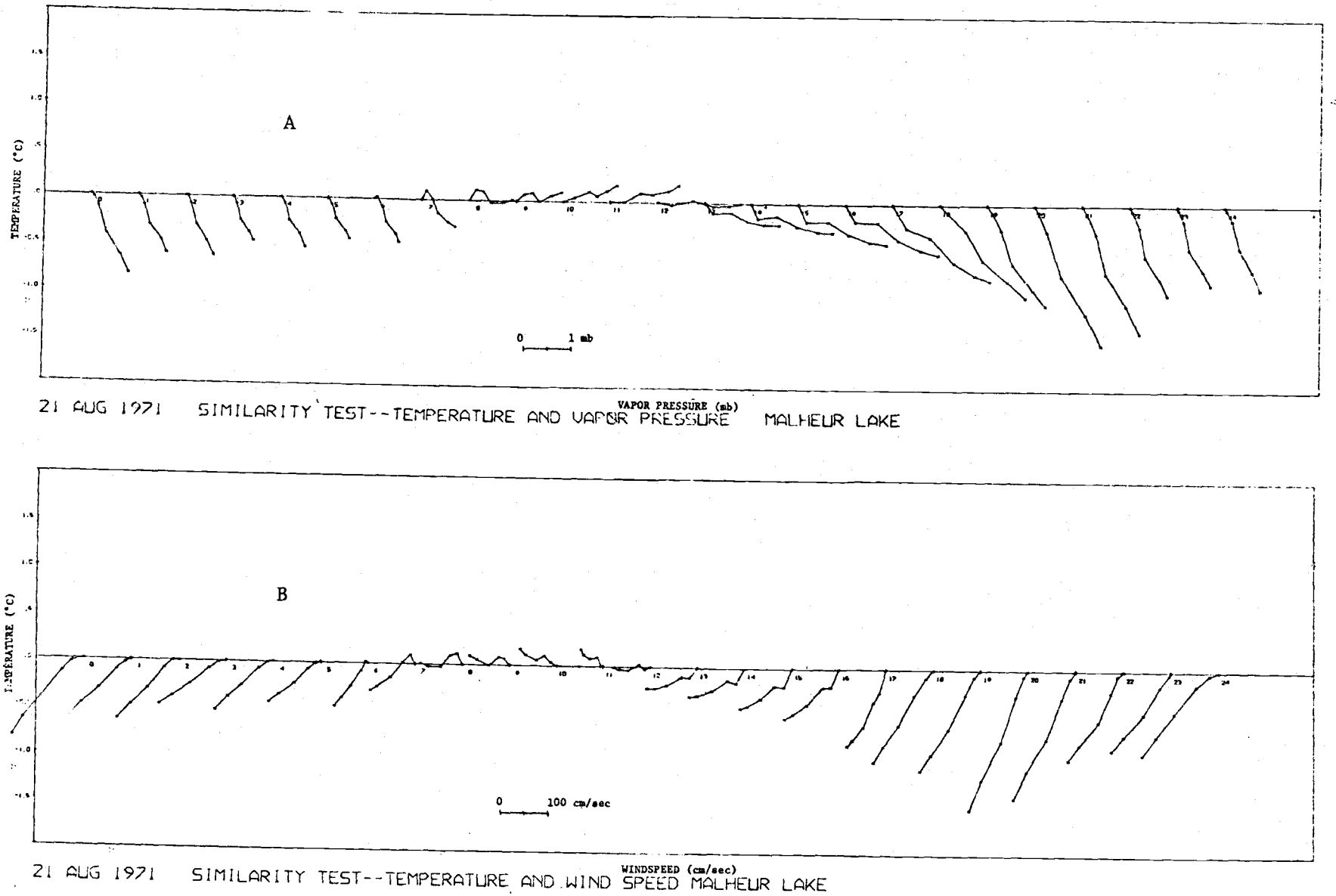

Figure 4-11. Similarity plots at the marsh, August 21, 1971. A. Temperature and vapor pressure. B. Temperature and wind. The value at the first level of measurement was subtracted from each reading to facilitate plotting. The plots begin at hour 0 and continue through hour 24.

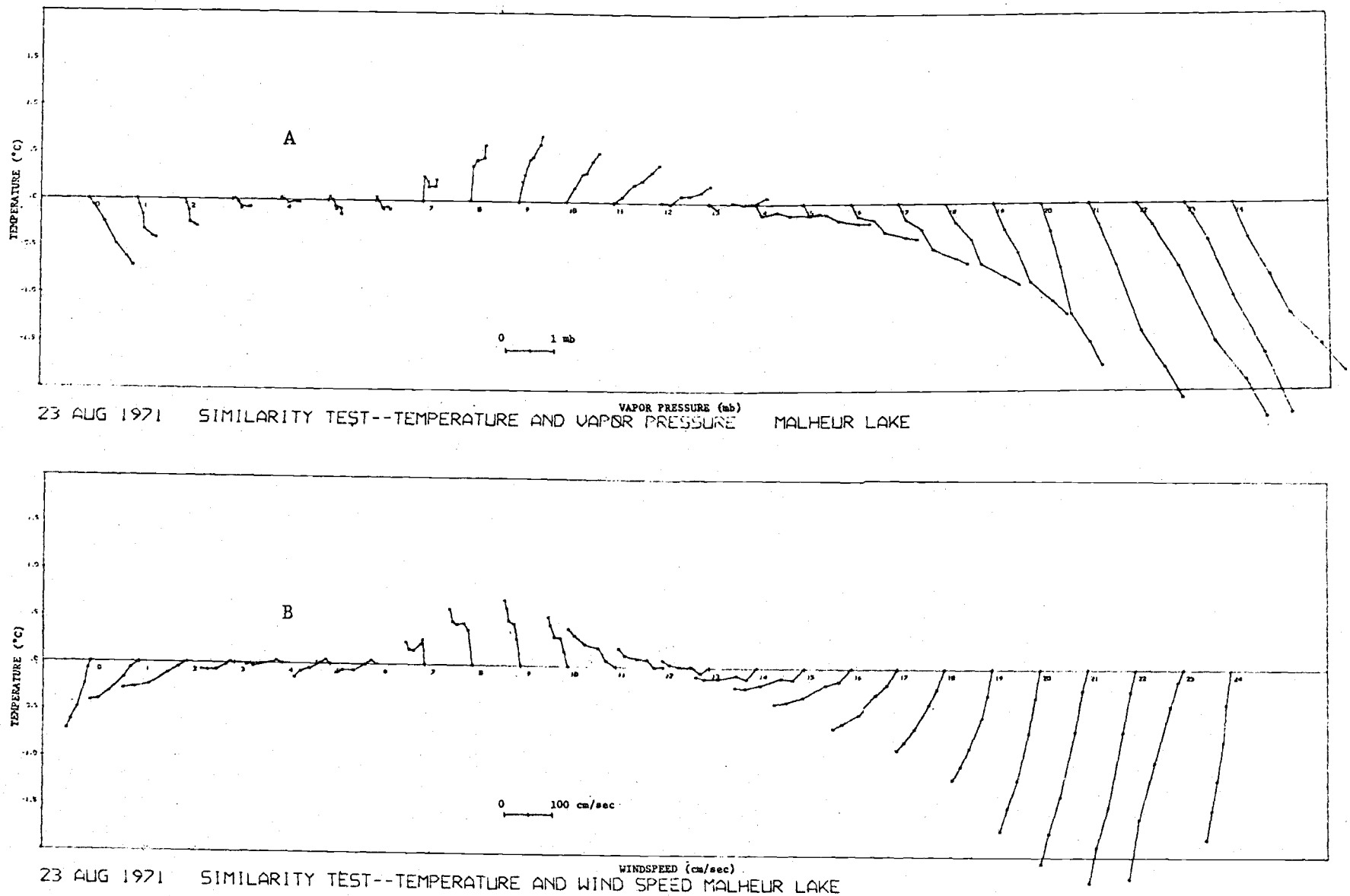

Figure 4-12. Similarity plots at the marsh, August 23, 1971. A. Temperature and vapor pressure. B. Temperature and wind. The value at the first level of measurement was subtracted from each reading to facilitate plotting. The plots begin at hour 0 and continue through hour 24.

uncertainties in the measurements. The differential gradient measurements are very critical for a variety of energy budget analyses. The uncertainties calculated for typical values are: temperature differences, $\pm$ 0.017°C; vapor pressure differences, $\pm$ 0.052 mb; and wind speed differences, $\pm$ 1 cm/sec.

The field performance of the instruments and the adequacy of the experimental design was further tested by a plotting technique. Similarity plots of temperature against wind speed, confirmed the accuracy of the field measurements. Further, the plots proved useful in selecting the appropriate instrument levels to be used in subsequent analyses, and also in interpretation of the energy exchange phenomena taking place at the surfaces.

4.5 Literature Cited.

Duebbert, H. F. 1969. The ecology of Malheur Lake and management implications. U.S. Dept. Interior, Bureau of Sport Fisheries and Wildlife. Refuge Leaflet No. 412, November 1969. 24 pp.

Holbo, R. 1972. The energy budget of a pumice desert. Ph.D. Thesis, Oregon State University, Corvallis. 142 pp.

IGY Instruction Manual. (1958). Part VI. Radiation instruments and measurements. Ann. IGY 5:365-466.

Oregon Water Resources Research Institute. 1971. Environmental considerations and the water resources of the Silvies Basin. WRRI-6. Oregon WRRI, Oregon State University. Corvallis, February 1971. 49+ pp.

Scarborough, J. B. 1966. Numerical Mathematical Analysis. Johns Hopkins Press. 6th edition.

Tanner, C. B. 1963. Basic instrumentation and measurements for plant environment and micrometeorology. Soils Bull. 6, Univ. Wisconsin, Madison.

5. RESULTS AND DISCUSSION

Thermal properties play an important role in the transformation of energy at a natural surface. The major input of energy is by radiation; dissipation is by reradiation, convection, evaporation and storage. The application of transfer models to the microclimate data collected at each site will define the energy budgets and aid in identifying those surface properties that have the greatest influence upon the energy exchange processes. This will then help us to predict and interpret the effects of changes in surface characteristics. There are few reports available that permit a comparison among energy budgets of dissimilar surfaces. Miller (1965) summarized reports from a variety of sources, and Aizenshtat (1960) has compared the energy budgets of several surfaces in an arid region.

The radiation exchange processes will be examined first, for they provide the major source of energy to the surface. The other modes of thermal energy transfer will then be examined in order to evaluate the dissipation of energy by the surface.

5.1 Radiation Budget Results

Net radiation (Q*) over a surface is the residual value of the incoming radiation minus that leaving the surface. The net radiation term thus represents the amount of energy that is transformed from radiant to non-radiant forms. The properties of the surface play an important role in the transformation process and thus influence the net amount of radiation that is transformed, or made available, at the surface. These surface properties can be examined through measurements of the different components of the radiation budget. This has been done in Miller's (1965) synthesis of energy exchange reports, by Reifsnyder and Lull (1965), by Gay (1971) and Gay and Knoerr (1970).

The incoming components are shortwave radiation from the sun ($K\downarrow$) and longwave radiation from the atmosphere ($L\downarrow$). The components leaving the surface are reflected shortwave ($K\uparrow$) and outgoing longwave ($L\uparrow$). The reflected fraction of shortwave radiation is called "albedo" (α) and may be expressed in percent. Outgoing longwave radiation actually consists of three parts. The major portion (Lg) is that emitted in relation to the emissivity and absolute temperature of the surface. A small portion is that fraction of incoming longwave reflected at the surface ($rL\downarrow$) in proportion to the coefficient of reflectivity (r) for longwave radiation. The value of r over vegetated surfaces is in the order of 1 percent. Another small portion of outgoing longwave is that emitted by the layer of the atmosphere between the surface and the radiometer; this may be symbolized as $A\uparrow$. In practice, however, we shall not attempt to break down the value of $L\uparrow$ measured at the level of the radiometer several meters above the surface.

The diurnal course of the mean hourly radiation budget components is plotted in Figures 5-1 through 5-4 for the pumice, meadow, forest and marsh sites. The mean daily radiation budget components and albedo values are summarized in Table 5-1 for the period of measurements.

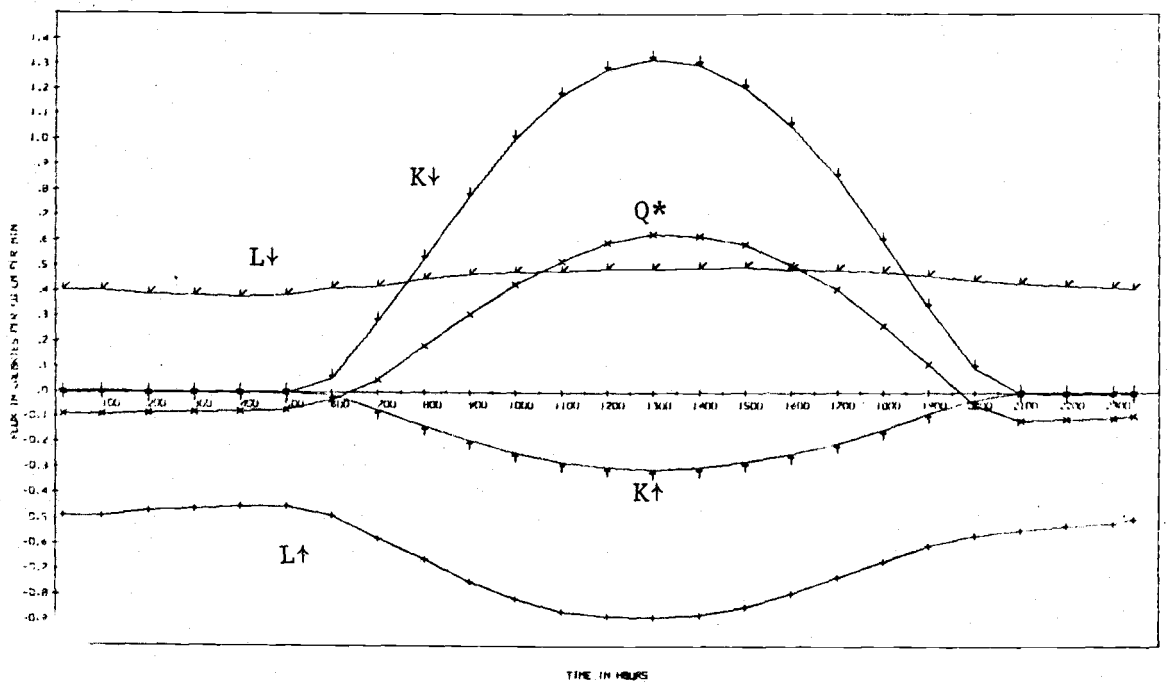

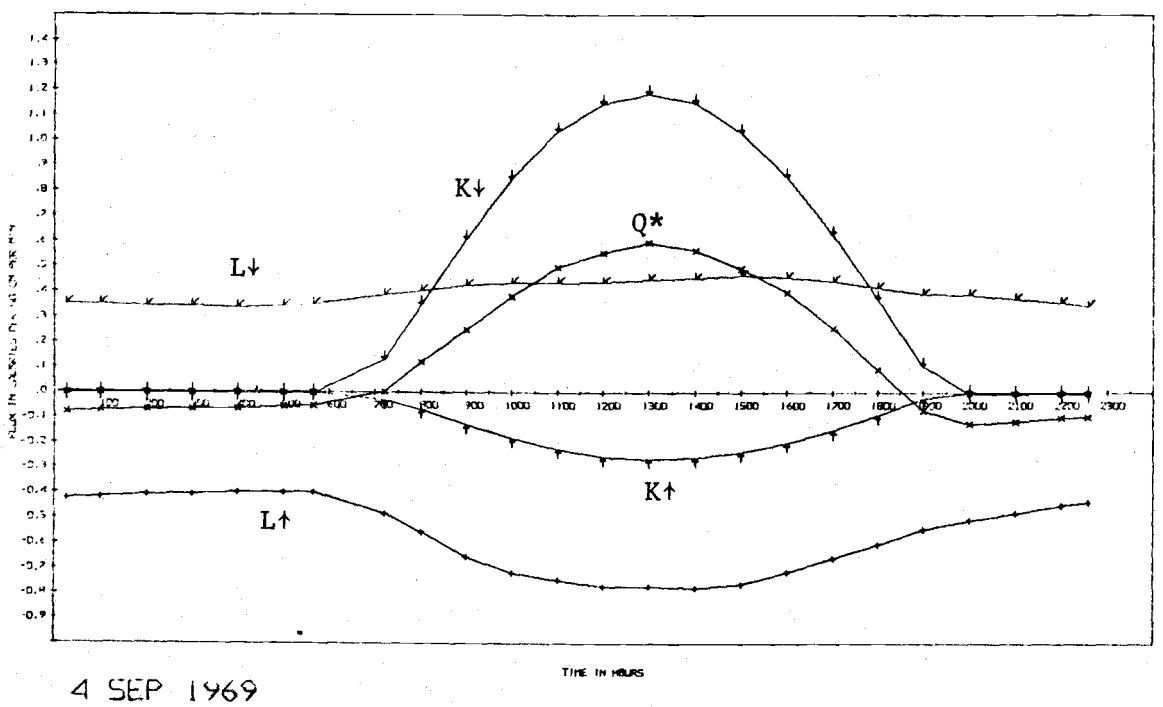

Figure 5-1. The diurnal course of the radiation budget components at the pumice site. Symbols are defined in the text.

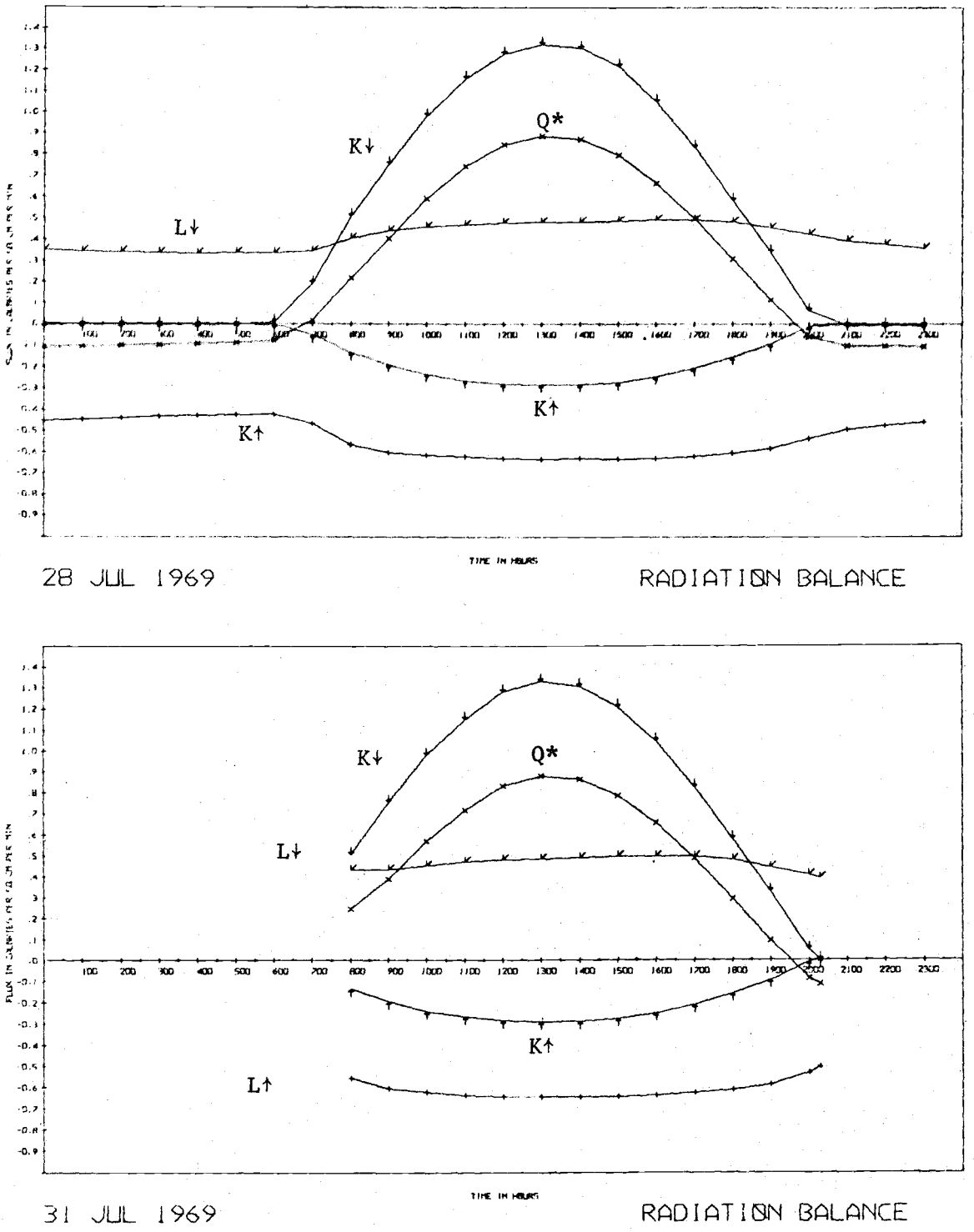

Figure 5-2. The diurnal course of the radiation budget components at the meadow site. Symbols are defined in the text.

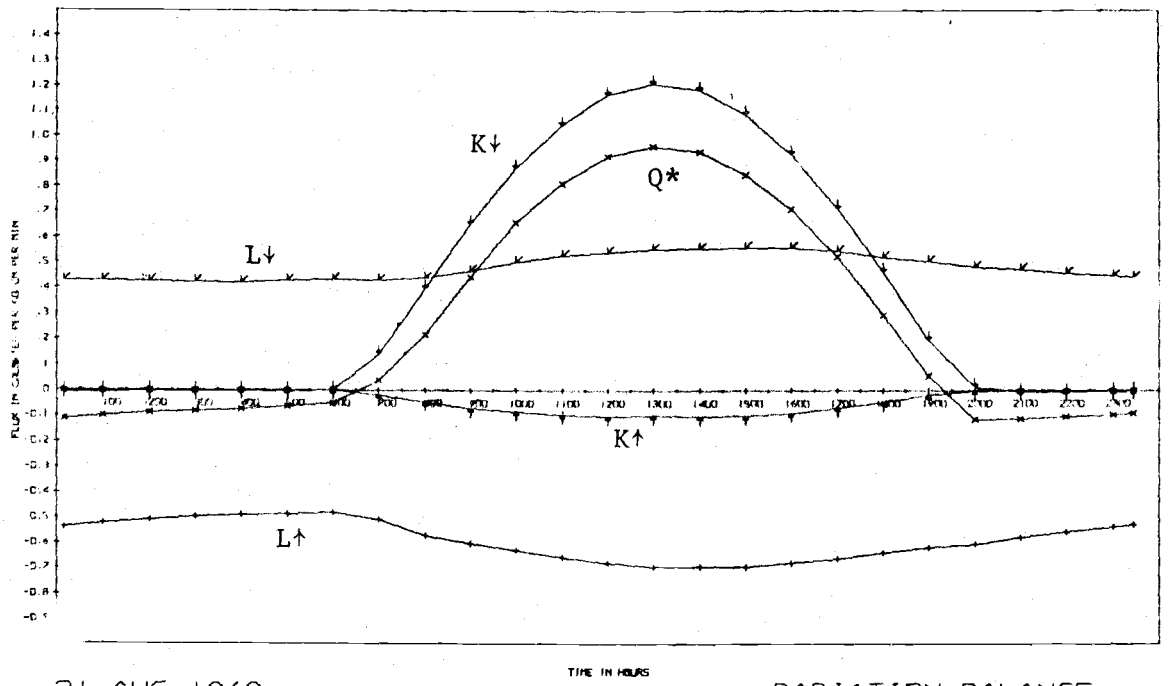

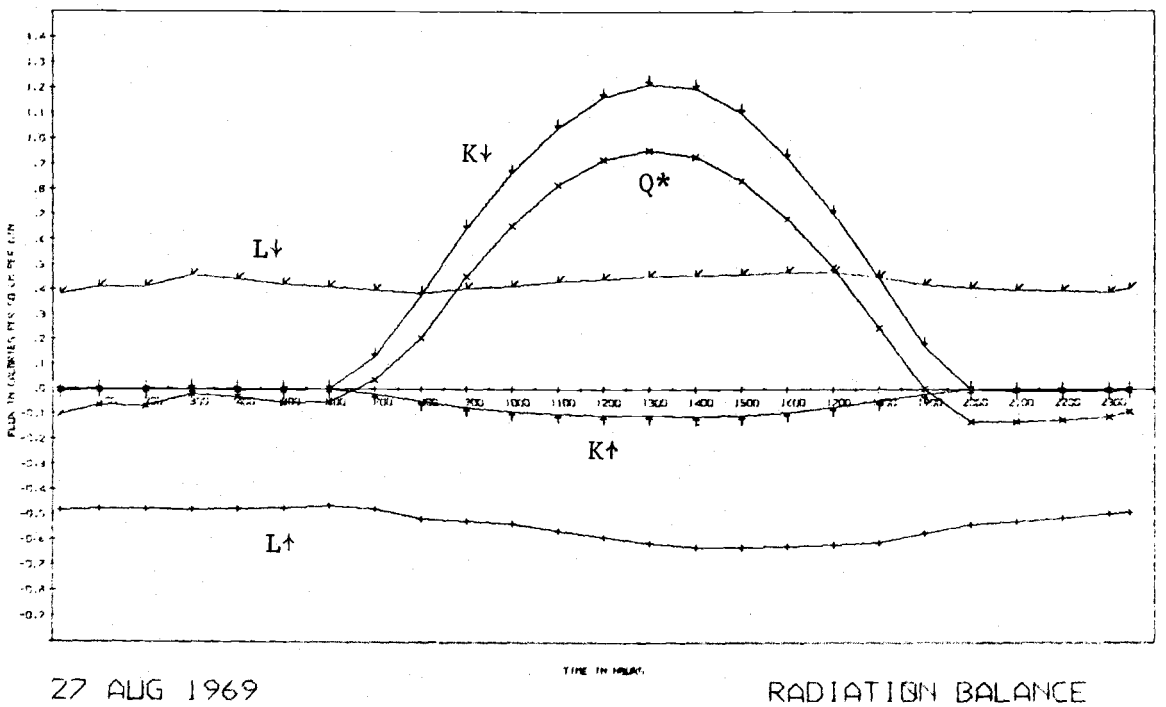

Figure 5-3. The diurnal course of the radiation budget components at the forest site. Symbols are defined in the text.

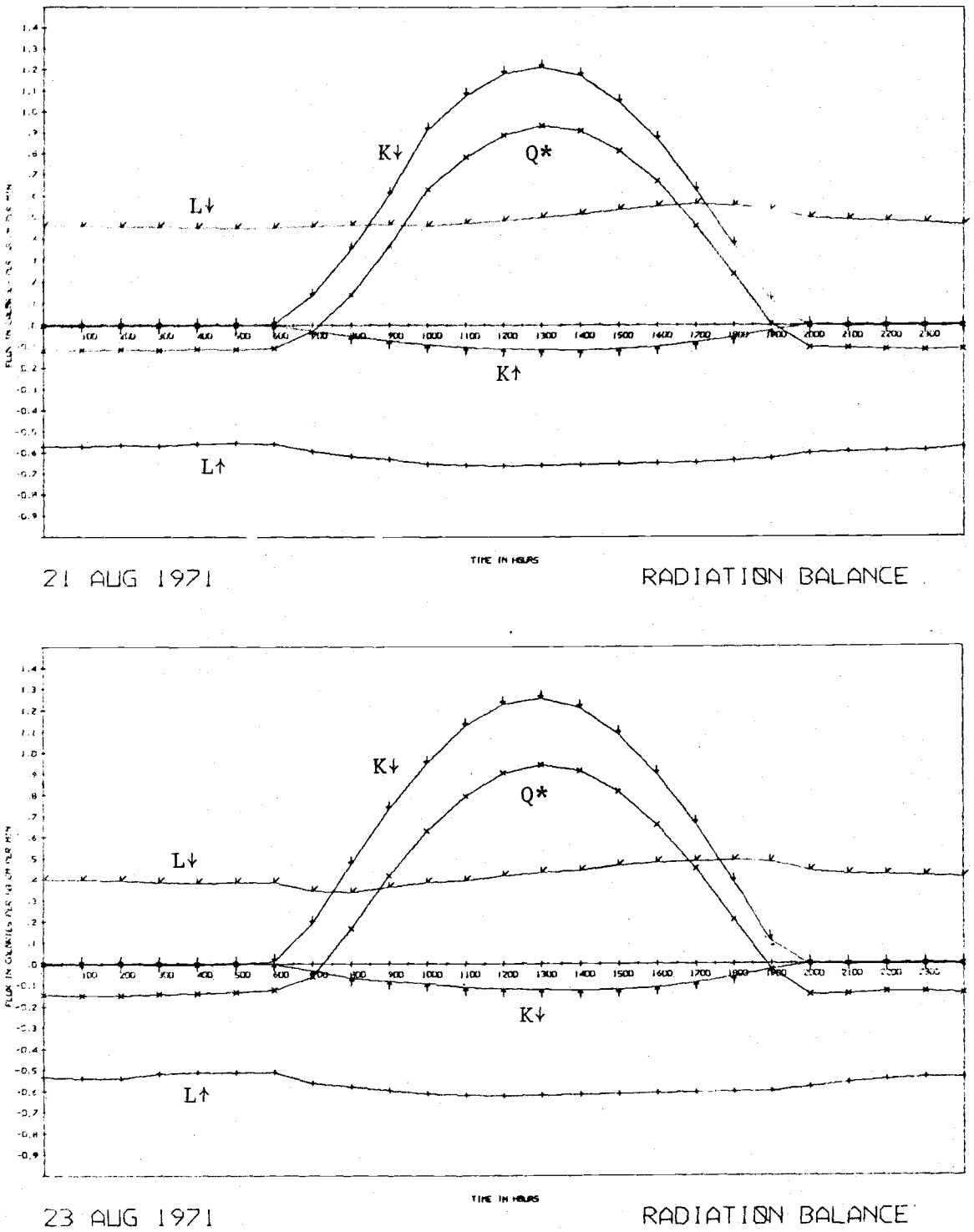

Figure 5-4. The diurnal course of the radiation budget components at the marsh site. Symbols are defined in the text.

Table 5-1. Mean radiation budgets for the four sites. Flux units are cal/cm^2/day, and albedo (α) is in percent.

Surface	albedo α	Shortwave $K\downarrow$	$K\uparrow$	K^*	Longwave $L\downarrow$	$L\uparrow$	L^*	Allwave $Q\downarrow$	$Q\uparrow$	Q^*
Pumice	23%	637	148	489	605	868	-263	1242	1016	226
Meadow	25%	694	164	529	596	773	-177	1288	937	351
Forest	10%	602	58	544	652	812	-160	1254	870	384
Marsh	11%	598	69	529	650	854	-204	1248	923	325

5.2 Radiation Budget Discussion

Several factors should be kept in mind during the discussion of the radiation measurements. For example, the measurements were not made at the same time and under strictly comparable conditions. Also, the accuracy of measurement of the shortwave components is in the order of 5 percent, while the longwave and net components may be only within 10 percent. However, the measurement days exhibit the same cloudless sky pattern, and they all fell within a seven week period from mid-July to early September. Within these limitations of precision and similarity, the budget components can be examined for information on the way the various surfaces transform radiation.

5.2.1 Shortwave Exchange.

The albedo of a surface plays a major role in the availability of energy for transformation. The data in Table 5-1 suggest that the four surfaces fall into two groups. The pumice and the meadow are relatively poor absorbers with albedos measuring 23 percent and 25 percent, respectively. The forest and the marsh, in contrast, are good absorbers with albedos of only 10 and 11 percent, respectively.

The 25 percent value of the meadow albedo is close to values reported elsewhere for surfaces covered with low, dense vegetation. Monteith (1959), for example, proposed a generalized albedo of 26 percent for field crops based upon his measurements of both individual leaves and plant communities. The low albedos for the forest and the marsh are also corroborated by other reports (Gay and Knoerr, 1970).

The major effect of the albedo differences can be seen in the shortwave absorption totals (K^*) in Table 5-1. Even though the pumice and meadow sites received the most shortwave radiation ($K\downarrow$) during the period of measurement, the forest and marsh absorbed the most. The relatively large quantities of absorbed solar radiation at the forest and marsh sites must then be dissipated through other energy exchange processes.

5.2.2 Longwave Exchange

The gain and loss of longwave radiation also affects the radiant energy available to a surface. The net exchange of longwave radiation (L^*) in Table 5-1 suggests that the surfaces can again be ordered into two groups. The emission of longwave radiation by the pumice surface far exceeds the gain from the atmosphere; the net loss is -263 cal/cm^2/day. The marsh had the second largest longwave loss, totaling -204 cal/cm^2/day. The meadow and forest, on

the other hand, showed lower net losses in the order of -170 cal/cm^2/day. The differences among the last three surfaces are small, however, and thus may not be significant.

The net longwave totals indicate that the pumice surface maintains a relatively warm surface temperature for a given regime of energy exchange. Energy dissipation processes other than radiation exchange enter into the development of a warm surface temperature, and these will be discussed in a later section.

5.2.3 Allwave Exchange

The total radiant energy supplied to the surfaces is also of interest. The totals can be deduced from Table 5-1. Summing K↓ and L↓ yields incoming radiation totals (Q↓) of 1242, 1288, 1254, and 1248 cal/cm^2/day for the pumice, meadow, forest and marsh respectively. In other words, the total radiation incident upon the four surfaces varied approximately 2 percent about a mean of 1258 cal/cm^2/day. The total radiation input was unexpectedly uniform for the four sites.

Net radiation for each site depends upon the characteristics of each surface that control the absorption and subsequent dissipation of the radiation. Some of these differences are associated with albedo. Others, however, require further consideration of the energy budget components for understanding. Note for example, that the net transformed radiation (Q*) over the pumice is much less than over the meadow, even though the albedos are similar. In our later examination of energy budget results, we shall see that the meadow is more efficient than the pumice in transforming absorbed radiation into non-radiant forms of energy, principally the latent heat of evaporation.

Because of the interaction between radiation properties and energy budget processes, it is not possible to deduce complete information from measured values of net radiation alone. The forest, for example, had the greatest net radiation. In fact, Q* over the forest was 170 percent of that over the pumice. Without information on the other radiation fluxes, however, one can not determine whether the observed difference is related to the input of radiant energy, to the surface albedo, or to the efficiency of the surface in transforming radiation into the non-radiative dissipation processes of convection, evaporation, and storage. For the example of the pumice and forest, we observe that the radiant energy input was almost the same (1242 cal/cm^2 versus 1254 cal/cm^2). The net radiation differences at these two surfaces are associated with albedo (23 percent over the pumice and 10 percent over the forest), and with the transformation efficiency of the surface.

We have now examined some of the factors affecting radiation exchange, and in the next section, we will look further at the processes governing other modes of energy transfer.

5.3 Energy Budget Results.

The following comments apply to the results of the energy budget calculations from each of the four uniform sites during mid-summer conditions of clear skies and warm temperatures.

5.3.1 Pumice Desert Energy Budget.

The procedures used to evaluate the energy budget components at the pumice desert site have been described in detail by Holbo (1972) so only a summary will be given here.

The convective heat flux (H) was calculated using the aerodynamic model, Equation [1-5a], with an empirically determined stability correction (Holbo, 1971). The latent energy flux (λE) was then calculated as a residual in Equation [1-1]. The soil heat flux (G) was based upon the temperature and volumetric heat capacity measurements.

The pumice results are tabulated in Table 5-2 for July 17, and September 4, 1969. The data represent mean hourly rates in units of calories per square centimeter per minute. For convenience, the daily integrals ($cal/cm^2/day$) are also included in the Table.

The pumice site energy fluxes are plotted in Figure 5-5. The plots show the smoothness of the diurnal curves of the transformed radiation (Q^*), the change in storage (G), convection (H), and latent energy (λE).

5.3.2 Meadow Energy Budget

The Bowen ratio method, Equation [1-4], was used to evaluate the latent and convective energy fluxes at the meadow site. The soil heat flux was measured directly with heat flux plates at the -5 cm level; this was the approximate depth of the interface between the fiberous roots and the soil matrix. No correction was applied to the soil heat flux for changes in storage in the 5 cm layer between the flux plates and the surface. This affects the magnitude of the hourly values, but should not affect the daily means.

The energy budget analyses for the meadow site are tabulated in Table 5-3 for mean hourly rates ($cal/cm^2/min$) and for daily integrals ($cal/cm^2/day$). The diurnal cycle of energy exchange for the meadow is plotted in Figure 5-6.

5.3.3 Forest Energy Budget

The Bowen ratio method, Equation [1-4], was used to evaluate the latent and convective fluxes over the lodgepole pine forest. The soil heat flux was measured directly with soil heat flux plates positioned 5 cm below the interface between the litter layer and the mineral soil. As in the meadow, no correction was applied for the energy storage changes in the soil and litter layer above the flux plates.

The energy budget analyses for the lodgepole pine stand are tabulated in Table 5-4, and plotted in Figure 5-7.

5.3.4 The Marsh Energy Budget

The marsh energy budget was developed from aerodynamic estimates of latent and convective energy. The application of Equations [1-5, 1-6] at the marsh site requires additional considerations that should be mentioned here.

Table 5-2. The energy budget components at the pumice site, July 17, and September 4, 1969. Tabulated data have units of cal/cm^2/min, while the integrated units are cal/cm^2/day.

Pumice Site	17 JUL 1969	Instrument levels: 80 and 320 cm			Pumice Site	4 SEP 1969	Instrument levels: 40 and 240 cm		
Period	Q*	G	H	E	Period	Q*	G	H	E
30- 130	-0.0902	.0642	.0221	.0039	30- 130	-0.0723	.0555	.0011	.0156
130- 230	-0.0850	.0944	.0085	-0.0179	130- 230	-0.0535	.0718	.0047	-0.0070
230- 330	-0.0809	.0885	.0133	-0.0209	230- 330	-0.0667	.0630	.0017	.0020
330- 430	-0.0771	.0870	.0016	-0.0116	330- 430	-0.0649	.0631	.0034	-0.0016
430- 530	-0.0711	.0805	.0029	-0.0123	430- 530	-0.0577	.0556	.0041	-0.0020
530- 630	-0.0324	.0526	.0017	-0.0218	530- 630	-0.0452	.0440	.0040	.0028
630- 730	.0486	-0.0157	-0.0466	.0137	630- 730	-0.0100	0	-0.0079	.0179
730- 830	.1371	-0.0889	-0.0927	-0.0014	730- 830	.1223	-0.0655	-0.0298	-0.0270
830- 930	.3093	-0.1569	-0.1400	-0.0124	830- 930	.2505	-0.1022	-0.0866	-0.0618
930-1030	.4281	-0.1915	-0.2034	-0.0333	930-1030	.3802	-0.1114	-0.2336	-0.0352
1030-1130	.5204	-0.1930	-0.2379	-0.0835	1030-1130	.4977	-0.1019	-0.3798	-0.0159
1130-1230	.5940	-0.1977	-0.3801	-0.0262	1130-1230	.5566	-0.1118	-0.4447	-0.0001
1230-1330	.6268	-0.1641	-0.3730	-0.0898	1230-1330	.5961	-0.1000	-0.5228	.0266
1330-1430	.6139	-0.1367	-0.4169	-0.0664	1330-1430	.5645	-0.0962	-0.4587	-0.0096
1430-1530	.5864	-0.0957	-0.4327	-0.0680	1430-1530	.4914	-0.0776	-0.3712	-0.0425
1530-1630	.5078	-0.0357	-0.4051	-0.0670	1530-1630	.3959	-0.0359	-0.3483	-0.0117
1630-1730	.4097	.0127	-0.3107	-0.1103	1630-1730	.2571	.0002	-0.2341	-0.0232
1730-1830	.2669	.0560	-0.2238	-0.0992	1730-1830	.0837	.0240	-0.1010	-0.0127
1830-1930	.1135	.0919	-0.0877	-0.1176	1830-1930	-0.0722	.0679	.0087	-0.0044
1930-2030	-0.0510	.1177	.0121	-0.1524	1930-2030	-0.1250	.0895	.0162	.0193
2030-2130	-0.1116	.1231	.0268	-0.0383	2030-2130	-0.1145	.0808	.0337	-0.0009
2130-2230	-0.1070	.1051	.0532	-0.0512	2130-2230	-0.0984	.0971	.0080	-0.0063
2230-2330	-0.1071	.0915	.0251	-0.0135	2230-2330	-0.0900	.0126	.0695	.0078
2330- 30	-0.0966	.0778	.0236	-0.0048	2230- 30	-0.0811	.0340	.0301	.0170
INTEGRAL	258	-7	-197	-54	INTEGRAL	194	-2	-180	-11

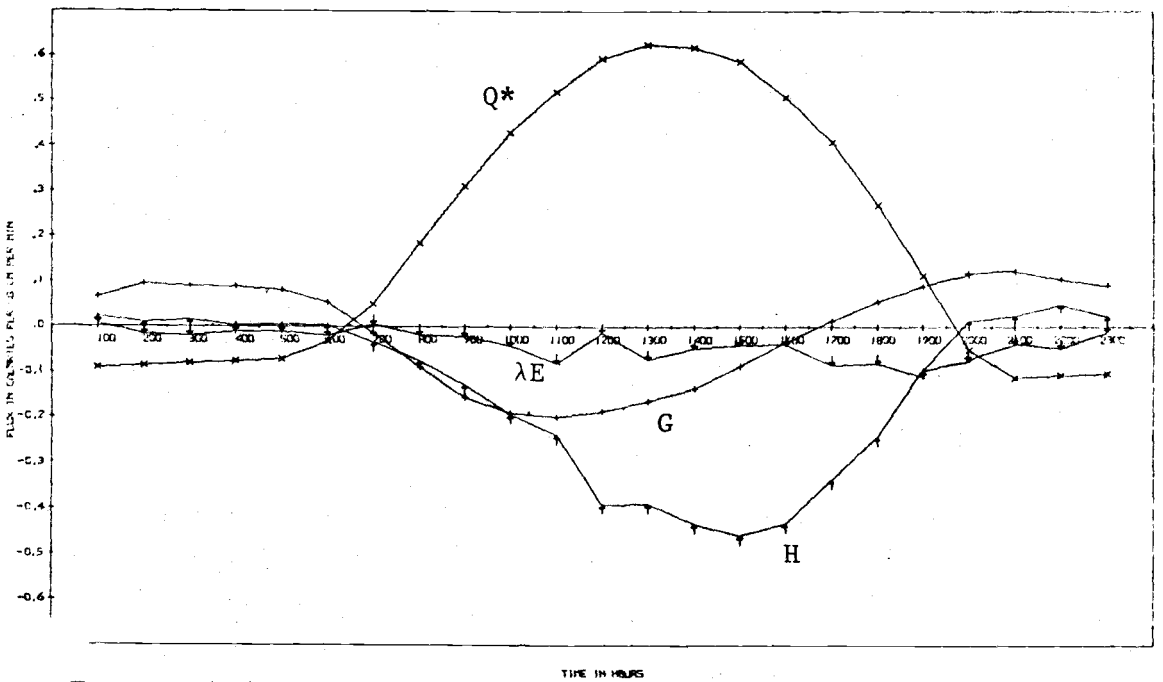

17 JUL 1969 ENERGY BUDGET--PUMICE SITE

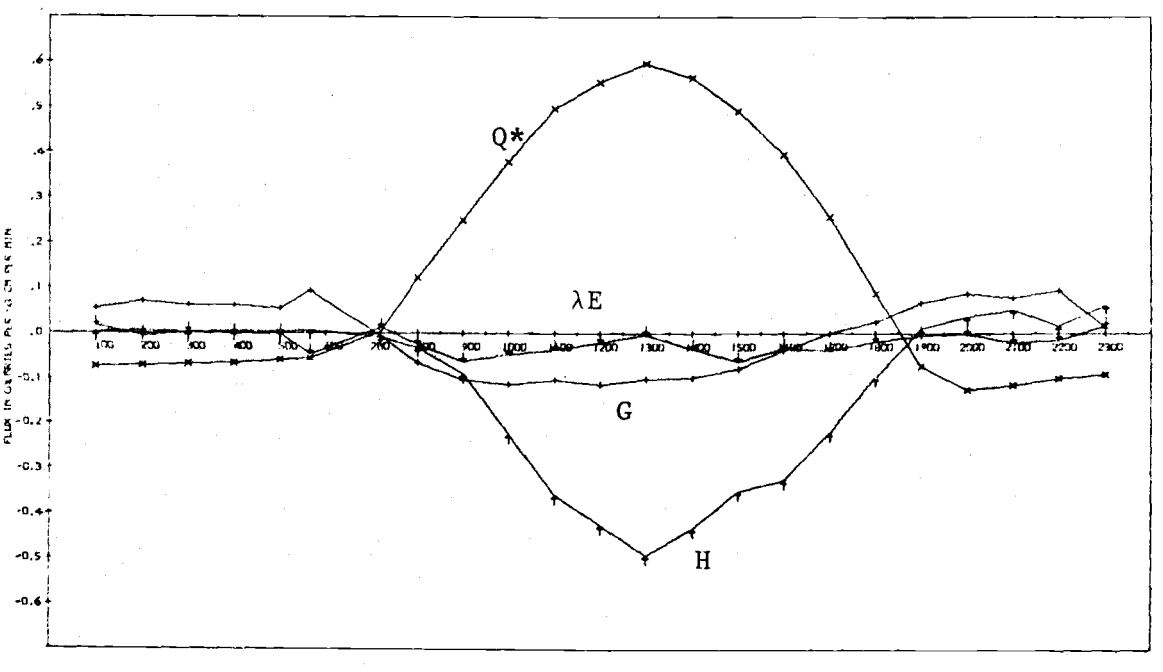

4 SEP 1969 ENERGY BUDGET--PUMICE SITE

Figure 5-5. The diurnal course of the energy budget components at the pumice site. Symbols are defined in the text.

Table 5-3. The energy budget components at the meadow site, July 28 and 31, 1969. Tabulated data are in units of cal/cm^2/min, while the integrated units are cal/cm^2/day.

Meadow	28 JUL 1969	Instrument levels: 20 and 160 cm		
Period	Q*	SHF	H	E
30- 13	-0.1076	.0430	.1719	-0.1073
130- 23	-0.1029	.0441	.0633	-0.0045
230- 33	-0.0996	.0452	.0334	.0210
330- 43	-0.0952	.0462	.0445	.0046
430- 53	-0.0912	.0465	.0390	.0056
530- 63	-0.0793	.0463	.0281	.0049
630- 73	.0199	.0434	-0.0679	.0046
730- 83	.2175	.0291	-0.0939	-0.1437
830- 93	.4020	-0.0154	-0.0520	-0.3346
930-103	.5930	-0.0544	.0021	-0.5407
1030-113	.7450	-0.0834	.0125	-0.6740
1130-123	.8457	-0.0967	-0.0081	-0.7409
1230-133	.8883	-0.0990	-0.0414	-0.7488
1330-143	.8720	-0.0884	-0.0291	-0.7544
1430-153	.7964	-0.0708	-0.0376	-0.6890
1530-163	.6669	-0.0548	-0.0365	-0.5756
1630-173	.4994	-0.0374	-0.0212	-0.4408
1730-183	.3098	-0.0212	.0180	-0.3066
1830-193	.1156	-0.0054	.0566	-0.1668
1930-203	-0.0639	.0086	.1838	-0.1284
2030-213	-0.1018	.0231	.0850	-0.0063
2130-223	-0.1030	.0334	.0575	.0122
2230-233	-0.1061	.0388	.0600	.0073
2330- 3	-0.1102	.0417	.0917	-0.0232
INTEGRAL	354	-8	33	-379

Meadow	31 JUL 1969	Instrument levels: 20 and 240 cm		
PERIOD	Q(1)	SHF	H(B)	E(B)
730- 830	.2484	.0188	-0.0952	-0.1721
830- 930	.3874	-0.0154	-0.0621	-0.3449
930-1030	.5694	-0.0527	-0.0429	-0.4747
1030-1130	.7161	-0.0797	-0.0569	-0.5795
1130-1230	.8299	-0.0959	-0.0493	-0.6846
1230-1330	.8779	-0.1001	-0.0615	-0.7164
1330-1430	.8632	-0.0944	-0.0932	-0.6756
1430-1530	.7838	-0.0800	-0.0738	-0.6300
1530-1630	.6560	-0.0626	-0.0592	-0.5342
1630-1730	.4864	-0.0416	-0.0333	-0.4115
1730-1830	.2928	-0.0230	-0.0103	-0.2594
1830-1930	.0927	-0.0063	.0558	-0.1422
1930-2030	-0.0848	.0098	.1483	-0.0724

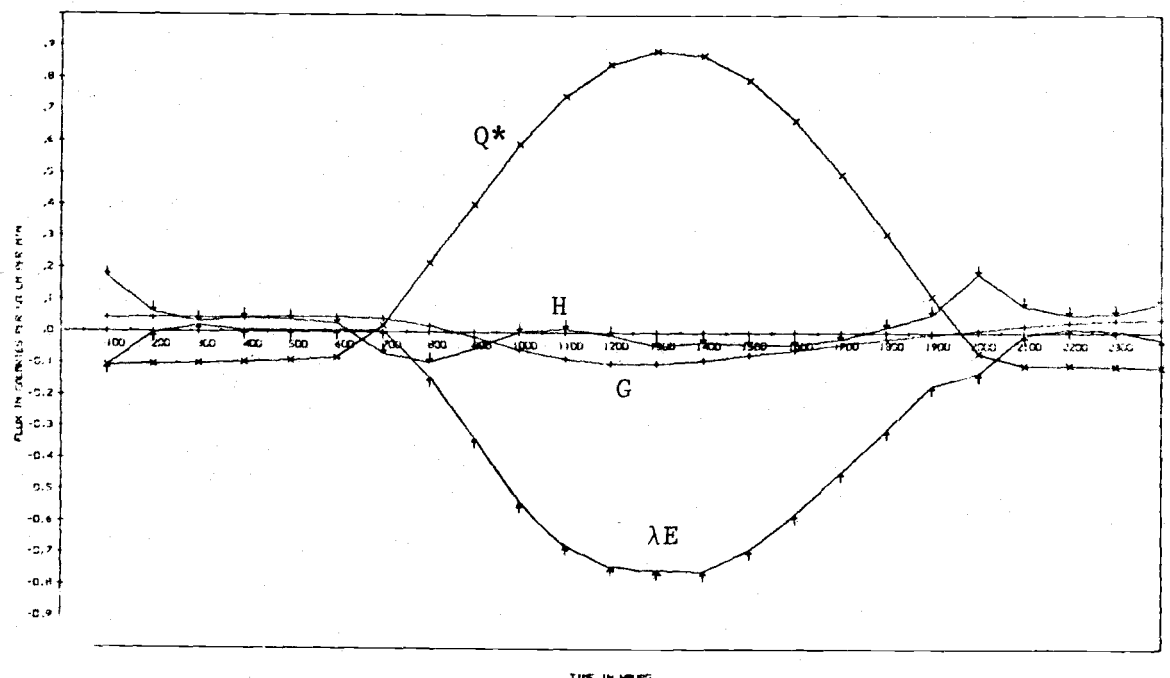

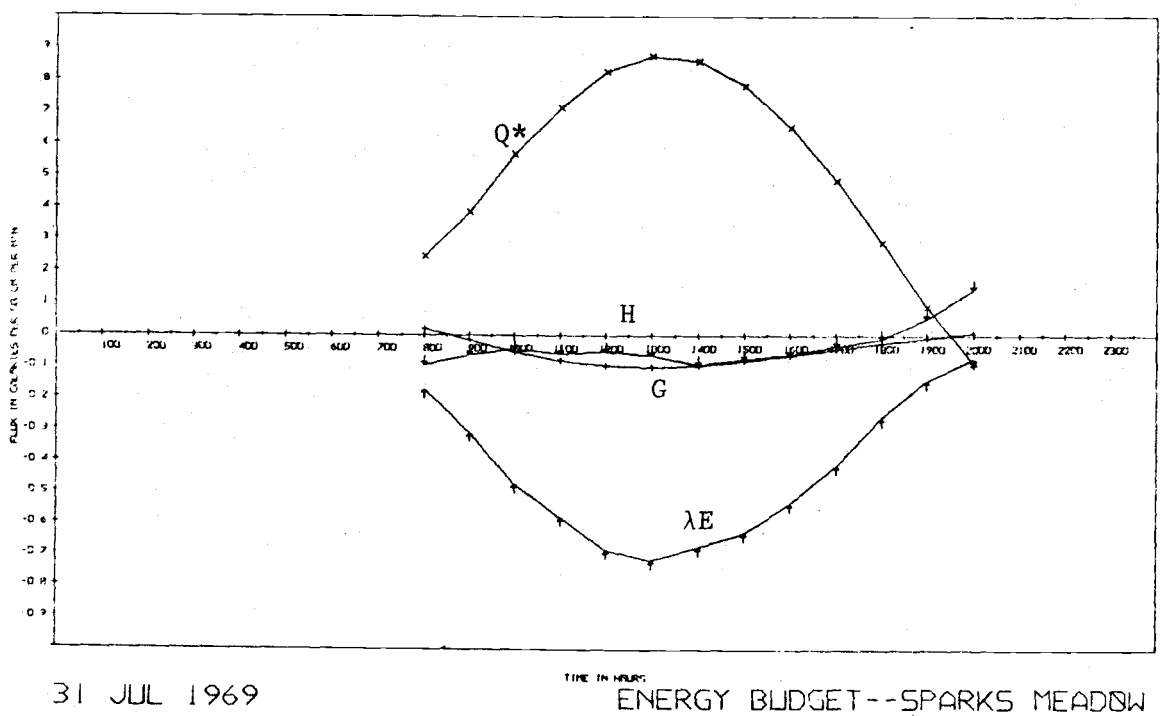

Figure 5-6. The diurnal course of the energy budget components at the meadow site. Symbols are defined in the text.

Table 5-4 The energy budget components at the lodgepole forest site, August 21 and 27, 1969. Tabulated data is in units of cal/cm^2/min, while the integrated units are cal/cm^2/day.

Lodgepole Forest	21 AUG 1969	Instrument levels: 707 and 1207 cm			Lodgepole forest	27 AUG 1969	Instrument levels: 707 and 957 cm		
PERIOD	Q(1)	SHF	H(B)	E(B)	PERIOD	Q(1)	SHF	H(B)	E(B)
0- 30	-0.1134	.0073	.0910	.0152	0- 30	-0.1011	.0143	.3563	.0315
30- 130	-0.1000	.0090	.0565	.0345	30- 130	-0.0639	.0138	.3266	.0235
130- 230	-0.0873	.0110	.0449	.0314	130- 230	-0.0650	.0125	.0303	.0223
230- 330	-0.0805	.0120	.0369	.0315	230- 330	-0.0196	.0096	.0052	.0046
330- 430	-0.0744	.0127	.0341	.0277	330- 430	-0.0322	.0096	.0120	.0110
430- 530	-0.0620	.0130	.0256	.0234	430- 530	-0.0530	.0102	.0229	.0139
530- 630	-0.0495	.0130	.0201	.0164	530- 630	-0.0488	.0127	.0197	.0164
630- 730	.0367	.0116	-0.0252	-0.0230	630- 730	.0388	.0115	-0.0179	-0.0331
730- 830	.2151	-0.0006	-0.0994	-0.1154	730- 830	.2064	.0022	.0019	-0.0130
830- 930	.4407	-0.0135	-0.1460	-0.2811	830- 930	.4537	-0.0076	-0.2954	-0.1637
930-1030	.6550	-0.0246	-0.3287	-0.3816	930-1030	.6571	-0.0190	-0.4495	-0.1885
1030-1130	.8123	-0.0303	-0.3949	-0.3871	1030-1130	.8172	-0.0234	-0.5263	-0.2875
1130-1230	.9187	-0.0256	-0.4092	-0.4039	1130-1230	.9174	-0.0197	-0.6597	-0.2391
1230-1330	.9605	-0.0511	-0.5240	-0.3854	1230-1330	.9547	-0.0427	-0.6308	-0.2812
1330-1430	.9368	-0.0403	-0.5023	-0.3942	1330-1430	.9299	-0.0308	-0.6540	-0.2491
1430-1530	.8475	-0.0532	-0.4385	-0.3558	1430-1530	.8357	-0.0946	-0.5866	-0.1591
1530-1630	.7107	-0.0215	-0.3416	-0.3476	1530-1630	.6850	-0.0115	-0.5309	-0.1426
1630-1730	.5218	-0.0221	-0.2253	-0.2744	1630-1731	.4895	-0.0078	-0.3696	-0.1220
1730-1830	.2931	-0.0122	-0.1091	-0.1719	1730-1830	.2469	-0.0033	-0.1517	-0.0920
1830-1930	.0559	-0.0060	-0.0032	-0.0466	1830-1930	.0025	.0022	-0.0008	-0.0240
1930-2030	-0.1152	-0.0001	0.0800	-0.0353	1930-2030	-0.1295	.0061	.1765	-0.0931
2030-2130	-0.1133	.0048	.1131	-0.0045	2030-2130	-0.1288	.0067	.1080	.0122
2130-2230	-0.1043	.0073	.0717	.0253	2130-2230	-0.1227	.0093	.0960	.0234
2230-2330	-0.0964	.0095	.0541	.0327	2230-2330	-0.1079	.0123	.0660	.0296
2330- 0	-0.0920	.0106	.0454	.0360	2330- 0	-0.0861	.0125	.0481	.0256
INTEGRAL	386	-11	-182	-193	INTEGRAL	383	-8	-256	-119

*H(B), E(B) interpolated this hour

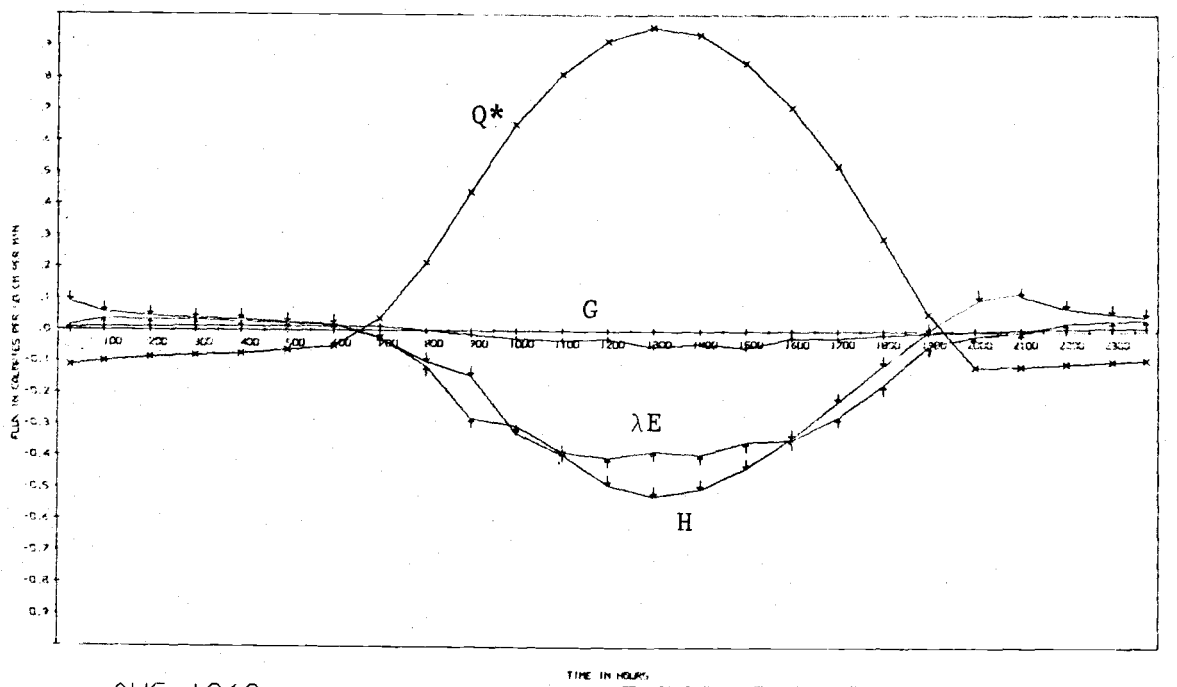

AUG 1969 ENERGY BUDGET--LODGEPOLE FOREST

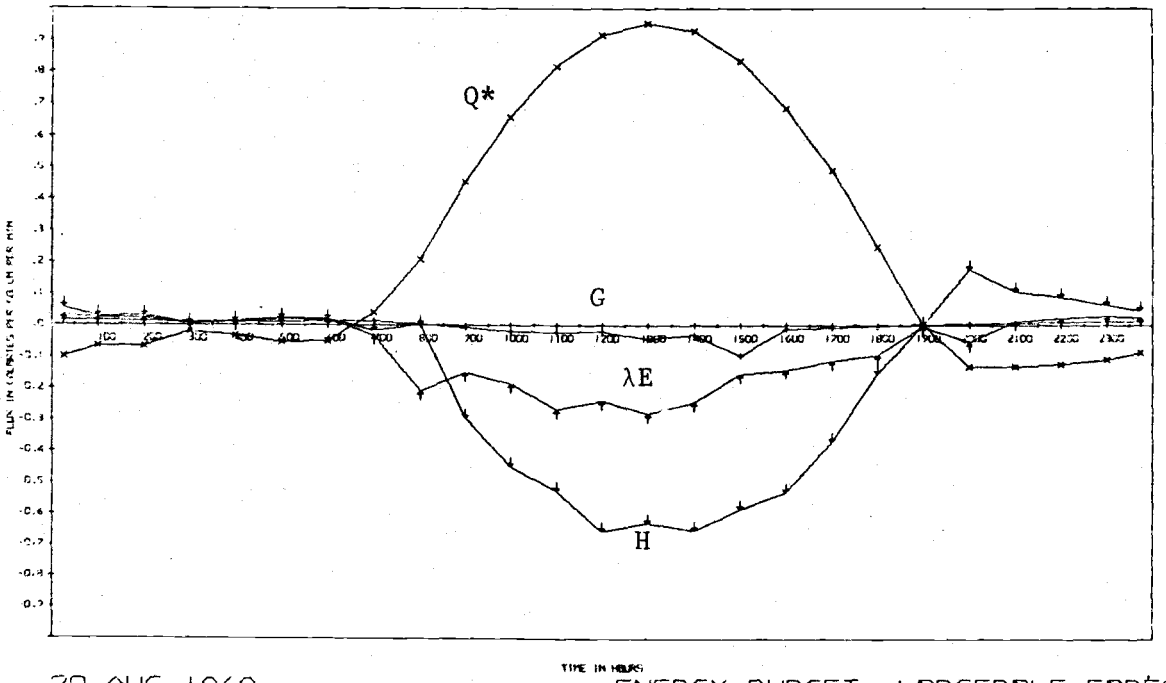

28 AUG 1969 ENERGY BUDGET--LODGEPOLE FOREST

Figure 5-7. The diurnal course of the energy budget components at the forest site. Symbols are defined in the text.

The heights used in the aerodynamic formulas must be measured above a reference level established at the point where the wind speed is zero. In the non-vegetated pumice desert, this is taken at the surface. In the presence of vegetation, however, the "zero-plane" is displaced upward, while the heights of the instruments remain fixed with respect to the ground (or water) level.

The displacement height, D, of the zero plane can be estimated by using all levels of wind and temperature data during conditions of neutral stability, e.g. Ri = 0. The graphical procedure used to estimate D involves plotting the log of instrument height (ln z) against the windspeed at that height (u), for all 6 levels of measurement. The instrument heights were then adjusted by subtracting a trial displacement height and replotting. This procedure was repeated until a straight line obtained and the profile was governed by the equation (Tanner, 1963, p. W-9)

$$u = \text{constant} \cdot \ln ((z-D)/z_o). \qquad [5\text{-}1]$$

The roughness parameter z_o is estimated by the intersection of line with the ordinate.

The mean values of D = 114 cm and z_o = 10 cm were established by examination of a number of neutral profiles. The actual height of the marsh vegetation was about 230 cm above the water while the bulk of the biomass was within 150 cm of the water level.

The correction term, ϕ, in Equations [1-5, 1-6] is based upon Paulson's (1970) formulation of the Businger-Dyer model which suggests that α and γ are equal to 15 and 0.75 respectively. Our earlier tests revealed that levels 4 and 6 at nominal heights of 360 and 520 cm above the water best met the requirements for similarity. The heights of these levels above the zero plane were 246 and 406 cm; these were the heights used in the analysis.

The latent and convective fluxes were estimated by the aerodynamic approach, and the change in stored energy evaluated as a residual. This approach was used because the large heat capacity of the marsh made it difficult to obtain direct measurements of the storage term. The Bowen ratio model could not be used at the marsh without a good estimate of G.

The energy fluxes at the marsh are tabulated in Table 5-5, and plotted in Figure 5-8.

5.4 Energy Budget Discussion

For clear weather periods, the supply of radiant energy available for transformation at the surface was shown earlier to be largely dependent upon the albedo, or reflectivity of the surface for solar radiation. The subsequent disposition of the transformed radiant energy can be examined through an energy budget analysis. Such an accounting will assist in understanding the importance of differences in various surface characteristics.

The mean energy budget data for the surfaces are summarized in Table 5-6. The aspects to be considered include the magnitudes of the three non-radiative components of the budget and the phase relationships among all four components.

Table 5-5. The energy budget components at Malheur Lake, August 21 and 23, 1971. Tabulated data is in units of cal/cm^2/min, while the integrated units are cal/cm^2/day.

Malheur Marsh	21 AUG 1971	Instrument levels: 360 and 520 cm		
Period	Q*	H	E	G
30- 130	-0.1168	.1230	-0.2573	.2534
130- 230	-0.1168	.1329	-0.2654	.2493
230- 330	-0.1185	.1063	-0.2339	.2461
330- 430	-0.1137	.1015	-0.2100	.2222
430- 530	-0.1146	.0764	-0.1800	.2182
530- 630	-0.1092	.0372	-0.0787	.1507
630- 730	-0.0313	.0428	-0.1805	.1690
730- 830	.1389	-0.0079	-0.3467	.2157
830- 930	.3654	-0.0416	-0.4017	.0779
930-1030	.6299	-0.0446	-0.3392	-0.2461
1030-1130	.7841	-0.0280	-0.3583	-0.3978
1130-1230	.8921	-0.0034	-0.3002	-0.5885
1230-1330	.9378	.0177	-0.4146	-0.5409
1330-1430	.9128	.0293	-0.4919	-0.4502
1430-1530	.8170	.0340	-0.4156	-0.4354
1530-1630	.6716	.0513	-0.4631	-0.2598
1630-1730	.4635	.0347	-0.2191	-0.2791
1730-1830	.2338	.1100	-0.4276	.0838
1830-1930	.0054	.1557	-0.4142	.2531
1930-2030	-0.1058	.2437	-0.4848	.3469
2030-2130	-0.1106	.2336	-0.4466	.3236
2130-2230	-0.1157	.1547	-0.3059	.2669
2230-2330	-0.1179	.1669	-0.3330	.2840
2330- 30	-0.1153	.1630	-0.3081	.2381
INTEGRAL	334	114	-472	24

Malheur-Marsh	23 AUG 1971	Instrument levels: 360 and 520 cm		
Period	Q*	H	E	G
30- 130	-0.1506	.0286	-0.1989	.2306
130- 230	-0.1505	.0284	-0.1299	.2510
230- 330	-0.1471	.0042	-0.0836	.2225
330- 430	-0.1392	.0008	-0.0428	.1812
430- 530	-0.1342	.0195	-0.0401	.1548
530- 630	-0.1254	.0113	-0.0927	.2068
630- 730	-0.0626	-0.0255	-0.0950	.1831
730- 830	.1656	-0.0809	-0.1575	.0719
830- 930	.4146	-0.1699	-0.2895	.0437
930-1030	.6281	-0.1444	-0.3268	-0.1569
1030-1130	.7927	-0.0825	-0.3418	-0.3684
1130-1230	.9079	-0.0414	-0.3744	-0.4881
1230-1330	.9445	-0.0217	-0.3589	-0.5639
1330-1430	.9145	-0.0020	-0.4950	-0.4175
1430-1530	.8168	.0198	-0.5099	-0.3267
1530-1630	.6576	.0435	-0.5737	-0.1274
1630-1730	.4500	.0629	-0.4834	-0.0295
1730-1830	.2089	.0441	-0.2650	.0120
1830-1930	-0.0285	.0477	-0.1814	.1622
1930-2030	-0.1462	.0667	-0.1363	.2158
2030-2130	-0.1444	.0877	-0.1812	.2379
2130-2230	-0.1331	.0897	-0.2063	.2479
2230-2330	-0.1333	.0800	-0.1650	.2183
2330- 30	-0.1396	.0219	-0.0632	.1869
INTEGRAL	316	5	-342	21

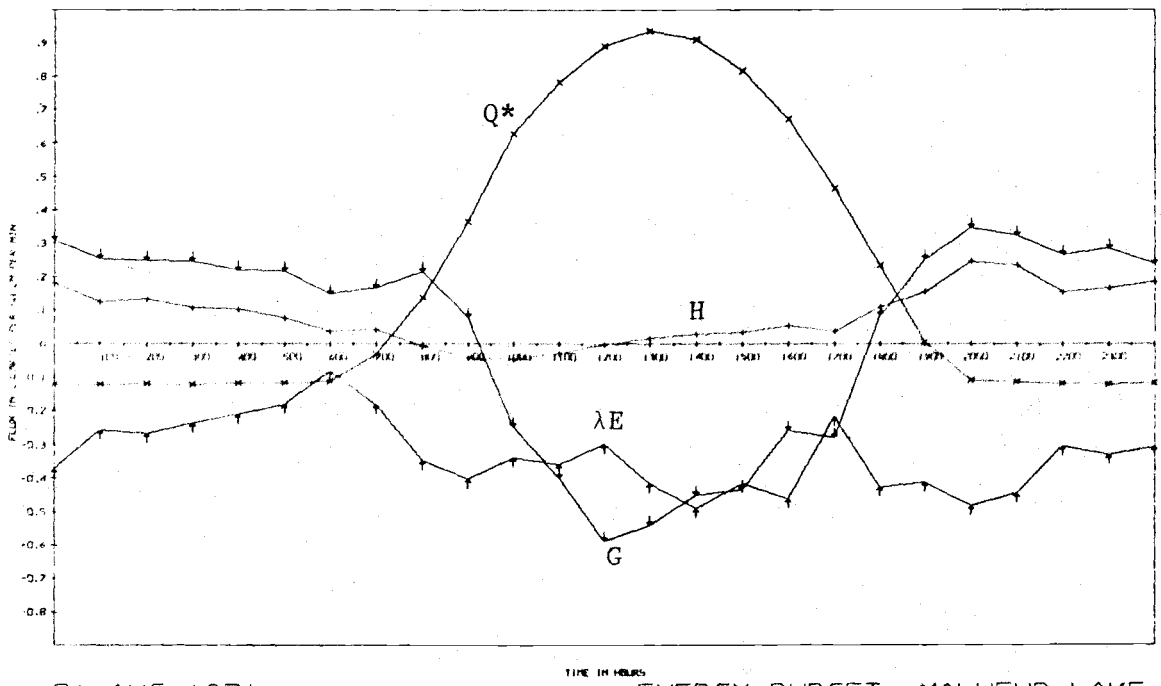

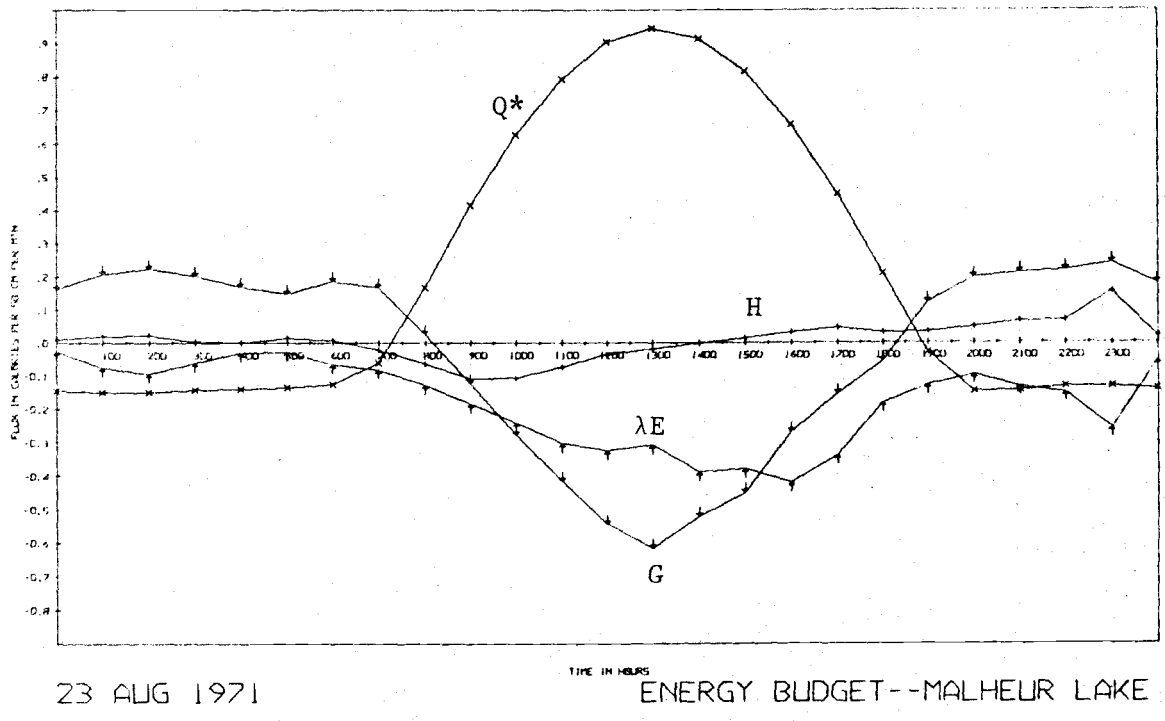

Figure 5-8. The diurnal course of the energy budget components at the marsh site. Symbols are defined in the text.

Table 5-6. Mean energy budgets for the experimental sites. Units are $cal/cm^2/day$.

	$\bar{Q}^*$	$\bar{G}$	$\bar{H}$	$\lambda\bar{E}$
Pumice	226	- 5	-188	- 33
Meadow	351	- 9	19	-361
Lodgepole	384	-10	-219	-155
Marsh	325	22	60	-407

5.4.1. Magnitudes

The magnitude of the heat storage component is small on a daily basis. The pumice, meadow and lodgepole sites show a daily loss in the order of -5 to -10 cal/cm^2, while the marsh gained 22 cal/cm^2. The daily totals, however, do not indicate the role that storage may play in the partitioning of energy at the surface. The hourly totals must be examined to show this effect.

The diurnal storage changes may be seen in the hourly energy budget plots (Figures 5-5 through 5-8). The hourly storage term is generally large at the marsh, even though the daily total approaches zero. The pumice desert also shows an appreciable change in storage throughout the day, while the meadow and forest sites, in contrast, show only a very small diurnal cycle in the change in stored heat.

The marsh site has an appreciable storage term because of the large heat capacity of the water and mud. The heat capacity of pumice material is smaller, but the storage changes still remain large at that site because of the high temperatures achieved by the pumice surface. The higher temperature is associated with the way the pumice surface partitions absorbed energy into the convective and the storage components in an environment where water is relatively unavailable.

The much smaller storage changes in the meadow and forest soils are associated with higher evaporation rates. High evaporation also prevails at the marsh, but as noted earlier, the mud and water there readily stores large quantities of thermal energy. The method of measurement at the meadow and forest site also minimizes the estimate of stored energy. The values at these two sites, as noted in the discussion of field procedures, are measured directly by soil heat flux plates and no correction has been added for the overlying layer of soil and vegetation. This omission could be important at the forest site, because of the biomass quantity found there.

Convection rates are related to the configuration of the surface, and to the availability of water for latent energy transfer. For example, the forest and pumice sites have the highest totals of convective transfer. Further examination of these surfaces will help explain the factors contributing to the large convection totals.

The lodgepole pine stand possesses many attributes of an efficient heat exchanger. The canopy elements are small. Since convective exchange is enhanced by small elements, they are thus effectively coupled to the temperature of the air. Another factor is the large canopy surface area, which is perhaps five

times greater than the area of the pumice surface. The forest canopy is effective in transferring absorbed energy into the air by convection. One should also recall that the forest is effective in absorbing energy; this increases the amount of energy available for dissipation.

The pumice surface also dissipates a large amount of energy by convection. In fact, on a proportional basis, it loses more available energy through the convection process than does the forest. This partitioning is primarily a consequence of the nonavailability of water at the pumice site. The smaller absolute convection for the pumice, in contrast to the large relative value of convection, appears associated with the less effective absorption of radiation by that surface.

The meadow and the marsh both show positive values of convection for the day. The surroundings of these sites are not plentifully supplied with water, and they therefore serve as sources of sensible energy. This energy is transported by the atmosphere to the cooler, evaporating surfaces of the meadow and marsh. The positive values are rather small on a daily basis, as the meadow gained 19 cal/cm^2 and the marsh 60 cal/cm^2. Evaporation is also affected by convection.

The positive convection values enhance the supply of energy available for dissipation by the other modes of energy transfer. The marsh, for example, gained the most from convection, and also lost the most latent energy by vaporization. The marsh evapotranspiration totaled -407 cal/cm^2 while the meadow was not far behind at -361 cal/cm^2. The forest was intermediate with a latent energy loss of -155 cal/cm^2, while the pumice lost only -33 cal/cm^2 for the day.

The evaporation equivalents of the latent energy terms are also of interest. Based on a nominal value of 590 cal/cm^3 for the latent heat of evaporation, the mean depth of water evaporated from each surface is: marsh, 6.9 mm; meadow, 6.1 mm; forest, 2.6 mm; and pumice, 0.6 mm. The two surfaces most plentifully supplied with water lost the greatest amounts, although the forest also lost an appreciable depth of water during the period of measurement.

The relative efficiency with which each surface partitions available energy into latent heat or convection can be examined through the Bowen ratio defined earlier as H/E. The mean daily values are small and negative for the marsh and meadow, being respectively -0.15 and -0.05, while the forest and pumice ratios are 1.4 and 5.7. The negative value of the ratio for the marsh and meadow indicates an advective situation where convection is positive, while the near-zero value reaffirms that latent energy transfer there is large with respect to convection. The positive values indicate that latent and sensible energy transfer are proceeding in the same direction over the forest and pumice. At these two drier sites, both fluxes are away from the surface. The large value of the ratio indicates that convection is becoming larger in relation to the latent energy term.

The mean Bowen ratios are helpful for visualizing the efficiency with which each surface partitions available energy into latent or sensible forms. However, one must also consider the efficiency of the surface in making energy "available" for partitioning. Since the change in heat storage is relatively small on a diurnal basis, the radiation properties play the major role in establishing

the quantity of available energy. The direction of the convective flux may also be important. For example, the Bowen ratio of 5.7 over the pumice confirms that evaporation is rather low in relation to convection. However, the energy available at the pumice surface (221 cal/cm^2) is only 54 percent of that available to the marsh (407 cal/cm^2) under similar conditions of incoming solar radiation. These values are obtained by summing net radiation and change in heat storage, plus positive values of convection where they exist.

5.4.2 Phase Relationships

The partitioning of energy among the dissipative fluxes is generally in phase with the diurnal curve of net radiation at all four sites. This will occur at a given site as long as the surfaces do not selectively partition the transformed energy into one of the dissipation fluxes at the expense of the others.

Deviations from this generalization are evident at the pumice and the marsh site, both of which have large diurnal changes in the rate at which energy enters or leaves storage. The magnitude of the storage changes at these two sites is sufficient to reduce the net radiant energy available for convection and evaporation in the morning hours, when the surface is heating up. In a similar fashion, energy that leaves storage as the surface cools in the evening enhances the amount available for convection and evaporation.

Several investigators (Black and McNaughton, 1971; Gay, 1972) have reported measurements over forests in which the latent energy curve was shifted in phase toward the afternoon. Black and McNaughton (1971) reported that this shift kept the latent energy exchange proportional to the vapor pressure deficit which ordinarily rises as air temperature increases in the afternoon. Stewart and Thom[1] have also concluded that the latent energy flux is controlled by vapor pressure deficit in their evaluation of the interplay between the large internal (stomatal) and small external (boundary layer) resistances to transfer. The ratio of these resistances for their pine site was in the order of 20:1. This ratio of resistances may vary from site to site, and may well be an important subject for future studies.

Thus in summary, the phase relationships show no marked displacement with respect to net radiation, except in the case of the heat storage term. This did contribute to small phase changes among the fluxes at the desert and meadow sites.

---

[1]J. B. Stewart and A. S. Thom. Energy budgets in pine forest. Institute of Hydrology, Wallingford, Berks., U. K. Unpublished manuscript, 1972.

5.5 Literature Cited.

Aizenshtat, B. A. 1958. The heat balance and microclimate of certain landscapes in a sandy desert. Translated by G. S. Mitchell from: M. I. Budyko (ed.). 1958. Glavnaia Geofizicheskaia Observatoriia im A. I. Voeikova.: Sovremennye problemy meteorologii prizemnogo sloia vozdukha. Sbornik statei pod red. Leningrad. Gidrometeoizdat., 1958, pp. 67-130. U.S. Weather Bureau, Washington, D. C. 1960. 90 pp.

Black, T. A. and K. G. McNaughton. 1971. Psychrometric apparatus for Bowen-ratio determination over forests. Bound. Layer Meteorol. 2:246-254.

Gay, L. W. 1971. The regression of net radiation upon solar radiation. Arch. Meteorol. Geophy. Biokl, B. 19:1-14.

Gay, L. W. 1972. Energy flux studies in a coniferous forest ecosystem. Pp. 243-253, in: J. F. Franklin, L. J. Dempster, and R. H. Waring (Eds.). Proceedings - research on coniferous forest ecosystems - a symposium. Pacific Northwest Forest and Range Experiment Station, Portland, Oregon. 322 p.

Gay, L. W., and K. R. Knoerr. 1970. The radiation budget of a forest canopy. Arch. Meteorol. Geophys. Biokl., B. 18:187-196.

Holbo, H. R. 1971. Development of a stability correction for estimating convective transfer. Dept. Atmospheric Sci. Tech. Report 71-7. Oregon State Univ., Corvallis. 10 pp.

Holbo, H. R. 1972. The energy budget of a pumice desert. Ph.D. thesis, Oregon State University, Corvallis. 142 pp.

Miller, D. H. 1965. The heat and water budget of the earth's surface. Advan. Geophys. 11:176-277.

Monteith, J. L. 1959 . The reflection of shortwave radiation by vegetation. Quart. J. Roy. Meteorol. Soc. 85:386-392.

Paulson, C. A. 1970. The mathematical representation of wind speed and temperature profiles in the unstable atmospheric surface layer. Journal of Applied Meteorology 9:857-861.

Reifsnyder, W. E., and H. W. Lull. 1965. Radiant energy in relation to forests. U.S. Forest Serv., Tech. Bull. 1344, Washington, D. C. 111 pp.

Tanner, C. B. 1963. Basic instrumentation and measurements for plant environment and micrometeorology. Dept. Soil Science, Soils Bull. 6, Univ. Wisconsin, Madison.

6. CONCLUSIONS

A landscape can be considered as a mosaic, made up of elements that may have widely differing thermal properties. Energy transfer characteristics are influenced by these properties; local and regional climates are affected by spatial integration of the energy exchange over many types of surface elements.

The landscape elements can be classified for study. On a coarse scale, the important elements in central Oregon include pumice desert, lodgepole pine forest, meadow and marsh. The energy exchange processes of these types of surfaces were examined during clear weather periods in mid- to late summer. This is the time when maximum inputs of energy occur, and the effects of different thermal properties will therefore be most apparent.

Major differences exist in the effectiveness with which these landscape elements absorb incident solar radiation. Under uniform conditions, the lodgepole forest absorbed 90 percent of the solar radiation. The marsh was close behind (89 percent), followed by the pumice (77 percent) and the meadow (75 percent). The absorption was greatest in areas with a well-developed canopy layer of appreciable thickness. This configuration apparently "traps" the radiation so that most is ultimately absorbed within the canopy.

It is often more meaningful to consider net radiation instead of incident solar radiation. Net radiation represents the amount of energy transformed from radiative to non-radiative forms of energy. There are three non-radiative forms of importance: convective and latent energy, and change in stored thermal energy. In a common view, net radiation is simply a measure of the income of allwave radiation, less the quantity lost by reflection and emission from the surface. The forested surface had the largest net radiation at 384 cal/cm^{2}day. Net radiation over the meadow (351 cal/cm^{2}day) exceeded that over the marsh (325 cal/cm^{2}day) even though the marsh was found to have greater absorptivity for solar radiation. Net radiation over the pumice desert was much smaller (226 cal/cm^{2}day) than over the other three surfaces.

The apparent anomaly of net radiation being higher over the meadow, despite the marsh's greater absorptivity for solar radiation, can be explained only by consideration of the other energy fluxes. When this is done, it then becomes apparent that the net radiation over the marsh is effectively reduced by the transfer of heat to the evaporating surface through convection (advection) from the warmer surroundings, and by transfer from storage. In other words, less radiant energy is required to sustain a given evaporation rate at the marsh, as compared to the meadow, because additional energy comes from the surroundings and from the substrate.

The magnitude of the three non-radiant energy transfer processes is of interest for these four types of surfaces. The latent energy term is of the most practical concern, as it represents a direct loss of water that would otherwise appear as stream flow. Convection plays a role in turbulence, diffusion and mixing in the lower atmosphere. Also, the thermal factors that control heat storage influence the temperature regime at the surface on microscale, as well as the regional scale.

The greatest amount of latent energy exchange took place at the marsh site (-407 cal/cm^{2}day), followed by the meadow (-351 cal/cm^{2}day) and the forest

(-155 cal/cm^{2}day). The water equivalent of this energy is respectively 6.9 mm, 6.1 mm and 2.6 mm. The pumice transformed only a negligible amount of latent energy during the study period.

The high latent energy loss at the marsh is related to the availability of water at this site and to the amount of sensible energy conveyed by convection from the arid surroundings. The marsh was undergoing a cooling phase during the late summer period of measurements, and the energy moving out of storage also augmented the evaporation.

Of the four surfaces examined, the forest was the most effective exchanger of energy. A relatively modest exchange of latent energy (-155 cal/cm^{2}day) was accompanied by the largest convective exchange (-219 cal/cm^{2}day) of any of the surfaces. It was surprising to note that the convection from the forest exceeded that from the pumice site (-188 cal/cm^{2}day). The pumice surface became much warmer at midday than did the lodgepole canopy, but the small elements that make up the canopy have a large total surface area and are effective in transferring convective energy into the atmosphere.

The energy budget results serve to provide some insight into changes that could be made in the surface characteristics, and of possible consequences resulting from such changes.

Timber cutting is the most common agent of change throughout the central Oregon region. Clear-cut areas in this region will lose less water by evaporation, and there may be some slight decrease in mixing, as well. However, the energy exchange characteristics of the cut-over pumice soil areas will tend to resemble those that were observed at the pumice desert site. The large diurnal temperature range of the pumice surface, from 50°C at midday to -5°C at night, has adverse effects on the establishment and growth of regeneration. Thus potential water savings derived from timber cutting must be viewed in perspective with the possible consequence to reestablishment of the forest cover. It is of course possible that silvicultural treatments and timber harvest practices will be devised that will minimize problems in regeneration.

It may also be feasible to impound some of the annual runoff before it reaches areas such as the Malheur marsh. This would provide control of water that now maintains the marsh; this water is to a large extent lost by evaporation. This paper will not assess the benefits to be gained by water management versus the loss associated with the marsh. However, one must note that reservoirs also lose a large quantity of water to evaporation, especially when located in arid areas such as that surrounding the marsh. Thus decisions upon whether or not to proceed with water control structures in the basin containing the Malheur marsh should be based on factors other than evaporation savings.

The results presented in this study should be more valuable for assessing the scale of ongoing natural processes, than for planning for modifications that could be made in the surface energy budget. The comparisons can be drawn from data collected during weather conditions associated with maximum rates of energy exchange. The results in particular provide an improved basis for estimating maximum evapotranspiration losses in the semi-arid region of central Oregon. The results also point out that additional research into energy exchange processes can be helpful in planning certain land management activities so as to achieve the maximum possible benefits.